UNIVERSITY OF CALIFORNIA

Los Angeles

MRI Biomarkers and Modifiable Health Factors of Aging and Dementia

A dissertation submitted in partial satisfaction

of the requirements for the degree Doctor of Philosophy

in Neuroscience

by

Sarah Kate Madsen

2013

ABSTRACT OF THE DISSERTATION

MRI Biomarkers and Modifiable Health Factors of Aging and Dementia

by

Sarah Kate Madsen

Doctor of Philosophy in Neuroscience

University of California, Los Angeles, 2013

Professor Paul M. Thompson, Chair

Alzheimer's dementia is a rising public health crisis that will have an unprecedented social and economic impact in the near future, as elderly individuals make up the fastest growing segment of the population worldwide [1-3]. The greatest single risk factor for Alzheimer's disease is age, though many genetic and environmental factors also influence disease onset and progression [4-9]. While current treatment options are sparse and no cure exists, it is critical to (1) identify the disease at its earliest stages, before irreversible brain degeneration has occurred and (2) to develop alternative strategies for reducing dementia risk based on aspects of health that are currently modifiable, such as cardiovascular health as one example. If we can identify

individuals who are at high risk for developing Alzheimer's dementia, but who have not yet experienced major neurodegeneration, then it may be possible to apply these alternative strategies to preserve brain health into old age.

In regards to the first aim, brain MRI scans identify robust signatures of Alzheimer's dementia at early stages. In my work, we have expanded upon existing brain-based MRI biomarkers by demonstrating changes in caudate nucleus shape in Alzheimer's disease and by showing that patterns of thinner cortical gray matter are associated with longitudinal expansion of the lateral ventricles. The caudate nucleus is a subcortical gray matter structure typically associated with motor planning, but is also involved in procedural memory, and is affected by the molecular pathology of Alzheimer's disease. The lateral ventricles are a fluid-filled space located at the center of the brain, which expand as brain tissue is lost in aging and dementia, within the fixed volume of the skull. Both of these biomarkers can be automatically measured from brain scans with high reliability and often with less manual intervention compared to other brain structures (such as the hippocampus). These biomarkers makes are candidates for use in clinical trials or, in the case of the lateral ventricles, even in an individual to assist in dementia diagnosis. My studies provide further validation for the use of these biomarkers with additional information on the clinical implications of structural changes in these structures.

For the second aim, I investigated blood levels of two potentially modifiable compounds (thyroid hormones and homocysteine) that have been linked to dementia risk and cognition in the elderly. Alterations in thyroid hormone levels and elevated homocysteine levels have separately been associated with increased dementia risk and cognitive decline in the elderly [10-20]. My results demonstrate that homocysteine and thyroid hormones levels measured are significantly

associated with structural brain differences in the elderly. I found that elderly individuals with elevated homocysteine levels were more likely to have reduced cortical gray matter in bilateral frontal, right temporal, bilateral sensory, motor, and visual areas. In another study, we found that higher levels of thyroid hormone (free thyroxine, fT4) within the normal range were associated with both brain tissue expansion and contraction relative to lower levels. These two compounds are modifiable because interventions exist to modify the levels of these compounds and it's possible to measure their levels using a blood test. While these interventions are not without risk and involve special consideration in the elderly, it is important to understand the relationship between these modifiable health factors and brain structure in the elderly. As more evidence accumulates, if the connection between these health factors, dementia risk and brain deterioration is strong enough, we may discover new avenues for preserving brain health into old age.

The dissertation of Sarah Kate Madsen is approved.

Susan M. Bookheimer

Jamie D. Feusner

Arthur W. Toga

Paul M. Thompson, Committee Chair

University of California, Los Angeles

2013

TABLE OF CONTENTS

ACKNOWLEDGEMENTS

I give the deepest thanks to everyone who has supported me before and during my graduate studies. My remarkable family, colleagues, classmates, and friends have made this possible and will forever have my greatest appreciation.

Funding Agency Acknowledgements

Sarah Kate Madsen was partially supported by the Neuroscience Interdepartmental Program at UCLA and by the National Defense Science and Engineering Graduate (NDSEG) Fellowship (32 CFR 168a) from the DoD, and Air Force Office of Scientific Research.

Data collection and sharing for this project was funded by the Alzheimer's Disease Neuroimaging Initiative (ADNI) (National Institutes of Health Grant U01 AG024904). ADNI is funded by the National Institute on Aging, the National Institute of Biomedical Imaging and Bioengineering, and through generous contributions from the following: Abbott, AstraZeneca AB, Bayer Schering Pharma AG, Bristol-Myers Squibb, Eisai Global Clinical Development, Elan Corporation, Genentech, GE Healthcare, GlaxoSmithKline, Innogenetics, Johnson and Johnson, Eli Lilly and Co., Medpace, Inc., Merck and Co., Inc., Novartis AG, Pfizer Inc, F. Hoffman-La Roche, Schering-Plough, Synarc, Inc., and Wyeth, as well as non-profit partners the Alzheimer's Association and Alzheimer's Drug Discovery Foundation, with participation from the U.S. Food and Drug Administration. Private sector contributions to ADNI are facilitated by the Foundation for the National Institutes of Health (http://www.fnih.org/). The grantee

organization is the Northern California Institute for Research and Education, and the study is coordinated by the Alzheimer's Disease Cooperative Study at the University of California, San Diego. ADNI data are disseminated by the Laboratory for Neuro Imaging at the University of California, Los Angeles.

The research reported in this article was supported in part by funds from contract numbers N01-HC-80007, N01-HC-85079 through N01-HC-85086, N01-HC-35129, N01 HC-15103, N01 HC-55222, N01-HC-75150, N01-HC-45133, grant number U01 HL080295 from the National Heart, Lung, and Blood Institute, with additional contribution from the National Institute of Neurological Disorders and Stroke. Additional funds were provided by the National Institute on Aging to O.L.L. (AG020098), L.H.K. (AG15928), P.T. (EB008281), and the University of Pittsburgh (AG05133), and by subcontract (N01-HC-055222) to J.T.B. A full list of principal CHS investigators and institutions can be found at www.chs-nhlbi.org/pi.htm.

Additional support was provided by NIH grants P30 AG010129, K01 AG030514, and the Dana Foundation.

Co-author Acknowledgements

I would like to thank all of the following co-authors for their contributions. I would also like to thank all of the co-authors who I have published with in graduate school, but was not able to list below.

Madsen, S. K., Ho, A., Hua, X., Saharan, P. S., Toga, A. W., Jack, C. R., Weiner, M. W., Thompson, P. M., & the Alzheimer's Disease Neuroimaging Initiative. (2010). 3D maps localize caudate nucleus atrophy in 400 AD, MCI, and healthy elderly subjects. *Neurobiology of Aging: ADNI Special Issue*, 1312-1325; doi:10.1016/j.neurobiolaging.2010.05.002.

Madsen, S.K.,. Gutman, B. A., Joshi, S. H., Toga, A. W., Jack, C. R. Jr., Weiner, M. W., Thompson, P. M., for the Alzheimer's Disease Neuroimaging Initiative (ADNI) (2013). Mapping dynamic changes in ventricular volume onto baseline cortical surface in normal aging, MCI, and Alzheimer's disease, accepted at MBIA *MICCAI 2013*, Nagoya, Japan, Sept. 22-26 2013.

Madsen S. K., Rajagopalan, P., Joshi, S.H., Toga, A.W., Thompson, P.M. & the Alzheimer's Disease Neuroimaging Initiative (ADNI) (2013). Elevated homocysteine is associated with thinner cortical gray matter in 803 ADNI subjects, *Neurobiology of Aging*, under review May 1 2013.

Madsen S.K., Gutman, B.A., Joshi, S.H., Toga, A.W., Jack, C.R.Jr., Weiner, M.W., Thompson, P.M., for the Alzheimer's Disease Neuroimaging Initiative (ADNI) (2013). Relating longitudinal ventricular expansion to cortical gray matter thinning in the elderly, *Neurobiology of Aging (Special Issue on Novel Imaging Biomarkers for Alzheimer's Disease and Related Disorders)*, under review May 1 2013.

Madsen, S.K., Liang, L., Boyle, C. A., Rajagopalan, P., Cappola, A. R., Becker, J. T., Lopez, O. L., Thompson, P. M. (2013). Thyroid hormones are related to future differences in brain tissue in 495 healthy euthyroid elderly, in preparation for submission July 2013.

Madsen, S.K., Bohon, C., Feusner, J.D. (2013). Visual processing in anorexia nervosa and body dysmorphic disorder: similarities, differences, and future research directions. *Journal of Psychiatric Research*, available online July 1st, 2013.

Romero-Calderon, R., O'Hare, E., Suthana, N. A., Scott-Van Zeeland, A. A., Rizk-Jacson, A., Attar, A., **Madsen, S. K.,** Ghiani, C. A., Evans, C. J., Watson, J. B. (2012). Project Brainstorm: Using Neuroscience to Connect College Students with Local Schools, PLoS Biology, 10(4), e1001310. doi:10.1371/journal.pbio.1001310.

VITA

2003-2007	B.S., Neuroscience and Psychobiology, UCLA
	UCLA College Honors Program, Psychology Research Opportunities Program
	Undergraduate Research with Dr. A. W. Toga and Dr. M. S. Fanselow
2007-2009	Staff Research Associate with Dr. P. M. Thompson
2010-2013	National Defense Science and Engineering Graduate (NDSEG) Fellowship, Department of Defense, Air Force
	Brain Research Institute Graduate Student and UCLA Graduate Division Travel Awards
2010	Press Conference, Spotting and Treating Alzheimer's Disease, Annual Meeting of the Society for Neuroscience
	Graduate Student Fellow, New Horizons in Human Brain Imaging Meeting: A Pacific Rim Neuroimaging Conference
	Quality of Graduate Education Special Course Funding, Career Advancement for Scientists and Educational Course on Diffusion and Structural MRI
2011	Teaching Assistant for Project Brainstorm, Event Leader for Brain Awareness Week
	HHMI Mentor Award, Preparing Future Faculty
2011-2012	Teaching Assistant for Civic Engagement in Science and Technology at UCLA
2012	FSL/FreeSurfer Brain Image Analysis Software Course
2013	Young Investigator Scholarship, 7th Annual Drug Discovery for Neurodegeneration Conference: An Intensive Course on Translating Research into Drugs

SELECT PUBLICATIONS

Madsen, S. K., Ho, A., Hua, X., Saharan, P. S., Toga, A. W., Jack, C. R., Weiner, M. W., Thompson, P. M., & the Alzheimer's Disease Neuroimaging Initiative. (2010). 3D maps localize caudate nucleus atrophy in 400 AD, MCI, and healthy elderly subjects. *Neurobiology of Aging: ADNI Special Issue*, 1312-1325; doi:10.1016/j.neurobiolaging.2010.05.002.

Madsen, S.K.,. Gutman, B. A., Joshi, S. H., Toga, A. W., Jack, C. R. Jr., Weiner, M. W., Thompson, P. M., for the Alzheimer's Disease Neuroimaging Initiative (ADNI) (2013). Mapping dynamic changes in ventricular volume onto baseline cortical surface in normal aging, MCI, and Alzheimer's disease, accepted at MBIA *MICCAI 2013*, Nagoya, Japan, Sept. 22-26 2013 [8-page paper; peer-reviewed conference paper].

Madsen S. K., Rajagopalan, P., Joshi, S.H., Toga, A.W., Thompson, P.M. & the Alzheimer's Disease Neuroimaging Initiative (ADNI) (2013). Elevated homocysteine is associated with thinner cortical gray matter in 803 ADNI subjects, *Neurobiology of Aging)*, under review May 1 2013.

Madsen S.K., Gutman, B.A., Joshi, S.H., Toga, A.W., Jack, C.R.Jr., Weiner, M.W., Thompson, P.M., for the Alzheimer's Disease Neuroimaging Initiative (ADNI) (2013). Relating longitudinal ventricular expansion to cortical gray matter thinning in the elderly, *Neurobiology of Aging (Special Issue on Novel Imaging Biomarkers for Alzheimer's Disease and Related Disorders)*, under review May 1 2013.

Madsen, S.K., Liang, L., Boyle, C. A., Rajagopalan, P., Cappola, A. R., Becker, J. T., Lopez, O. L., Thompson, P. M. (2013). Thyroid hormones are related to future differences in brain tissue in 495 healthy euthyroid elderly. in preparation for submission July 2013.

Madsen, S.K., Bohon, C., Feusner, J.D. (2013). Visual processing in anorexia nervosa and body dysmorphic disorder: similarities, differences, and future research directions. *Journal of Psychiatric Research*, available online July 1st, 2013.

Romero-Calderon, R., O'Hare, E., Suthana, N. A., Scott-Van Zeeland, A. A., Rizk-Jacson, A., Attar, A., **Madsen, S. K.,** Ghiani, C. A., Evans, C. J., Watson, J. B. (2012). Project Brainstorm: Using Neuroscience to Connect College Students with Local Schools, PLoS Biology, 10(4), e1001310. doi:10.1371/journal.pbio.1001310.

CHAPTER 1

Introduction

There is great interest in understanding brain aging, both in health and in diseases such as Alzheimer's dementia. In the following chapters, I look at several aspects of brain structure and determined how these structural differences are related to clinical factors in healthy aging, mild cognitive impairment (a preliminary stage that often precedes the onset of dementia), and in Alzheimer's disease. Since restoring lost brain tissue is currently not possible, it's important to identify the earliest possible signs of dementia. We also want to identify ways in which elderly individuals might reduce their risk for dementia using the medical tools and scientific knowledge that are currently available. With this information, it may be possible to help preserve brain health in our rapidly expanding elderly populations.

Alzheimer's disease is the leading cause of dementia, affecting 24 million people worldwide [3]. This is a major public health issue and expanding problem. Individuals over the age of 80 years old, the so called "oldest old," represent the fastest growing segment of the population worldwide [1]. Age is the predominate risk factor for the development of Alzheimer's disease [21]. This increase in the number of very elderly individuals brings an increased burden of dementia, with the prevalence of Alzheimer's disease expected to double every twenty years [22]. There is no cure for the disease and current treatments slow the decline of cognitive symptoms in the short-term, without effecting underlying neurodegeneration [23, 24].

Improving brain MRI biomarkers of aging and dementia can help us identify the signs of dementia much sooner, before irreversible brain degeneration has occurred. In my work, I focus on brain structures that have ideal characteristics as MRI biomarkers in elderly populations. The caudate nucleus is a subcortical gray matter structure affected by Alzheimer's pathology and the lateral ventricles expand as brain tissue is lost in aging and dementia. These two structures can be reliably and accurately detected with automated methods, compared to other structures such as the hippocampus or cortical gray matter, which are more difficult to segment in elderly atrophied brains. The caudate nucleus and lateral ventricles were previously overlooked relative to these structures because it was less clear how changes in these two structures related to the specific clinical deficits seen in Alzheimer's disease. My work provides a deeper understanding of how structural changes in these structures relate to key aspects of dementia progression and clinical symptoms, enabling us to take advantage of their properties as biomarker properties while also inferring information about cognition.

The second focus in my work is to understand how *modifiable* risk factors for dementia are related to brain structure in the elderly. This is extremely important because current treatments for dementia cannot halt or slow neurodegeneration and there is no cure for this progressive neurodegenerative disorder. My work shows that levels of thyroid hormones and homocysteine, measured with a simple blood test, are related to brain structure differences in areas affected by Alzheimer's disease pathology and in other regions, suggesting that additional mechanisms specific to these aspects of health are also at play. The appeal of this research is that it may eventually suggest possible courses of action that individuals could take to preserve their brain health and reduce their risk of Alzheimer's disease, when applied appropriately.

1.1 Organization of the dissertation

The layout of the dissertation is as follows.

The second chapter covers my work on MRI biomarkers in elderly individuals who are cognitively normal, mildly impaired, or who have Alzheimer's disease. . In section 2.1, I present my results on shape differences in the caudate nucleus. In section 2.2, I present my results from mapping longitudinal change in lateral ventricle volumes onto cortical gray matter thickness.

The third chapter covers my work on relating modifiable Alzheimer's disease risk factors to brain structure in the elderly. In section 3.1, I present my work on subclinical alterations in thyroid hormone levels and future differences in regional brain volumes in a cognitively normal elderly sample. In section 3.2, I present my work on elevated homocysteine levels and reduced cortical gray matter in the elderly.

The fourth chapter includes related work completed during my graduate studies. In section 4.1, I present my review on visual processing in anorexia nervosa and body dysmorphic disorder, of which a major component was functional and structural brain imaging findings. In section 4.2 I present an article we published as part of the neuroscience outreach efforts at UCLA, for which I taught several classes and led large outreach events. In section 1.3, I list the co-authored papers that I completed during my graduate studies, which cover a broad range of brain imaging techniques in various populations.

The fifth chapter includes future works in planned and ongoing studies.

CHAPTER 2

MRI biomarkers of dementia

2.1 Caudate nucleus shape differences in dementia

This section is adapted from the following paper.

Madsen, S. K., Ho, A., Hua, X., Saharan, P. S., Toga, A. W., Jack, C. R., Weiner, M. W., Thompson, P. M., & the Alzheimer's Disease Neuroimaging Initiative. (2010). 3D maps localize caudate nucleus atrophy in 400 AD, MCI, and healthy elderly subjects. *Neurobiology of Aging: ADNI Special Issue*, 1312-1325; doi:10.1016/j.neurobiolaging.2010.05.002.

ELSEVIER

Neurobiology of Aging 31 (2010) 1312–1325

NEUROBIOLOGY OF AGING

www.elsevier.com/locate/neuaging

3D maps localize caudate nucleus atrophy in 400 Alzheimer's disease, mild cognitive impairment, and healthy elderly subjects

S.K. Madsen[a], A.J. Ho[a], X. Hua[a], P.S. Saharan[a], A.W. Toga[a], C.R. Jack Jr[b], M.W. Weiner[c,d], P.M. Thompson[a,*], The Alzheimer's Disease Neuroimaging Initiative[†]

[a] *Laboratory of Neuro Imaging, Department of Neurology, University of California, Los Angeles, School of Medicine, Los Angeles, CA, USA,*
[b] *Mayo Clinic College of Medicine, Rochester, MN, USA*
[c] *Departments of Radiology, Medicine, and Psychiatry, University of California, San Francisco, San Francisco, CA, USA*
[d] *VA Medical Center, San Francisco, CA, USA*

Received 15 February, 2010; received in revised form 29 April 2010; accepted 1 May 2010

Abstract

MRI research examining structural brain atrophy in Alzheimer's disease (AD) generally focuses on medial temporal and cortical structures, but amyloid and tau deposits also accumulate in the caudate. Here we mapped the 3D profile of caudate atrophy using a surface mapping approach in subjects with AD and mild cognitive impairment (MCI) to identify potential clinical and pathological correlates. 3D surface models of the caudate were automatically extracted from 400 baseline MRI scans (100 AD, 200 MCI, 100 healthy elderly). Compared to controls, caudate volumes were lower in MCI (2.64% left, 4.43% right) and AD (4.74% left, 8.47% right). Caudate atrophy was associated with age, sum-of-boxes and global Clinical Dementia Ratings, Delayed Logical Memory scores, MMSE decline 1 year later, and body mass index. Reduced right (but not left) volume was associated with MCI-to-AD conversion and CSF tau levels. Normal caudate asymmetry (with the right 3.9% larger than left) was lost in AD, suggesting preferential right caudate atrophy. Automated caudate maps may complement other MRI-derived measures of disease burden in AD.

Keywords: Alzheimer's disease; Mild cognitive impairment; Normal aging; Caudate nucleus; Brain mapping; Surface mapping; MRI; Atrophy; Alzheimer's Disease Neuroimaging Initiative

Alzheimer's disease (AD) is the most prevalent form of dementia, affecting over 24 million people worldwide and over 5 million in the USA alone (Jorm et al., 1987). Memory systems of the hippocampus and medial temporal lobes are among the first to be affected by plaque and tangle pathology, with subsequent cortical pathology and widespread neuronal loss leading to impairments in language, attention, orientation, visuospatial, and executive functions. Traditionally, AD research has focused on regions that degenerate earliest, and less attention has been paid to other subcortical brain regions involved in aging and AD (Rubin, 1999). Preferential caudate atrophy is more typical of motor disorders such as Parkinson's disease (Nakamura et al., 2001), but beta-amyloid and tau pathology also accumulate in the caudate in AD (Braak and Braak, 1990). Many earlier MRI studies of aging (Jernigan et al., 2001; Krishnan et al., 1990; Raz et al., 2003) and AD (Good et al., 2002; Rombouts et al., 2000) show progressive atrophy of the caudate. The caudate plays a vital functional role in forming new associations to acquire explicit memories, and in motor learning (Knowlton et al., 1996; Nakamura et al., 2001). Atrophy of the caudate nucleus may therefore be a valid

* Corresponding author at: Tel.: (310) 206 2101; fax: (310) 206 5518.
E-mail address: thompson@loni.ucla.edu (P.M. Thompson).

[†] Data used in the preparation of this article were obtained from the Alzheimer's Disease Neuroimaging Initiative database (www.loni.ucla.edu/ADNI). As such, investigators within the Alzheimer's Disease Neuroimaging Initiative (ADNI) contributed to the design and implementation of ADNI and/or provided data but did not participate in analysis or writing of this report. For a complete listing of ADNI investigators, please see: www.loni.ucla.edu/ADNI/Collaboration/ADNI_Manuscript_Citations.pdf.

0197-4580/$ – see front matter © 2010 Elsevier Inc. All rights reserved.
doi:10.1016/j.neurobiolaging.2010.05.002

target, in conjunction with others, in the search for AD biomarkers in the brain.

Despite some prior volumetric MRI studies, no study has mapped caudate atrophy and evaluated its clinical and pathological correlates in a large population of AD subjects. Here we extracted 3D models of caudate nucleus shape in 400 subjects from the Alzheimer's Disease Neuroimaging Initiative (ADNI), to test whether caudate atrophy was related to: (1) AD or MCI diagnosis at time of scanning; (2) baseline cognition assessed using the Mini-Mental State Examination (MMSE), clinical dementia rating (CDR), and immediate and delayed recall Wechsler Memory Scale (WMS); (3) future clinical decline (in MMSE, CDR) 1 year after scanning; (4) conversion from MCI to AD in the subsequent 1 or 2 years; (5) CSF biomarkers of AD (amyloid beta, tau, p-tau); and (6) other influential factors such as age and sex, Geriatric Depression (GD) scale, presence of tremor, abnormal gait, AD- and obesity-related ApoE and FTO genotypes, and body mass index (BMI). We also ranked the relative strength of factors associated with caudate atrophy, expecting strongest associations with global cognition, then with CSF markers, and then with risk-modifying genotypes. We also wanted to determine how AD interacts with the naturally occurring asymmetry in caudate anatomy (where the right caudate tends to be about 4% larger than the left), to see if there was asymmetry in the disease process.

1. Methods

1.1. Subjects

We analyzed 400 baseline T1-weighted structural MRI scans from the ADNI public database (www.loni.ucla.edu/ADNI/Data/), along with associated demographic information, ApoE and FTO genotypes, CSF biomarker measures (for amyloid beta, tau, p-tau), and clinical and cognitive assessments (detailed below). Data were downloaded on or before June 1, 2009, and reflect the status of the database at that point. ADNI is a 5-year study launched in 2004 by the National Institute on Aging (NIA), the National Institute of Biomedical Imaging and Bioengineering (NIBIB), the Food and Drug Administration (FDA), private pharmaceutical companies and nonprofit organizations, as a US$60mn public-private partnership. The primary goal of ADNI has been to test whether serial MRI, PET, biological markers, and clinical and neuropsychological assessments acquired at multiple sites (as in a typical clinical trial), can replicate results from smaller single site studies measuring the progression of MCI and early AD. A major focus of AD biomarker research is the pre-disease state known as mild cognitive impairment or MCI. Individuals with MCI have a 4–6-fold elevated risk for developing AD in the future, with 15% of MCI individuals developing AD within 1 year (Petersen et al., 1993). Determination of sensitive and specific markers for very early AD progression will aid researchers and clinicians in monitoring the effectiveness of new treatments, and lessen the time and cost of clinical trials. The Principal Investigator of this initiative is Michael W. Weiner MD, VA Medical Center and University of California, San Francisco.

ADNI collects a thorough battery of clinical and cognitive measures. We analyzed several scores that reflect cognitive decline in MCI and AD (Table 1). A total of 100 individuals diagnosed with probable AD (mean age: 75.86 ± 7.25 years), 200 with MCI (75.45 ± 7.03), and 100 healthy elderly controls (76.62 ± 4.83) were studied. The subject pool was age- and sex-matched within each diagnostic group. Data for all 400 subjects were available on each of the clinical measures analyzed in this study, leading to differing sample sizes for some of the following analyses.

Cognitive measures examined included: (1) the Mini-Mental State Examination (MMSE) – a global measure of mental status, evaluating five cognitive domains: orientation, registration, attention and calculation, recall, and language (Cockrell and Folstein, 1988); (2) the global and "sum-of-boxes" clinical dementia rating (CDR and CDR-SB respectively), which measures dementia severity by evaluating patients' performance in six domains: memory, orientation, judgment and problem solving, community affairs, home and hobbies, and personal care; CDR scores of

Table 1
Demographic and clinical data

	N	Women/Men	Age (years)	Education (years)	MMSE	CDR	CDR-SB
Control	100	53/47	76.62 (4.83)	15.87 (1.84)	29.14 (0.86)	0.47 (0.30)	0.02 (0.09)
MCI	200	100/100	75.45 (7.03)	15.61 (3.16)	26.94 (1.86)	0.43 (0.29)	1.48 (0.84)
AD	100	50/50	75.86 (7.25)	14.96 (3.31)	23.41 (1.86)	0.42 (0.33)	4.48 (1.56)

	Delayed Logical Memory	Immediate Logical Memory	MMSE change at 1 year	Diagnosis change after 1 year (number of AD conversions)	Diagnosis change after 2 years (number of AD conversions)	BMI
Control	12.99 (3.23)	14.11 (3.17)	−0.14 (1.42)	0	0	24.77 (3.18)
MCI	3.73 (2.79)	6.94 (3.24)	−1.21 (2.88)	36	24	25.91 (4.13)
AD	1.11 (1.74)	3.91 (2.82)	−2.62 (4.57)			25.49 (4.12)

Mean demographic and clinical data are shown by diagnostic group for all subjects at the time of scanning (baseline); standard deviations are in parentheses. Changes in MMSE scores were measured over a 1-year follow-up interval. Changes in diagnosis were determined after one- and 2-year follow-up intervals; the number of MCI and control subjects who converted to AD is also shown.

0, 0.5, 1, 2, and 3 represent no dementia, questionable, mild, moderate, and severe dementia, respectively, and CDR-SB scores range from 0 to 18 (Morris et al., 1993); and (3) immediate and delayed Logical Memory (LM) recall, which is a modified version of the episodic memory assessment from the Wechsler Memory Scale-Revised (WMS-R) (Wechsler, 1987); subjects were asked to recall a short story consisting of 25 pieces of information immediately after it was read to the subject (LM-im) and after a 30-minute delay (LM-del). It is a reasonable first step to survey a broad range of standard clinical tests of AD severity and memory impairment, because particular tests may be differentially associated with differences in caudate nucleus structure, and each test measures different aspects of cognitive performance. Also, it is important to compare different clinical measures to determine which tests associate best with atrophy for future clinical trials. This also enables direct comparison with a wide range of studies that have assessed these different measures.

We also examined Geriatric Depression (GD) scores (higher scores indicate greater depression severity), presence or absence of tremor, and normal versus abnormal gait to assess some of the emotional and motor functions traditionally associated with the caudate nucleus. Because recent studies have found that cardiovascular factors are associated with faster cognitive decline and more rapid progression of AD (Helzner et al., 2009), we also examined associations between atrophy and cardiovascular risk factors, such as BMI, which has been associated with brain atrophy in recent tensor-based morphometry studies of healthy elderly subjects (Raji et al., 2009) and in MCI and AD (Ho et al., 2010a). BMI was calculated as weight (kg) over height squared (m^2) − a simple but widely used measure for classifying obese and overweight subjects. We also tested for associations between atrophy and the FTO genotype, based on recent findings that a particular allele of the prevalent FTO gene is associated with higher weight and waist circumference. FTO genotype has also been linked to brain atrophy in a tensor-based morphometry study (Ho et al., 2010b).

1.2. MRI acquisition and preprocessing

Scans were acquired on 1.5T MR scanners at 60 sites across the USA and Canada. Different types of scanners (GE, Siemens, or Philips) and various software platforms were used, but a standardized MRI protocol ensured cross-site comparability (Jack et al., 2008). A typical 1.5T MR protocol involved a 3D sagittal MP-RAGE scan with repetition time (TR): 2,400 ms, minimum full excitation time (TE), inversion time (TI): 1,000 ms, flip angle: 8°, 24 cm field of view, and a 192 × 192 × 166 acquisition matrix in the x-, y-, and z-dimensions, yielding a voxel size of 1.25 × 1.25 × 1.2 mm^3, later reconstructed to 1 mm^3 isotropic voxels.

Image corrections were applied using a processing pipeline at the Mayo Clinic, consisting of: (1) correction of geometric distortion due to gradient nonlinearity (Jovicich et al., 2006), i.e. "grad warp" (2) "B1-correction" to adjust for image intensity inhomogeneity due to B1 nonuniformity (Jack et al., 2008), (3) "N3" bias field correction for reducing residual intensity inhomogeneity (Sled et al., 1998), and (4) geometric scaling to remove scanner- and session-specific calibration errors using a phantom scan acquired for each subject (Gunter et al., 2006). All original image files as well as all corrected images are available at www.loni.ucla.edu/ADNI/Data/.

To adjust for global differences in brain positioning and scale across individuals, all scans were linearly registered to the stereotaxic space defined by the International Consortium for Brain Mapping (ICBM-53) (Mazziotta et al., 2001) with a 9-parameter (9P) transformation (three translations, three rotations, three scales) using the Minctracc algorithm (Collins et al., 1994). This registration is one standard method to account for global differences in brain scale across subjects; alternatives include scaling each subject's caudate nucleus volume for overall head size, using scalp images, or covarying for total intracranial volume in a general linear model. Globally aligned images were resampled in an isotropic space of 220 voxels along each axis (x, y, and z) with a final voxel size of 1 mm^3.

1.3. Automated segmentation

We automatically extracted models of the caudate nucleus from each registered MRI scan, using an automated segmentation method based on adaptive boosting (Adaboost), that we recently developed and validated (Morra et al., 2008). Adaboost is a machine learning approach that learns to segment a structure in new images based on a small training set of expertly delineated tracings. As in our hippocampal studies (Morra et al., 2009a, 2009b), we created a small representative training set of 21 MRI scans (7 AD, 7 MCI, and 7 controls) that were expertly hand-labeled according to a validated protocol (Looi et al., 2007). These manual traces were then used to produce automated segmentations of the large (non-overlapping) testing set of 400 MRI scans. Using the image intensities and gradients in the training set scans, and statistical information on the likely position and geometry of the caudate, the algorithm learns a classification rule to designate each voxel as caudate or non-caudate. The automated segmentation incorporates ~13,000 features including intensity, combinations of x, y, and z coordinates, and gray matter, white matter, and cerebrospinal fluid tissue classifications. As is standard in machine learning, images used in the training set were excluded from all analyses presented here.

1.4. Volumetric analysis

For each subject, we determined left and right caudate volumes from the automatically generated segmentations. From these, we calculated the mean volume and a measure of asymmetry (L-R)/[2(L+R)] for each diagnostic group

and tested for group and hemispheric differences in caudate volume.

1.5. Statistical maps

Parametric surface models were created from the 400 automatically generated caudate segmentations, which were then used to create statistical maps associating local volumetric differences with clinical and cognitive scores (Csernansky et al., 2004; Wang et al., 2007). As shown in Figure 1, surface models were created from each subject's automatically generated binary segmentation (Thompson et al., 2004). A central curve was calculated through the longitudinal axis of each model; the radial distance from this medial line to each surface point was used as a highly localized measure of atrophy. This same approach was used in two prior papers based on manual tracings (Butters et al., 2008) and tracings from another automated segmentation algorithm (Becker et al., 2006). We have used the same radial distance mapping approach to map hippocampal and ventricular shape differences (Chou et al., 2009; Morra et al., 2009a, 2009b).

Based on a computed point-wise correspondence of the structure surfaces across subjects, geometric surface averaging was performed across all subjects in each diagnostic group. At each surface point, a correlation was run to compare diagnostic groups and determine the association of diagnosis or clinical scores with atrophy, as measured by differences in radial distance. In all maps shown, we used a multiple regression adjusted for age and sex. In these regressions, adjustments were made for age and sex by including them as covariates in the model. We did not adjust our maps for effects of ApoE genotype because we did not detect any significant effect of ApoE genotype on caudate nucleus shape in either the pooled sample or in any diagnostic group, considered separately. All maps presented in this manuscript refer to one-sided tests in the direction

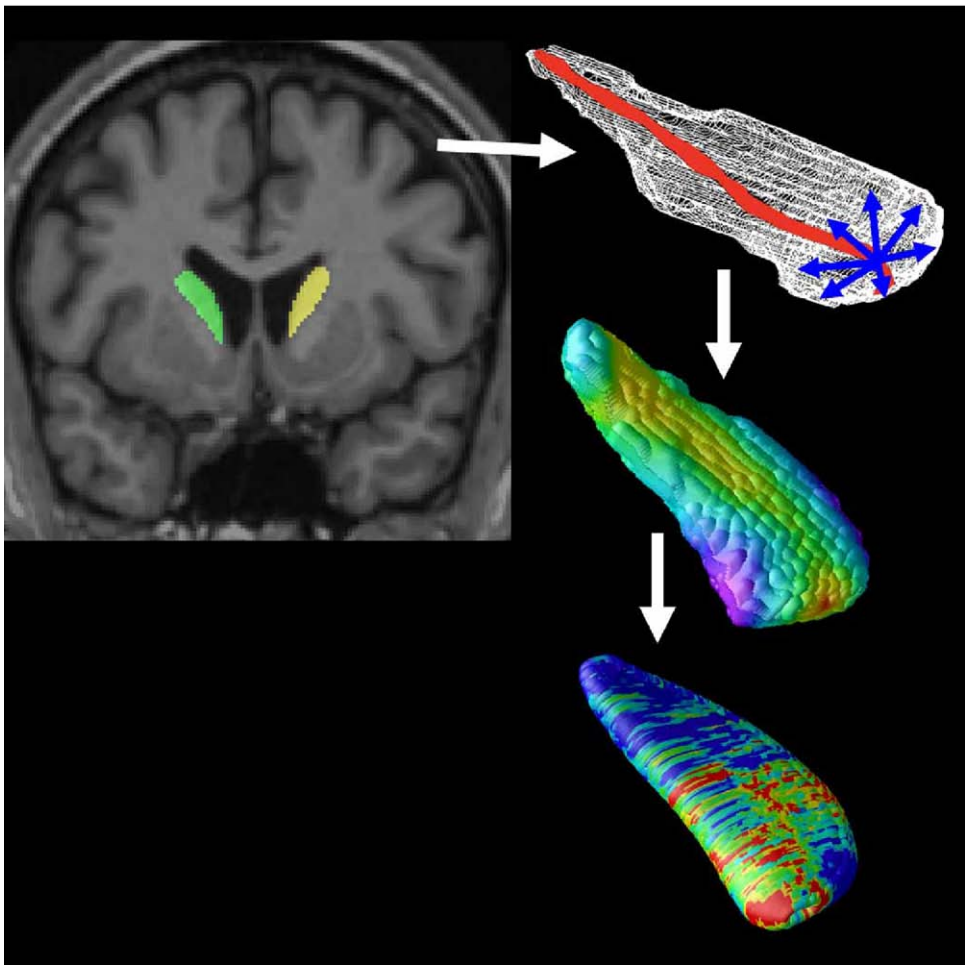

Fig. 1. Mapping caudate atrophy. After image preprocessing, our Adaboost algorithm automatically segments the caudate nucleus bilaterally. A central curve (top right) was calculated through the longitudinal axis of each caudate and the radial distance to each point in a 3D surface mesh was used as a highly localized measure of atrophy (middle right). *p*-values are calculated at each surface point (bottom right) showing the significance of differences in radial distances between diagnostic groups or their associations with clinical scores. These maps visualized the profile of local shape differences or their clinical correlates at a point-wise level.

expected for the values of each clinical measure. For example, a lower MMSE score indicates poorer cognitive performance, which is expected to correlate with caudate nucleus atrophy rather than expansion. For a measure such as MMSE, we used a positive one-sided test, corresponding to the hypothesis that a lower MMSE score (poorer performance) would be associated with volume reductions in the caudate nucleus. Negative one-sided tests were used for measures in which higher scores are expected with greater atrophy in the caudate, such as BMI, in which a lower score is generally considered indicative of better health.

Color coded p-values were mapped onto the average left and right caudate models. To correct for multiple comparisons across surface points, permutation tests provided an overall significance value for each statistical map. Specifically, the suprathreshold area (points with $p < 0.01$) in the map was compared with a null distribution for this same area, estimated from 100,000 random permutations of the covariates (Thompson et al., 2003).

2. Results

2.1. Volumetric results

First, we performed a volumetric analysis of the left and right caudate nucleus to demonstrate volumetric differences between normal aging and AD. As shown in Figure 2, controls had the highest bilateral caudate nucleus volume (mean: 3,777, SD = 1,017 mm^3), followed by MCI (mean: 3,648, SD = 1,062 mm^3; 3.42% lower), with AD subjects showing the lowest volumes (mean: 3,543, SD = 1,302 mm^3; 6.20% lower); this confirmed the expected trend of AD < MCI < controls.

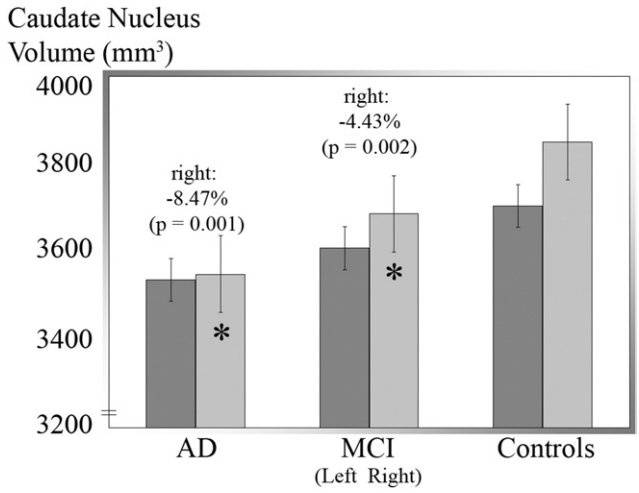

Fig. 2. Volumetric Analysis (N = 400). Mean volumes for left, right, and pooled (left plus right) caudate volumes in the three diagnostic groups; error bars denote standard errors of the mean. Compared with controls caudate volume is lower bilaterally in MCI and still lower in AD. Also, right caudate volume is greater than left in the whole sample ($p < 0.001$), MCI ($p = 0.005$), and controls ($p < 0.001$), but the asymmetry is not detected in AD. Between groups, the right caudate was smaller in AD (−300 mm^3, −8.47%, $p = 0.001$) and MCI (−163 mm^3, −4.43%, $p = 0.002$) than in controls.

Table 2
Effect size comparisons

	Caudate	Hippocampus	Ventricles	N
Cohen's d				
AD vs. Controls	0.378*	0.952*	−0.619*	193
MCI vs. Controls	0.252*	0.473*	−0.205	286
AD vs. MCI	0.148	0.485*	−0.401*	279
r-value				
MMSE	0.175*	0.349*	−0.205*	400
CDR	−0.062	−0.192*	0.143*	400
CDR-SB	−0.209*	−0.365*	0.225*	400
BMI	−0.177*	−0.197*	−0.028	373

Effect sizes for caudate nucleus, hippocampus, and lateral ventricle volumes. Cohen's d statistics are shown to indicate effect sizes for group differences in the pooled (left plus right) volumes of the caudate nucleus, hippocampus (Morra et al., 2009), and lateral ventricles (Chou et al., 2009, 2010). For the continuous variables (MMSE, CDR, CDR-SB, and BMI scores), partial correlations (r-values) are reported from a multiple regression model that controlled for age and sex. *Significant results are highlighted with an asterisk ($p < 0.05$). The ventricular effects have an opposite sign to the others as the ventricles tend to expand in AD while other subcortical structures become smaller. As expected, effect sizes are generally largest for the hippocampus, then the lateral ventricles, then the caudate.

We also calculated Cohen's d statistics to tabulate the effect sizes for group differences in pooled (left plus right hemisphere) volumes for the caudate nucleus, hippocampus, and lateral ventricles in a sample of ADNI subjects for whom all these structures were measured (AD: N = 93; MCI, N = 186; Controls: N = 100). While the values listed here in Table 2 were calculated using our current sample, the Cohen's d statistic allows for direct comparison with other past and future results from samples of different sizes. Previous studies have reported effect sizes around $D = 1.1$ for hippocampal volume comparisons of AD subjects versus controls and $D = 0.9$ for MCI versus controls (Shen et al., 2010), which is a little higher than those in Table 2. The hippocampal and ventricular volumes come from our previous papers that used validated methods in the ADNI baseline data (Chou et al., 2009, 2010; Morra et al., 2009b); the highest achievable N for these comparisons was 400; all three subcortical measures were available for all the subjects whose caudates were analyzed in this study.

For continuous variables (MMSE, CDR, CDR-SB, and BMI scores), we computed a partial correlation from a multiple regression model, controlling for sex and age. The results are shown in Table 2.

A significant rightward asymmetry was found (the right caudate was larger) in controls ($p < 0.001$, asymmetry = 3.86%) and in MCI ($p = 0.01$, asymmetry = 2.13%). This asymmetry was no longer detected in AD. This rightward asymmetry is subtle and not always detected in MRI studies (see Discussion). Between groups, right caudate volume was smaller in AD (−300 mm^3, −8.47%, $p = 0.001$) and MCI (−163 mm^3, −4.43%, $p = 0.002$) versus controls, but

left caudate volume was not significantly different between diagnostic groups.

We compared MCI subjects who converted to AD with those who remained in the MCI diagnostic group at future follow-ups. At both 1- and 2-year time points, we found significantly greater baseline atrophy in the right caudate among MCI-to-AD converters compared with nonconverting MCI subjects ($p = 0.033$, 0.99%; $p = 0.032$, 2.41% respectively for 1- and 2-year follow ups).

Next we examined correlations between caudate nucleus volume and a variety of clinical measures including MMSE, CDR, and Logical Memory scores, with the goal of ranking their strength of association. Poorer MMSE scores at baseline ($p < 0.001$, N = 400) and changes in MMSE scores from baseline at a 1-year follow-up ($p = 0.008$, N = 400) were both significantly correlated with greater right caudate atrophy at baseline, when all diagnostic groups were pooled. Similarly, greater atrophy of the right caudate was also correlated with poorer global CDR scores ($p = 0.013$, N = 400). Both right and left caudate atrophy were associated with worse "sum of boxes" CDR scores ($p = 0.010$, for the left; $p > 0.001$, for the right, N = 400) and with poorer Delayed Logical Memory recall ($p = 0.019$, for the left; $p = 0.005$, for the right, N = 395). Poorer Immediate Logical Memory recall was also correlated with right caudate atrophy ($p = 0.004$, N = 395).

2.2. Group difference maps

Next we created 3D maps showing the significance levels (p-values) for local caudate atrophy in AD and MCI versus controls (Fig. 3), after controlling for age and sex. Separate maps are shown for the left and right caudate nucleus.

Relative to controls, greater atrophy was detected in AD (left: $p = 0.022$, corrected; right: $p = 0.001$, corrected; N = 200) and MCI (left: $p = 0.023$, corrected; right: $p = 0.012$, corrected; N = 300), but not in AD versus MCI (left: $p = 0.383$, corrected; right: $p = 0.083$, corrected; N = 300).

2.3. Baseline association maps of clinical scores

Next we created maps of correlations for the clinical and cognitive scores that showed significant associations in our volumetric analyses (Fig. 3). These map-based results were largely in line with the analysis of overall volumes. Tests where poorer scores were associated with volume reduction

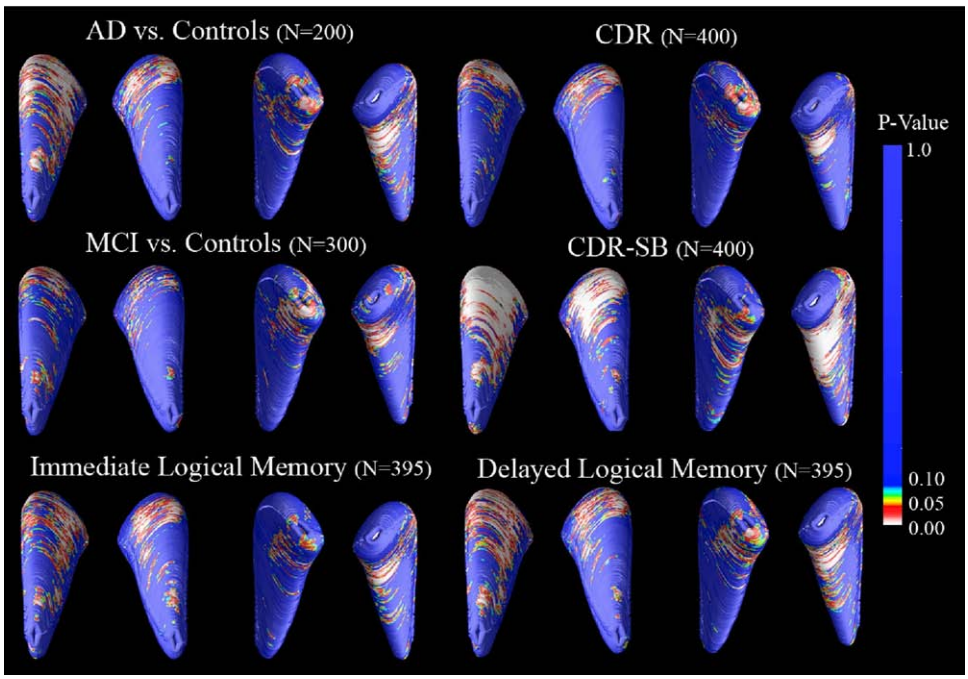

Fig. 3. Caudate atrophy in AD and MCI and baseline clinical scores. 3D maps show significant atrophy in AD and MCI versus controls, with p-values color-coded at each surface point. Red indicates areas where reduced caudate nucleus volume is associated ($p < 0.05$) with the poorer clinical diagnosis; yellow to blue areas are weakly or not associated. The top set of significance maps are labeled to indicate the orientation of the average caudate nucleus shapes, which is consistent in all figures in this paper (anterior caudate head points upward in this figure, posterior tail points downward; the left pair of maps represents the superior surface, while the right pair represents the inferior surface of the caudate nucleus, as seen from below). Permutation tests showed that the group differences between AD and controls (Left: $p = 0.022$, corrected; Right: $p = 0.001$, corrected; N = 200) and between MCI and controls (Left: $p = 0.023$, corrected; Right: $p = 0.012$, corrected; N = 300) are significant bilaterally. Association maps are significant bilaterally for CDR-SB (Left: $p = 0.002$, corrected; Right: $p < 0.001$, corrected; N = 400), CDR (Left: $p = 0.029$; Right: $p = 0.022$, corrected; N = 400), and Delayed Logical Memory (Left: $p = 0.015$, corrected; Right: $p = 0.003$, corrected; N = 395). Associations with Immediate Logical Memory (Right: $p = 0.006$, corrected; N = 395) were detected only for the right caudate nucleus.

bilaterally (CDR-SB, Delayed Logical Memory) also showed a significant bilateral effect in the maps. Bilateral atrophy was associated with greater impairment measured by CDR (right: $p = 0.029$, corrected; N = 400), CDR-SB (left: $p = 0.002$, corrected; right: $p < 0.001$, corrected; N = 400), and in Delayed Logical Memory (left: $p = 0.015$, corrected; right: $p = 0.003$, corrected; N = 395). Poorer Immediate Logical Memory scores (right: $p = 0.006$, corrected; N = 395) were associated with right caudate atrophy only, as in the volumetric analysis.

2.4. Associations with clinical scores 1 year later

To investigate the predictive value of our caudate maps, we associated baseline caudate anatomy with change in MMSE and CDR scores between baseline and 1-year later (Fig. 4). As suggested by our volumetric analysis, right caudate atrophy was highly associated with baseline MMSE scores in the full sample ($p = 0.001$, corrected, N = 400) and with 1-year change in MMSE scores in the MCI group (left: $p = 0.037$; right: $p = 0.001$, corrected, N = 200). Associations of 1-year change in MMSE scores were not significant for either AD or control groups; however we cannot rule out that these associations may be found over a longer time interval, greater than 1 year. Although associations with baseline CDR and CDR-SB were significant (Fig. 3), associations with 1-year change in these scores were not significant after multiple comparisons correction.

2.5. Greater atrophy in MCI-to-AD converters

To investigate the predictive value of local caudate nucleus atrophy, we created significance maps showing the association between caudate nucleus atrophy at baseline among MCI subjects who converted to AD (converters) versus those who remained classified as MCI (nonconverters) 1 or 2 years after their baseline scan (Fig. 4). Right caudate volumes were lower at baseline for those who had converted to AD 1 year later ($p = 0.008$, corrected; N = 174) or 2 years later ($p = 0.035$, corrected; N = 50).

2.6. Associations with CSF biomarkers

Right but not left caudate atrophy (Fig. 4) was associated with CSF tau concentrations (right: $p = 0.021$, corrected; N = 216, AD: N = 59, MCI: N = 102, controls: N = 55). Additionally, correlation analyses within each diagnostic group revealed that both left and right caudate nucleus volume are correlated with CSF tau concentration in the AD subjects (left: $r = 0.239$, $p = 0.034$; right: $r = 0.370$, $p = 0.002$; N = 59) but not in the MCI or control groups ($r < 0.1$, $p > 0.05$). Correlation maps of associations between radial atrophy and, concentrations of-tau and amyloid beta and ratio measures of tau/amyloid beta and p-tau/amyloid beta were also assessed, but these correlation maps did not pass permutation-based corrections for multiple comparisons. It would be interesting to see if the CSF associations

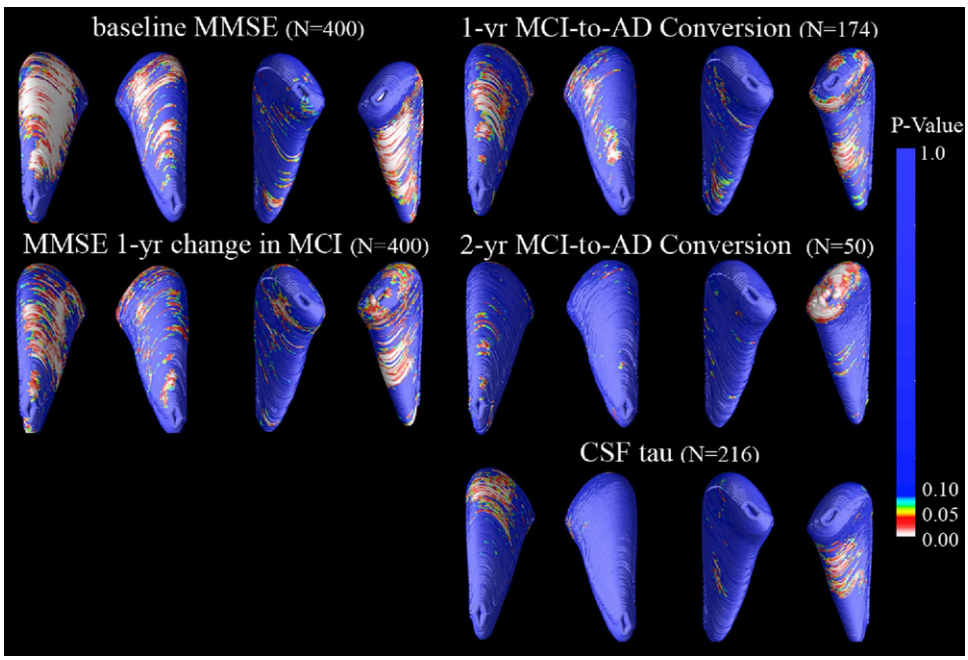

Fig. 4. Maps of associations with MMSE scores at baseline and 1 year later, MCI-to-AD conversion, and CSF concentrations of tau. 3D maps show areas of significant associations between local volumetric atrophy in the caudate and MMSE scores at baseline and after a 1-year follow-up interval, with *p*-values color-coded at each surface voxel. Associations were only detected in the right caudate nucleus for baseline MMSE scores (Right: $p = 0.001$, corrected). Change in MMSE score after a 1-year follow-up interval was bilaterally associated in the MCI group only (Left: $p = 0.037$; Right: $p = 0.001$, corrected; N = 200). Those who converted from MCI to AD after 1 year and 2 years showed greater right caudate atrophy at baseline than those who did not (1-year conversation: $p = 0.008$, corrected; 2-year conversation: $p = 0.035$, corrected). For CSF levels of tau at time of scanning, associations were significant for the right but not left caudate for the tau CSF biomarker ($p = 0.036$, corrected, N = 216).

hold up on a group-by-group level since other ADNI laboratories have found that tau concentrations increase progressively from controls to MCI to AD (Shaw et al., 2009); however, our current study did not have enough power to detect associations within each diagnostic group separately (as sample sizes with available CSF data are only around 50 subjects per group).

2.7. Associations with additional clinical variables

Significant associations were also found in maps for age (left: $p = 0.039$, corrected; right: $p = 0.001$, corrected; N = 400) and sex (left: $p < 0.001$, corrected; right, $p < 0.001$, corrected; N = 400), with smaller caudates in men than women (Fig. 5), and smaller caudates in older than younger people. Examining emotional domains, we also found significant associations between more impaired Geriatric Depression scores and atrophy of the right caudate nucleus (right, $p = 0.004$, corrected; N = 395). In our analysis of motor function, the presence of abnormal gait was significantly associated with volume reductions in the right caudate nucleus (right, $p = 0.027$, corrected; N = 395); however, maps of associations between atrophy and the presence of tremor in our subjects were not significant.

In line with recent tensor-based morphometry findings that higher BMI is associated with brain atrophy in the elderly, caudate atrophy was found here to be associated with higher BMI in our full sample (left: $p < 0.001$, corrected; right: $p = 0.002$, corrected; N = 393) and in the AD subjects considered separately (left: $p = 0.015$, corrected; right: $p = 0.005$, corrected; N = 96). Within-group associations for MCI and control groups were not significant.

Maps of associations with the FTO genotype, which is linked to higher BMI and with brain atrophy in elderly people (Ho et al., 2010b), were not significant after permutation-based correction for multiple comparisons. Maps associating local caudate nucleus volume with APOE genotype were also not significant after multiple comparisons correction.

2.8. Ranking effect sizes for different covariates

Results from our permutation-corrected significance maps agreed with our volumetric results for each statistical test performed, while providing a more detailed spatial profile of regional atrophy. Adjusting for age and sex in these regressions did not affect these associations materially, but slightly boosted effect sizes (data not shown). To rank the covariates in terms of their effect sizes, we ran the maps with randomly selected samples of 400, 300, 200, 96, and 50 subjects, to find the reduced sample size needed to detect each effect, using the results of the permutation test to correct for multiple comparisons. A sample size of 96 was chosen instead of 100 to allow inclusion of the associations for BMI in the AD group only, which consisted of 96 subjects. Only 50 subjects were needed to detect the BMI

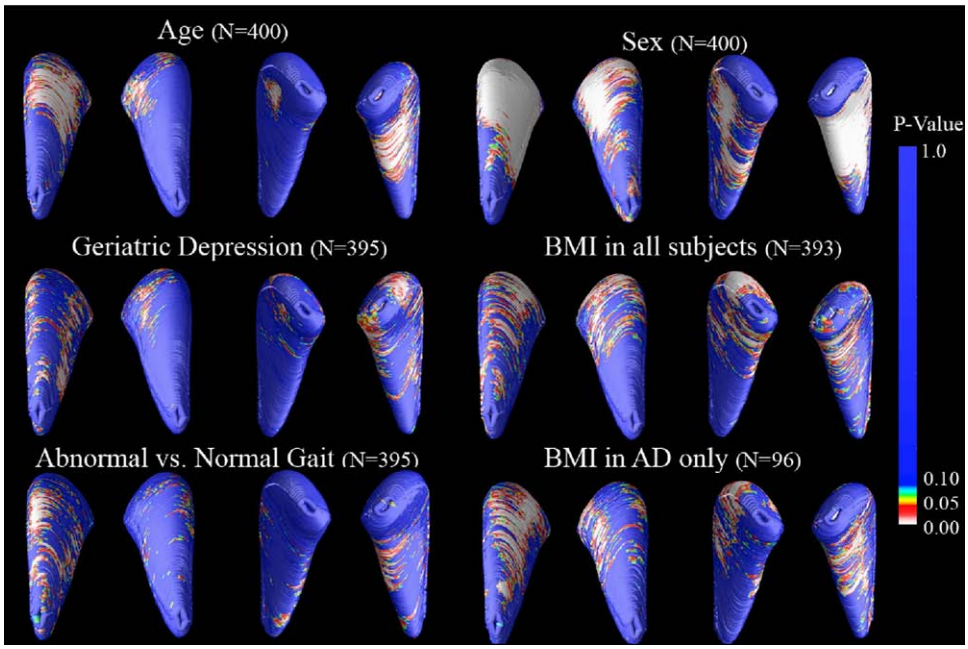

Fig. 5. Associations between caudate atrophy and additional clinical variables. 3D maps show areas of significant associations between local volumetric atrophy in the caudate nucleus and several additional clinical variables. Significant associations were found for age (Left: $p = 0.039$, corrected; Right: $p = 0.001$, corrected; N = 400) and sex (Left: $p < 0.001$, corrected; Right, $p < 0.001$, corrected; N = 400), with smaller caudates in men than women (8.58% bilaterally). Significant associations were also found in the right caudate nucleus for Geriatric Depression scores (Right, $p = 0.004$, corrected; N = 395) and for abnormal versus normal gait (Right, $p = 0.027$, corrected; N = 395). BMI scores at time of scanning for all subjects and for AD subjects only. For BMI, significant associations were found in all subjects (Left: $p < 0.001$, corrected; Right: $p = 0.0021$, corrected; N = 393) and in AD subjects only (Left: $p = 0.015$, corrected; Right: $p = 0.005$, corrected; N = 96).

effect in the AD group (left: $p = 0.024$, corrected; right: $p = 0.022$, corrected; N = 50). In a representative sample, 96 subjects were needed to detect effects of BMI (left: $p = 0.0031$, corrected; right: $p = 0.006$, corrected; N = 96), baseline CDR-SB scores (right: $p = 0.037$, corrected; N = 96), and the comparison of AD versus controls (right: $p = 0.038$, corrected; N = 96). Effects of baseline MMSE scores were first detected at 200 subjects (right: $p < 0.001$, corrected; N = 200).

3. Discussion

This study demonstrates that 3D maps of the caudate nucleus localize statistically significant regions of volume reduction associated with (1) diagnosis and clinical and cognitive scores, (2) future decline in MMSE scores at 1-year follow-up in the MCI group, (3) conversion from MCI to AD 1 and 2 years after scanning, (4) baseline CSF concentrations of tau, and (5) additional clinical measures including BMI, Geriatric Depression, and abnormal gait. The variables most strongly associated with caudate atrophy were found using a reduced N analysis, namely (in this rank order): BMI in the AD group only, BMI in all subjects, CDR-SB scores, group difference between AD and controls, and MMSE scores at baseline. It is interesting to note that cardiovascular measures and CDR-SB scores, which rely on interviews from both patients and informants, were more powerfully associated with caudate volume reductions in our 3D maps, compared with seemingly more direct measures of AD such as the MMSE. Although some of these measures are highly correlated and may be viewed as redundant, we felt that it was important to take a broad approach initially, in analyzing multiple measures of cognition and health. This has practical significance for the planning of clinical trials, which currently use a variety of similar tests, and also allows direct comparison with other studies that each may use different tests.

Caudate atrophy was generally localized to anterior regions and was specific to the right caudate for several variables assessed. Caudate atrophy in AD (vs. controls) was 2-fold greater on the right than the left. Further study is needed to confirm the greater vulnerability of the right caudate. The natural asymmetry of the caudate (right 3.9% larger than the left in controls) has been found in many but not all studies, and large samples are needed to detect it. Most literature supports a rightward (right larger than left) asymmetry in caudate nucleus volume (Giedd et al., 1996; Ifthikharuddin et al., 2000; Larisch et al., 1998; Peterson et al., 1993; Yamashita et al., 2009), but some studies have found leftward, gender-specific, or no asymmetry (Gunning-Dixon et al., 1998; Szabo et al., 2003). Based on our current findings and previous literature, it may be possible to view asymmetry findings in brain structures as a general indicator of poor brain health. Psychosis has been linked to genes involved in the development of cerebral asymmetry (Laval et al., 2004) and differences in laterality have been found to covary with, or predict, individual differences in susceptibility to stress pathology and drug sensitivity (Carlson and Glick, 1989). The presence or change in direction of asymmetry has been reported (but not always consistently) in disorders ranging from schizophrenia (Crow et al., 1996), ADHD (Castellanos et al., 1996), bipolar (Javadapour et al., 2010) affective mood disorders (Baumann et al., 1999), and Tourette syndrome (Klieger et al., 1997).

There may be some skepticism that the caudate is a natural place to look for clinical correlations in AD, but it may give additional power to detect associations with cognition and future decline, if used along with structures that are more commonly studied. For example, it is widely accepted that the hippocampus − target of most published AD morphometry studies − is challenging to segment reliably, with a notorious 2-fold difference in mean hippocampal volumes across studies and imaging centers (Frisoni et al., 2010). Prior studies using the same radial distance mapping technique with other brain structures in ADNI have also found correlations between hippocampal atrophy (Morra et al., 2009), ventricular expansion (Chou et al., 2009, 2010) and clinical variables such as MMSE, CDR, and CDR-SB scores. There are also differences between diagnostic groups in the volumes of all of these structures (AD vs. controls, MCI vs. controls). As shown in Table 2, and as might be expected, hippocampal volumes gave the greatest effect sizes for detecting group differences within ranges supported by previous studies (Shen et al., 2010), and for detecting correlations with clinical scores. Effect sizes for lateral ventricle volumes also gave relatively strong effect sizes, although they were generally weaker than the hippocampal effect sizes. Caudate effect sizes, while significant, were generally lower than those for the ventricles and hippocampus. As one exception to this rank order, the caudate gave marginally better effect sizes than ventricular volume for distinguishing MCI from controls. Even so, we did not perform statistical tests for differences in effect sizes across structures, as a stringent multiple comparisons correction would be needed. Despite these generally weaker effects, the current study of the caudate also found significant associations between reduced volume and MCI-to-AD conversion, and with decline in MMSE scores after a 1-year follow-up in the MCI group, whereas these associations were not detectable in studies of ventricular expansion (Chou et al., 2009) or hippocampal atrophy (Morra et al., 2009a, 2009b), using the same ADNI subject pool (with 240 and 490 subjects, respectively); the latter study also used the same Adaboost machine learning algorithm, applied to hippocampal segmentation. This is an intriguing finding, suggesting caudate volume at baseline may predict later clinical changes relatively well, perhaps because caudate atrophy is only severe when the disease is rapidly progressing.

The caudate has previously been implicated in AD through multiple lines of evidence including histological findings of tau and amyloid accumulations (Braak and Braak, 1990). Volumetric studies find reductions in caudate nucleus volume with normal aging (Jernigan et al., 2001; Krishnan et al., 1990; Raz et al., 2003), in AD versus controls (Rombouts et al., 2000), and in many other neurological, psychiatric and neurodevelopmental conditions including autism (Turner et al., 2006), fragile X syndrome (Gothelf et al., 2008), elderly depression (Butters et al., 2008), and HIV (Becker et al., 2006). Caudate lesions can produce deficits in executive control and cognitive processing speed (Rubin, 1999). Interestingly, a recent study also found subcortical brain volume reductions, encompassing the caudate nucleus, in elderly individuals with a higher BMI (Raji et al., 2009).

The anterior caudate head is the most closely involved in traditionally studied cognitive processes and integrates major inputs from the dorsolateral and orbitofrontal cortices, involved in attention and planning (Cummings, 1995). Disturbances in the hemispheric asymmetry of the caudate head are associated with ADHD and schizophrenia (Ballmaier et al., 2008; Blanton et al., 1999; Hynd et al., 1993). One study found significant caudate volume reductions in depressed elderly and created 3D maps using the same technique here, except on manually derived segmentations; however, their maps were not significant after permutation-based correction for multiple comparisons (Butters et al., 2008).

Beyond the caudate and the medial temporal lobes, additional basal ganglia and subcortical gray matter structures are implicated in AD and age-related neurodegeneration. Putamen and thalamus volumes are reduced in AD, and volume decreases correlate with cognitive deficits (de Jong et al., 2008). Putamen volumes are reduced in frontotemporal lobe degeneration, but not in AD (Looi et al., 2009). A recent study of individuals with Down's syndrome—a group at heightened risk for developing AD—found significant associations in those who developed AD and bilateral volume reductions in the hippocampus, caudate, right amygdala, and right putamen (Beacher et al., 2009). *In vivo* imaging with [11C]-PIB PET, which is thought to map the profile of amyloid deposition in the living brain, has correlated increased amyloid signal with increased atrophy in the hippocampus and amygdala (Frisoni et al., 2009). In addition, post-mortem studies have localized diffuse amyloid plaques in the caudate nucleus in AD (Ikonomovic et al., 2008).

In a PET study of dopamine D1 and D2 receptors, researchers found a 14% reduction in mean signal for D1 receptors for the caudate and putamen in AD, but no difference in D2 receptor signal (Kemppainen et al., 2000). The basal ganglia also have the highest iron content of any brain region, which is interesting because AD patients exhibit disrupted iron metabolism that may relate to oxidative damage and higher iron levels are found in the caudate and putamen in AD patients compared with controls (Bartzokis et al., 2000).

A common limiting factor in neuroimaging studies of AD is the labor-intensive task of manually segmenting subcortical structures on large MRI datasets, requiring long-term effort from expertly trained neuroanatomists. Fortunately, automated methods now exist to efficiently segment many subcortical structures including the hippocampus and caudate nucleus (Fischl et al., 2002; Powell et al., 2008; Yushkevich et al., 2006). Here we used an automated method based on adaptive boosting, that we recently developed and validated (Morra et al., 2008). Using this method, we efficiently created caudate nucleus segmentations in 400 ADNI brain MRI scans. The resulting 3D maps had enough statistical power to detect local volume differences associated with a wide variety of clinical variables in AD. Our maps detected associations between caudate atrophy and CSF levels of tau, which have not always been associated with other MRI-derived measures in the same cohort (Chou et al., 2009). CSF levels of tau are significantly associated with higher rates of temporal lobe atrophy (Leow et al., 2009), but only showed a trend level of association with the rate of hippocampal atrophy (Schuff et al., 2009). In prior amyloid PET studies, amyloid deposition has been noted in the caudate nucleus (Ikonomovic et al., 2008). Here we did not detect a relation between the level of CSF amyloid and the volume of the caudate. In the future, a direct PET-based brain measure of amyloid in the caudate may correlate better with atrophy than CSF-based measures of amyloid burden. Limited sample sizes may have also made it hard to detect an association; even so, the sample was large enough for tau levels to be reliably correlated with maps of atrophy for the right caudate nucleus in the pooled sample and bilaterally for the volumetric summaries in the AD group.

A possible confounding factor in some voxel-based morphometric studies of the caudate is the potential for misregistration of anatomy across subjects along the ventricles, especially in elderly subjects with substantial brain degeneration. Because the caudate nucleus is a gray matter structure that lies just below the boundary of the lateral ventricles, some volumetric studies may be confounded by poor or biased registration along the lateral ventricular surface. This effect is unlikely in the current study as our measures of radial atrophy are intrinsic, meaning they are independent of whether the structure is translated in space. They are computed from a centerline traced down the center of the structure, and do not rely on the correct registration of images across subjects, as some voxel-based averaging methods do.

The etiology of caudate atrophy in AD and MCI is of interest. One probable explanation is that we are assessing neuronal atrophy, secondary to the accumulation of amyloid plaque pathology and tau neurofibrillary tangles (Braak and Braak, 1990). The caudate may also experience a loss of afferent projections from other brain regions. As such, a

limitation of the study is that the associations between caudate atrophy and cognition may in reality be mediated by atrophy occurring in other brain structures, such as the hippocampus. The intent in this study was to identify correlates of caudate atrophy, but it is likely that the more immediate causes of the clinical differences may be atrophy (or functional compromise) of structures elsewhere in the brain, not necessarily those assessed here.

A further limitation of the current study is that the available sample sizes made it necessary to use a pooled sample including both patients and controls for several analyses. Pooling subjects allowed us to achieve sufficient statistical power to detect important findings, but there is also a risk of recovering group sampling effects due to the differences between diagnostic groups in cognitive measures. Where sample sizes and effect sizes were sufficient for within-group correlations to be detected, we did find statistically significant associations in 1-year change in MMSE score in the MCI group and with BMI in the AD group. It is possible that there are additional within-group associations for these and other measures that did not survive the sample size reduction. It can also be argued that AD, MCI, and healthy elderly controls represent stages on a continuum − in that case, binning the subjects into diagnostic groups could limit the power of correlations found across the spectrum and lead to false negative results.

In this study, we report correlations between atrophy and cognitive or CSF-derived measures in a pooled ADNI sample (combining patients with AD, MCI and controls), while also reporting several within-groups correlations split by diagnosis ("disaggregated" analyses of AD subjects only, for example). Both types of analysis are complementary and each has its own limitations. When analyzing a mixed cohort of subjects, our goal is to determine (1) the cognitive correlates of atrophy in the entire sample, and (2) whether the chosen biomarker of disease burden is linked with decline across the full spectrum of controls, MCI, and AD subjects. As the whole cohort is arguably a continuum, it is vital to look beyond diagnostic categories to analyze relationships between atrophy and particular measures of cognitive function. A within-group analysis of AD subjects only, for example, may not be able to detect these correlations due to a "restricted range" effect seen when looking at a limited range of differences in brain structure and cognitive performance. By running split analyses only, many important correlations may be missed. For instance, brain atrophy correlates well with CSF-derived measures of tau pathology across the continuum from healthy aging to MCI and to AD. However, it is possible that no correlation will be detected if we subselect a group such as MCI, with a very narrow range of disease burden. Furthermore, it is a fallacy to preselect groups that are defined partly on cognitive measures, and then later test for correlations with these same cognitive scales. If the selection criterion for the group correlates with the variable of interest, we will find many false negatives due to the truncated range, making the results uninterpretable.

Pooled analyses have limitations to consider, as well. When cognitive measures are correlated with diagnosis, correlations in a pooled cohort may show similar patterns to those found when directly comparing AD subjects with controls. Another consideration when using pooled cohorts such as ADNI, is that correlations may be influenced by the proportion of subjects in each diagnostic group. By design, ADNI oversampled subjects with cognitive decline, including a 1:2:1 ratio of AD: MCI: controls. Correlations in this particular sample may not be detected to the same degree in other population studies with different proportions of subjects or within each diagnostic group. For these reasons, we chose to use a combination of both pooled and split analyses, which have complementary value in understanding the cognitive and pathological correlates of atrophy.

Because it can be difficult to tease apart contributions of each individual brain region in a disease such as AD, studying effects of the disease on specific anatomical structures, beyond those most commonly targeted, may help to piece together relevant circuitry affected by AD pathology. Multiple AD biomarkers can be used in a mutually reinforcing way to identify subjects most likely to decline to AD in a sample (Kohannim et al., 2010), with caudate atrophy may inform the classification of AD, MCI or the prediction of future decline. Another line of work involves genome-wide association studies of caudate volume in large subject cohorts such as ADNI. This information will improve our understanding of the mechanistic processes involved in brain aging and AD.

Disclosure statement

The authors have no potential financial or personal conflicts of interest including relationships with other people or organizations within 3 years of beginning the work submitted that could inappropriately influence this work.

Acknowledgements

Data collection and sharing for this project was funded by the Alzheimer's Disease Neuroimaging Initiative (ADNI) (National Institutes of Health, Grant U01 AG024904). ADNI is funded by the National Institute on Aging, the National Institute of Biomedical Imaging and Bioengineering, and through generous contributions from the following: Abbott, AstraZeneca AB, Bayer Schering Pharma AG, Bristol-Myers Squibb, Eisai Global Clinical Development, Elan Corporation, Genentech, GE Healthcare, GlaxoSmithKline, Innogenetics, Johnson and Johnson, Eli Lilly, and Co., Medpace, Inc., Merck and Co., Inc., Novartis AG, Pfizer, Inc, F. Hoffman-La Roche, Schering-Plough, Synarc, Inc., and Wyeth, as well as nonprofit partners the Alzheimer's Association and Alzheimer's Drug Discovery Foundation, with participation from the US Food

and Drug Administration. Private sector contributions to ADNI are facilitated by the Foundation for the National Institutes of Health (www.fnih.org/). The grantee organization is the Northern California Institute for Research and Education, and the study is coordinated by the Alzheimer's Disease Cooperative Study at the University of California, San Diego. ADNI data are disseminated by the Laboratory of Neuro Imaging at the University of California, Los Angeles. This research was also supported by NIH Grants P30 AG010129, K01 AG030514, and the Dana Foundation.

References

Ballmaier, M., Schlagenhauf, F., Toga, A.W., Gallinat, J., Koslowski, M., Zoli, M., Hojatkashani, C., Narr, K.L., Heinz, A., 2008. Regional patterns and clinical correlates of basal ganglia morphology in non-medicated schizophrenia. Schizophr Res 106, 140–147.

Bartzokis, G., Sultzer, D., Cummings, J., Holt, L.E., Hance, D.B., Henderson, V.W., Mintz, J., 2000. In vivo evaluation of brain iron in Alzheimer disease using magnetic resonance imaging. Arch Gen Psychiatry 57, 47–53.

Baumann, B., Danos, P., Krell, D., Diekmann, S., Leschinger, A., Stauch, R., Wurthmann, C., Berstein, H.G., Bogerts, B., 1999. Reduced volume of limbic system-affiliated basal ganglia in mood disorders: Preliminary data from a postmortem study. J Neuropsychiatr Clin Neurosci 11, 71–78.

Beacher, F., Daly, E., Simmons, A., Prasher, V., Morris, R., Robinson, C., Lovestone, S., Murphy, K., Murphy, D.G., 2009. Alzheimer's disease and Down's syndrome, an in vivo MRI study. Psychol Med 39, 675–684.

Becker, J.T., Davis, S.W., Hayashi, K.M., Meltzer, C.C., Toga, A.W., Lopez, O.L., Thompson, P.M., 2006. Three-dimensional patterns of hippocampal atrophy in mild cognitive impairment. Arch Neurol 63, 97–101.

Blanton, R.E., Levitt, J., Thompson, P.M., Badrtalei, S., Capetillo-Cunliffe, L., Toga, A.W., 1999. Average 3-dimensional caudate surface representations in a juvenile-onset schizophrenia and normal pediatric population. NeuroImage Abstracts, 9, s621.

Braak, H., Braak, E., 1990. Alzheimer's disease, striatal amyloid deposits and neurofibrillary changes. J Neuropathol Exp Neurol 49, 215–224.

Butters, M.A., Aizenstein, H.J., Hayashi, K.M., Meltzer, C.C., Seaman, J., Reynolds, C.F., Toga, A.W., Thompson, P.M., Becker, J.T., IMAGe Research Group, 2008. Three-dimensional mapping of the caudate nucleus in late-life depression. Am J Geriatr Psychiatry 17, 4–12.

Carlson, J.N., Glick, S.D., 1989. Cerebral lateralization as a source of interindividual differences in behavior. Cell Mol Life Sci 45, 788–798.

Castellanos, F.X., Giedd, J.N., Marsh, W.L., Hamburger, S.D., Vaituzis, A.C., Dicktein, D.P., Sarfatti, S.E., Vauss, Y.C., Snell, J.W., Lange, N., Kaysen, D., Krain, A.L., Ritchie, G.F., Rajapakse, J.C., Rapoport, J.L., 1996. Quantitative brain magnetic resonance imaging in attention-deficit hyperactivity disorder. Arch Gen Psychiatry 35, 607–616.

Chou, Y.Y., Lepore, N., Avedissian, C., Madsen, S.K., Parikshak, N., Hua, X., Shaw, L.M., Trojanowski, J.Q., Weiner, M.W., Toga, A.W., Thompson, P.M., the Alzheimer's Disease Neuroimaging Initiative, 2009. Mapping correlations between ventricular expansion and CSF amyloid and tau biomarkers in 240 subjects with Alzheimer's disease, mild cognitive impairment and elderly controls. Neuroimage 46(2), 394–410.

Chou, Y.Y., Lepore, N., Saharan, Madsen, S.K., Hua. X Jack, C.J. Jr., Shaw, L., Trojanowski, J.Q., Weiner, M.W., Toga, A.W., Thomspon, P.M., the Alzheimer's Disease Neuroimaging Initiative. 2010. Ranking the Clinical and Pathological Correlates of Ventricular Expansion Mapped in 804 Alzheimer's Disease, MCI, and Normal Elderly Subjects. Neurobiology of Aging [in press].

Cockrell, J.R., Folstein, M.F., 1988. Mini-Mental State Examination (MMSE). Psychopharmacol Bull 24, 689–692.

Collins, D.L., Neelin, P., Peters, T.M., Evans, A.C., 1994. Automatic 3D intersubject registration of MR volumetric data in standardized Talairach space. J Comput Assist Tomogr 18, 192–205.

Crow, T.J., Done, D.J., Sacker, A., 1996. Cerebral lateralization is delayed in children who later develop schizophrenia. Schizophr Res 22, 181–185.

Csernansky, J.G., Wang, L., Joshi, S.C., Ratnanather, J.T., Miller, M.I., 2004. Computational anatomy and neuropsychiatric disease: Probabilistic assessment of variation and statistical inference of group difference, hemispheric asymmetry, and time-dependent change. Neuroimage 23(suppl 1), S56–S68.

Cummings, J.L., 1995. Anatomic and behavioural aspects of frontal-subcortical circuits. Ann NY Acad Sci 769, 1–14.

de Jong, L.W., van der Hiele, K., Veer, I.M., Houwing, J.J., Westendorp, R.G., Bollen, E.L., de Bruin, P.W., Middelkoop, H.A., van Buchem, M.A., van der Grond, J., 2008. Strongly reduced volumes of putamen and thalamus in Alzheimer's disease, an MRI study. Brain 131, 3277–3285.

Fischl, B., Salat, D.H., Busa, E., Albert, M., Dieterich, M., Haselgrove, C., van der Kouwe, A., Killiany, R., Kennedy, D., Klaveness, S., Montillo, A., Makris, N., Rosen, B., Dale, A.M., 2002. Whole brain segmentation, Automated labeling of neuroanatomical structures in the human brain. Neuron 33, 341–355.

Frisoni, G.B., Lorenzi, M., Caroli, A., Kemppainen, N., Någren, K., Rinne, J.O., 2009. In vivo mapping of amyloid toxicity in Alzheimer disease. Neurology 72, 1504–1511.

Giedd, J.N., Snell, J.W., Lange, N., Rajapakse, J.C., Casey, B.J., Kozuch, P.L., Vaituzis, A.C., Vauss, Y.C., Hamburger, S.D., Kaysen, D., Rapoport, J.L., 1996. Quantitative magnetic resonance imaging of human brain development, ages 4–18. Cereb Cortex 6, 551–560.

Good, C.D., Scahill, R.I., Fox, N.C., Ashburner, J., Friston, K.J., Chan, D., Crum, W.R., Rossor, M.N., Frackowiak, R.S.J., 2002. Automatic Differentiation of anatomical patterns in the human brain: validation with studies of degenerative dementias. Neuroimage 17, 29–46.

Gothelf, D., Furfaro, J.A., Eckert, M.A., Hall, S.S., O'Hara, R., Erba, H.W., Ringel, J., Hayashi, K.M., Patnaik, S., Golianu, B., Kraemer, H.C., Thompson, P.M., Piven, J., Reiss, A.L., 2008. Neuroanatomy of Fragile X Syndrome is Associated with Aberrant Behavior and FMRP. Ann Neurol 63, 40–51.

Gunning-Dixon, F.M., Head, D., McQuain, J., Acker, J.D., Raz, N., 1998. Differential aging of the human striatum, a prospective MR imaging study. AJNR Am J Neuroradiol 19, 1501–1507.

Gunter, J., Bernstein, M., Borowski, B., Felmlee, J., Blezek, D., Mallozzi, R., 2006. Validation testing of the MRI calibration phantom for the Alzheimer's Disease Neuroimaging Initiative study. ISMRM 14th Scientific Meeting and Exhibition, Seattle, WA.

Helzner, E.P., Luchsinger, J.A., Scarmeas, N., Cosentino, S., Brickman, A.M., Glymour, M.M., Stern, Y., 2009. Contribution of vascular risk factors to the progression in Alzheimer Disease. Arch Neurol 66, 343–348.

Ho, A.J., Raji, C.A., Becker, J.T., Lopez, O.L., Kuller, L.W., Hua, X., Lee, S., Hibar, D., Dinov, I.D., Stein, J.L., Jack, C.R., Weiner, M.W., Toga, A.W., Thompson, P.M., 2010a. Obesity and Brain Structure in 700 AD and MCI Patients. Neurobiology of Aging, Special Issue on ADNI [in press].

Ho, A.J., Stein, J.L., Hua, X., Lee, S., Hibar, D.P., Leow, A.D., Dinov, I.D., Toga, A.W., Saykin, A.J., Shen, L., Foroud, T., Pankratz, N., Huentelman, M.J., Craig, D.W., Gerber, J.D., Allen, A.N., Corneveaux, J.J., Stephan, D.A., DeCarli, C.S., Dechairo, B.M., Potkin, S.G., Jack, C.R. Jr., Weiner, M.W., Raji, C.A., Lopez, O.L., Becker, J.T., Carmichael, O.T., Thompson, P.M., the Alzheimer's Disease Neuroimaging Initiative., 2010b. A commonly carried allele of the obesity-related

FTO gene is associated with reduced brain volume in the healthy elderly. PNAS. Published online April 9, 2010.

Hynd, G.W., Hern, K.L., Novey, E.S., Eliopulos, D., Marshall, R., Gonzalez, J.J., Voeller, K.K., 1993. Attention deficit-hyperactivity disorder and asymmetry of the caudate nucleus. J Child Neurol 8, 339–347.

Ifthikharuddin, S.F., Shrier, D.A., Numaguchi, Y., Tang, X., Ning, R., Shibata, D.K., Kurlan, R., 2000. MR volumetric analysis of the human basal ganglia, normative data. Acad Radiol 7, 627–634.

Ikonomovic, M.D., Klunk, W.E., Abrahamson, E.E., Mathis, C.A., Price, J.C., Tsopelas, N.D., Lopresti, B.J., Ziolko, S., Bi, W., Paljug, W.R., Debnath, M.L., Hope, C.E., Isanski, B.A., Hamilton, R.L., deKosky, S.T., 2008. Post-mortem correlates of *in vivo* PiB-PET amyloid imaging in a typical case of Alzheimer's disease. Brain 131, 1630–1645.

Jack, C.R., Bernstein, M.A., Fox, N.C., Thompson, P., Alexander, G., Harvey, D., Borowski, B., Britson, P.J., Whitwell, J., Ward, C., Dale, A.M., Felmlee, J.P., Gunter, J.L., Hill, D.L., Killiany, R., Schuff, N., Fox-Bosetti, S., Lin, C., Studholme, C., deCarli, C.S., Krueger, G., Ward, H.A., Metzger, G.J., Scott, K.T., Mallozzi, R., Blezek, D., Levy, J., Debbins, J.P., Fleisher, A.S., Albert, M., Green, R., Bartzokis, G., Glover, G., Mugler, J., Weiner, M.W., 2008. The Alzheimer's Disease Neuroimaging Initiative (ADNI), MRI methods. J Magn Reson Imaging 27, 685–691.

Javadapour, A., Malhim, G.S., Ivandovski, B., Chen, X., Wen, W., Sachdev, P., 2010. Hippocampal volumes in adults with bipolar disorder. J Neuropsychiatr Clin Neurosci 22, 55–62.

Jernigan, T.L., Archibald, S.L., Fennema-Notestine, C., Gamst, A.C., Stout, J.C., Bonner, J., Hesselink, J.R., 2001. Effects of age on tissues and regions of the cerebrum and cerebellum. Neurobiol Aging 22, 581–594.

Jorm, A.F., Korten, A.E., Henderson, A.S., 1987. The prevalence of dementia, a quantitative integration of the literature. Acta Pscyhiatr Scan 765, 465–479.

Jovicich, J., Czanner, S., Greve, D., Haley, E., van der Kouwe, A., Gollub, R., Kennedy, D., Schmitt, F., Brown, G., Macfall, J., Fischl, B., Dale, A., 2006. Reliability in multi-site structural MRI studies, Effects of gradient non-linearity correction on phantom and human data. Neuroimage 30, 436–443.

Kemppainen, N., Ruottinen, H., Nâgren, K., Rinne, J.O., 2000. PET shows that striatal dopamine D1 and D2 receptors are differentially affected in AD. Neurology 55, 205–209.

Klieger, P.S., Fett, K.A., Dimitsopulos, T., Kurlan, R., 1997. Asymmetry of basal ganglia perfusion in Tourette syndrome shown by technetium-99m-HMPAO SPECT. J Nucl Med 38, 188–191.

Knowlton, B.J., Mangels, J.A., Squire, L.R., 1996. A Neostriatal Habit Learning System in Humans. Science 273, 1399–1402.

Kohannim, O., Hua, X., Hibar, D.P., Lee, S., Chou, Y.Y., Toga, A.W., Jack, C.R. Jr., Weiner, M.W., Thompson, P.M., the Alzheimer's Disease Neuroimaging Initiative, 2010. Boosting power for clinical trials using classifiers based on multiple biomarkers. Neurobiology of Aging, Special Issue on ADNI studies [in press].

Krishnan, K.R., Husain, M.M., McDonald, W.M., Doraiswamy, P.M., Figiel, G.S., Boyko, O.B., Ellinwood, E.H., Nemeroff, C.B., 1990. In vivo stereological assessment of caudate volume in man, effect of normal aging. Life Sci 47, 1325–1329.

Larisch, R., Meyer, W., Klimke, A., Kehren, F., Vosberg, H., Muller-Gartner, H.W., 1998. Left–right asymmetry of striatal dopamine D2 receptors. Nucl Med Commun 19, 781–787.

Laval, S.H., Dann, J.C., Butler, R.J., Loftus, J., Rue, J., Leask, S.J., Bass, N., Comazzi, M., Vita, A., Nanko, S., Shaw, S., Peterson, P., Shields, G., Smith, A.B., Stewart, J., Delisi, L.E., Crow, T.J., 2004. Evidence for linkage to psychosis and cerebral asymmetry (relative hand skill) on the X chromosome. Am J Med Genet B Neuropsychiatr Genet 81, 420–427.

Leow, A.D., Yanovsky, I., Parikshark, N., Hua, X., Lee, S., Toga, A.W., Jack, C.R., Jr, Bernstein, M.A., Britson, P.J., Gunter, J.L., Ward, C.P., Borowski, B., Shaw, L.M., Trojanowski, J.Q., Fleisner, A.S., Harvey, D., Kornak, J., Schuff, N., Alexander, G.E., Weiner, M.W., Thompson, P.M.. the Alzheimer's Disease Neuroimaging Initiative, 2009. Alzheimer's Disease Neuroimaging Initiative: A 1-year follow up study using tensor-based morphometry correlating degenerative rates, biomarkers, and cognition. Neuroimage 45(3), 645–655.

Looi, J.C.L., Lindberg, O., Liberg, B., Tatham, V., Kumar, R., Maller, J., Millard, E., Sachdev, P., Hogberg, G., Pagani, M., Botes, L., Engman, E.L., Yi, Z., Svensson, L., Wahlun, L.O., 2007. Volumetrics of the caudate nucleus, Reliability and validity of a new manual tracing protocol. Psychiatry Res Neuroimaging 163, 279–288.

Looi, J.C., Svensson, L., Lindberg, O., Zandbelt, B.B., Ostberg, P., Orndahl, E., Wahlund, L.O., 2009. Putaminal volume in frontotemporal lobar degeneration and Alzheimer's disease, differential volumes in dementia subtypes and controls. AJNR Am J Neuroradiol 30, 1552–1560.

Mazziotta, J., Toga, A., Evans, A., Fox, P., Lancaster, J., Zilles, K., Woods, R., Paus, T., Simpson, G., Pike, B., Holmes, C., Collins, L., Thompson, P., MacDonald, D., Iacoboni, M., Schormann, T., Amunts, K., Palomero-Gallagher, N., Geyer, S., Parsons, L., Narr, K., Kabani, N., Le Goualher, G., Boomsma, D., Cannon, T., Kawashima, R., Mazoyer, B., 2001. A probabilistic atlas and reference system for the human brain, International Consortium for Brain Mapping (ICBM). Philos Trans R Soc Lond B Biol Sci 356, 1293–1322.

Morra, J. H., Tu, Z., Apostolova, L.G., Green, A.E., Avedissian, C., Madsen, S.K., Parikshak, N., Hua, X., Toga, A.W., Jack, C.R., Weiner, M.W., Thompson, P.M., the Alzheimer's Disease Neuroimaging Initiative, 2008. Validation of a fully automated 3D hippocampal segmentation method using subjects with Alzheimer's disease, mild cognitive impairment, and elderly controls. Neuroimage 43(1), 59–68.

Morra, J.H., Tu, Z., Apostolova, L.G., Green, A.E., Avedissian, C., Madsen, S.K., Parikshak, N., Hua, X., Toga, A.W., Jack, C.R., Jr, Schuff, N., Weiner, M.W., Thompson, P.M., the Alzheimer's Disease Neuroimaging Initiative, 2009a. Automated 3D mapping of hippocampal atrophy and its clinical correlates in 400 subjects with Alzheimer's disease, mild cognitive impairment, and elderly controls. Hum Brain Mapp 30(90), 2766–2788.

Morra, J.H., Tu, Z., Apostolova, L.G., Green, A.E., Avedissian, C., Madsen, S.K., Parikshak, N., Toga, A.W., Jack, C.R., Jr, Schuff, N., Weiner, M.W., Thompson, P.M., the Alzheimer's Disease Neuroimaging Initiative, 2009b. Automated mapping of hippocampal atrophy in 1-year repeat MRI data from 490 subjects with Alzheimer's disease, mild cognitive impairment, and elderly controls. Neuroimage 45(1S), S3–S15.

Morris, J.C., Edland, S., Clark, C., Galasko, D., Koss, E., Mohs, R., van Belle, G., Fillenbaum, G., Heyman, A., 1993. The consortium to establish a registry for Alzheimer's disease (CERAD). Part IV. Rates of cognitive change in the longitudinal assessment of probable Alzheimer's disease. Neurology 43, 2457–2565.

Nakamura, T., Ghilardi, M.F., Mentis, M., Dhawan, V., Fukuda, M., Hacking, A., Moeller, J.R., Ghez, C., Eidelberg, D., 2001. Functional networks in motor sequence learning, abnormal topographies in Parkinson's disease. Hum Brain Mapp 12, 42–60.

Peterson, B.S., Riddle, M.A., Cohen, D.J., Katz, L.D., Smith, J.C., Leckman, J.F., 1993. Human basal ganglia volume asymmetries on magnetic resonance images. Magn Reson Imaging 11, 493–498.

Powell, S., Magnotta, V.A., Johnson, H., Jammalamadaka, V.K., Pierson, R., Andreasen, N.C., 2008. Registration and machine learning-based automated segmentation of subcortical and cerebellar brain structures. Neuroimage 39, 238–247.

Raji, C.A., Ho, A.J., Parikshak, N.N., Becker, J.T., Lopez, O.L., Kuller, L.H., Hua, X., Leow, A.D., Toga, A.W., Thompson, P.M., 2009. Brain Structure and Obesity. Hum Brain Mapp, 47, S109.

Raz, N., Rodrigue, K.M., Kennedy, K.M., Head, D., Gunning-Dixon, F., Acker, J.D., 2003. Differential aging of the human striatum, longitudinal evidence. AJNR Am J Neuroradiol 003, 1849–1856.

Rombouts, S.A., Barkhof, F., Witter, M.P., Scheltens, P., 2000. Unbiased whole-brain analysis of gray matter loss in Alzheimer's disease. Neurosci Lett 285, 231–233.

Rubin, D.C., 1999. Frontal-striatal circuits in cognitive aging, evidence for caudate involvement. Aging Neuropsych Cog 6, 241–259.

Schuff, N., Woerner, N., Boreta, L., Kornfield, T., Shaw, L.M., Trojnakowski, J.Q., Thompson, P.M., Jack, C.R., Jr, Weiner, M.W., the Alzheimer's Disease Neuroimaging Initiative, 2009. MRI of hippocampal volume loss in early Alzheimer's disease in relation to ApoE genotype and biomarkers. Brain 132, 1067–1077.

Shaw, L.M., Vanderstichele, H., Knapik-Czajka, M., Clark, C.M., Aisen, P.S., Petersen, R.C., Blennow, K., Soares, H., Simon, A., Lewczuk, P., Dean, R., Siemers, E., Potter, W., Lee, V.M.Y., Trojanowski, J.Q., the Alzheimer's Disease Neuroimaging Initiative, 2009. Cerebrospinal fluid biomarker signature in Alzheimer's Disease Neuroimaging Initiative subjects. Annals of Neurology 65(4), 403–413.

Shen, L., Saykin, A.J., Kim, S., Firpi, H.A., West, J.D., Risacher, S.L., McDonald, B.C., McHugh, T.L., Wishart, H.A., Flashman, L.A., 2010. Comparison of Manual and Automated Determination of Hippocampal Volumes in MCI and Early AD. Brain Imaging Behav 4, 86–95.

Sled, J.G., Zijdenbos, A.P., Evans, A.C., 1998. A nonparametric method for automatic correction of intensity nonuniformity in MRI data. IEEE Trans Med Imaging 17, 87–97.

Szabo, A., Lancaster, J.L., Xiong, J., Cook, C., Fox, P., 2003. MR Imaging Volumetry of Subcortical structures and cerebellar hemispheres in normal persons. AJNR Am J Neuroradiol 24, 644–647.

Thompson, P.M., Hayashi, K.M., de Zubicaray, G., Janke, A.L., Rose, S.E., Semple, J., Herman, D., Hong, M.S., Dittmer, S.S., Doddrell, D.M., Toga, A.W., 2003. Dynamics of gray matter loss in Alzheimer's disease. J Neurosci 23, 994–1005.

Thompson, P.M., Hayashi, K.M., De Zubicaray, G.I., Janke, A.L., Rose, S.E., Semple, J., Hong, M.S., Herman, D.H., Gravano, D., Doddrell, D.M., Toga, A.W., 2004. Mapping hippocampal and ventricular change in Alzheimer disease. Neuroimage 22, 1754–1766.

Turner, K.C., Frost, L., Linsenbardt, D., McIlroy, J.R., Müller, R.A., 2006. Atypically diffuse functional connectivity between caudate nuclei and cerebral cortex in autism. Behav Brain Funct 2, 34.

Wang, L., Beg, F., Ratnanather, T., Ceritoglu, C., Younes, L., Morris, J.C., Csernansky, J.G., Miller, M.I., 2007. Large deformation diffeomorphism and momentum based hippocampal shape discrimination in dementia of the Alzheimer type. IEEE Trans Med Imaging 26, 462–470.

Wechsler, D., 1987. Wechsler Memory Scale—Revised. Psychological Corporation, Texas.

Yamashita, K., Yoshiura, T., Hiwatashi, A., Noguchi, T., Togao, O., Takayama, Y., Nagao, E., Kamano, H., Hatakenaka, M., Honda, H., 2009. Volumetric Asymmetry and Differential Aging Effect of the Human Caudate Nucleus in Normal Individuals, A Prospective MR Imaging Study. J Neuroimaging 2009, 29.

Yushkevich, P.A., Piven, J., Hazlett, H.C., Smith, R.G., Ho, S., Gee, J.C., Gerig, G., 2006. User-guided 3D active contour segmentation of anatomical structures, Significantly improved efficiency and reliability. Neuroimage 31, 1116–1128.

2.2 Mapping longitudinal changes in lateral ventricle volume onto cortical gray matter

This section is adapted from the following paper.

Madsen S. K., Rajagopalan, P., Joshi, S.H., Toga, A.W., Thompson, P.M. & the Alzheimer's Disease Neuroimaging Initiative (ADNI) (2013). Elevated homocysteine is associated with thinner cortical gray matter in 803 ADNI subjects, *Neurobiology of Aging*, under review May 1 2013.

Mapping ventricular expansion onto cortical gray matter thinning in the elderly

Sarah K. Madsen[a], Boris A. Gutman[a], Shantanu H. Joshi[a], Arthur W. Toga[a],

Clifford R. Jack, Jr.[b], Michael W. Weiner[c,d], Paul M. Thompson[a,e],

for the Alzheimer's Disease Neuroimaging Initiative (ADNI)

[a]Imaging Genetics Center, Laboratory of Neuro Imaging, Dept. of Neurology, UCLA
[b]Mayo Clinic
[c]Departments of Radiology, Medicine, Psychiatry, UCSF
[d]Department of Veterans Affairs Medical Center
[e]Department of Psychiatry, Semel Institute, UCLA

Submitted to *Neurobiology of Aging – Special Issue on Novel Imaging Biomarkers for Alzheimer's Disease and Related Disorders*

May 1, 2013

*Data used in preparing this article were obtained from the Alzheimer's Disease Neuroimaging Initiative database (www.loni.ucla.edu/ADNI). As such, many investigators within the ADNI contributed to the design and implementation of ADNI and/or provided data but most did not participate in analysis or writing of this report. For a complete listing of ADNI investigators, please see: http://adni.loni.ucla.edu/wp-content/uploads/how_to_apply/ADNI_Authorship_List.pdf

Abstract

Dynamic changes in the brain's lateral ventricles on MRI are powerful biomarkers of disease progression in mild cognitive impairment (MCI) and Alzheimer's disease (AD). Ventricular measures can represent accumulation of diffuse brain atrophy with very high effect sizes. Despite having no direct role in cognition, ventricular expansion co-occurs with volumetric loss in gray and white matter structures. To better understand relationships between ventricular and cortical changes over time, we related ventricular expansion to atrophy in cognitively-relevant cortical gray matter surfaces, which are more challenging to segment. In elderly ADNI subjects, percent change in ventricular volumes at one- (N=677) and two-year (N=536) intervals was significantly associated with baseline cortical thickness in the full sample controlling for age, sex, and diagnosis, and in MCI separately. Ventricular expansion in MCI was associated with thinner GM in frontal, temporal, and parietal regions affected by AD. Ventricular expansion reflects cortical atrophy in early AD, offering a useful biomarker for clinical trials of interventions to slow AD progression.

Keywords

biomarkers; Alzheimer's disease; mild cognitive impairment; brain imaging; magnetic resonance imaging (MRI); cortical; gray matter; atrophy; thickness; volume; surface area; brain structure; longitudinal

Introduction

As brain tissue is lost in normal aging and dementia, the volume of cerebral spinal fluid (CSF) in the lateral ventricles and surrounding the brain expands to fill the space, within the fixed volume of the skull. The clear tissue contrast between CSF and brain tissues makes it easier to reliably segment and measure the lateral ventricles in standard T1-weighted anatomical MRI scans, even in populations that present challenges for segmentation of other brain structures (Ferrarini et al., 2008, Qiu et al., 2009). The lateral ventricles can be reliably segmented with semi- or fully-automated methods that measure their overall volume (Jack et al., 2004, Nestor et al., 2008, Resnick et al., 2003), shape (Chou, 2007, Ferrarini et al., 2006, Gong, 2011), radial width (Apostolova et al., 2012, Frisoni et al., 2002, Thompson et al., 2004), or boundary shift integral (Ridha et al., 2008, Schott et al., 2005). By comparison, accurate and reliable segmentation of the cortical gray matter surface is somewhat challenging in elderly brains, as gray and white matter (GM, WM) contrast decreases with age and the cortical surface may also become increasingly complex and irregular in shape as more brain tissue is lost. Time-consuming manual editing is often required even with the most sophisticated, widely-used cortical GM segmentation packages (Fischl and Dale, 2000, Sanchez-Benavides et al., 2010). Some of these issues can be alleviated by collecting scans with specialized protocols to increase the signal to noise ratio at the cortical boundary. Some researchers advocate averaging two or more MRI scans within subject to improve the accuracy of cortical segmentation, although collecting several scans is not always feasible (Perlman, 2007). Relating expansion of the lateral ventricles to detailed 3D maps of cortical GM thinning takes advantage of a subcortical brain structure that is very easily segmented in standard MRI data from elderly populations, while also allowing interpretations of the likely cortical changes, which have more direct clinical relevance.

Ventricular measures achieve some of the highest possible effect sizes for tracking longitudinal changes in the human brain. Ventricular volume is a powerful MRI biomarker that has been widely-used in studies of normal aging, mild cognitive impairment (MCI), and Alzheimer's disease (AD) (Apostolova et al., 2012, Chou, 2007, Ferrarini et al., 2006, Fleisher et al., 2008, Jack et al., 2008, Jack et al., 2004, Jack et al., 2005, Nestor et al., 2008, Qiu et al., 2009, Thompson et al., 2004, Wang et al., 2002). In comparative studies, fewer subjects may be needed[1] (Hua et al., 2013) to detect statistical effects of disease-modifying interventions in clinical trials using ventricular biomarkers compared to using many other neuroimaging measures. One study demonstrated, for example, that approximately 60 subjects are needed to detect a fixed percentage of slowing of ventricular expansion versus 90 subjects needed to detect slowing in hippocampal atrophy and 300 subjects needed to detect the same proportional slowing of the rate of decline on neuropsychological tests (Ridha et al., 2008).

Larger or expanding ventricles are linked with a broad range of brain-related health factors in the elderly, including current cognitive status and future memory decline (Coffey et al., 2001, Murphy et al., 2010), the brain reserve or general resiliency against neurodegeneration (Cavedo et al., 2012), depression, language scores, CSF measures of amyloid beta, APOE genotype (Chou et al., 2010), poorer cardiovascular health (Isaac et al., 2011), vitamin D deficiency (Annweiler et al., 2013), elevated homocysteine levels (Feng et al., 2013), post-operative cognitive dysfunction (Bourne et al., 2012, Kline et al., 2012), decreased survival in dementia (Olesen et al., 2011), and conversion to MCI and AD (Carmichael et al., 2007b, Fleisher et al., 2008, Jack et al., 2004, Nestor et al., 2008).

[1] Head-to-head comparisons of effect sizes for brain biomarkers require many caveats, as therapeutic interventions may affect each biomarker differently. Also, simply reducing the numerical rate of change for different biomarkers many have different functional or clinical consequences for the patient. Some of these issues are discussed in Hua et al., 2013.

Although the ventricles provide several practically useful MRI biomarkers, the structure does not play a direct role in cognition. Therefore it is vital to determine how the changes in brain regions of functional and cognitive significance in AD relate to expansion in lateral ventricles. Lateral ventricle expansion co-occurs with degeneration of gray and white matter globally and nearby subcortical regions (Ferrarini et al., 2008, Qiu et al., 2009). By associating ventricular expansion with detailed profiles and patterns in cortical GM thickness, we can make good use of the reliability and ease of ventricular segmentation, relating changes to likely differences in cortical structures that are somewhat more difficult or time-consuming to segment, but which are more directly susceptible to AD-related pathologies.

2. Methods

2.1. Study population

We analyzed subjects that underwent high-resolution, T1-weighted structural MRI scanning of the brain, as part of phase 1 of the Alzheimer's Disease Neuroimaging Initiative (ADNI1). Our subject sample included only subjects listed in the standard set of N=817 baseline, N=685 one-year follow-up, and N=544 two-year follow-up scans obtaining during the ADNI1 phase of data collection that was created to promote rigor and more meaningful comparability across ADNI studies (Wyman et al., 2012). In the ventricle analysis, two baseline scans and one scan from the one-year follow-up time-point were not included, even though they are currently listed in the standard set, because they were added to the list after we had competed data processing. In the cortical GM analysis, all standard subjects were processed.

ADNI was launched in 2004 by the National Institutes of Health, the Food and Drug Administration, private pharmaceutical companies, and non-profit organizations to identify and evaluate biomarkers of AD for use in multisite studies. All ADNI data are publicly available at adni.loni.ucla.edu. All ADNI studies are conducted in compliance with the Good Clinical Practice guidelines, the Declaration of Helsinki, and the US 21 CFR Part 50–Protection of Human Subjects, and Part 56–Institutional Review Boards. Written informed consent was obtained from all ADNI participants prior to the study. ADNI is a multi-site, longitudinal study of patients with Alzheimer's disease (AD), mild cognitive impairment (MCI) and healthy elderly controls (HC). Standardized protocols maximize consistency across scan sites.

All individuals received a thorough clinical and cognitive evaluation near the time of their scan. The examination included the mini-mental state examination (MMSE, a standardized and widely-used 30 point questionnaire, with scores of 24-30 typically indicating normal cognition or MCI, and scores of 20-26 indicating probable AD (Folstein et al., 1975)) and diagnosis of probable AD, MCI, or cognitively normal. A diagnosis of cognitively normal is made for participants with no signs of depression, MCI, or dementia. A diagnosis of MCI is made for participants who have reported a subjective memory concern without impairment in other cognitive domains and no signs of dementia. A diagnosis of probable AD was made for subjects who met the NINCDS/ADRDA criteria. Inclusion and exclusion criteria are detailed in the ADNI protocol (Mueller et al., 2005) and is available online at http://adni.loni.ucla.edu/wp-content/uploads/2010/09/ADNI_GeneralProceduresManual.pdf.

2.2. Image acquisition

High-resolution structural MRI scans of the brain were acquired for subjects included in the standardized ADNI list (Wyman et al., 2012) on 1.5T scanners from General Electric (Milwaukee, Wisconsin, USA), Siemens (Germany), or Philips (The Netherlands) using a standardized MRI protocol for three-dimensional sagittal magnetization-prepared rapid gradient-echo sequences (Jack et al., 2008).

For lateral ventricle segmentation, we analyzed baseline (N=834), one-year (N=677), and two-year (N=536) follow-up brain MRI scans (1.5-Tesla, T1-weighted 3D MP-RAGE, TR/TE = 2400/1000 ms, flip angle = 8˚, slice thickness = 1.2 mm, final voxel resolution = 0.9375 x 0.9375 x 1.2 mm^3). Raw MRI scans were pre-processed to reduce signal inhomogeneity and linearly registered to a template (using 9 parameter registration). Segmentations were assessed visually for defects from multiple views. All subjects passed QC for ventricular segmentations.

For cortical GM segmentation, we analyzed baseline (N=677), one-year (N=646), and two-year (N=507) follow-up brain MRI scans (1.5-Tesla, T1-weighted 3D MP-RAGE, TR/TE = 2400/1000 ms, flip angle = 8˚, slice thickness = 1.2 mm, 24-cm field of view, a 192×192×166 acquisition matrix, final voxel resolution = 1.25×1.25×1.2 mm^3, later reconstructed to 1 mm isotropic voxels). Six subjects at baseline, 35 subjects at one-year follow-up, and 33 subjects at two-year follow-up were excluded during QC of cortical GM surfaces.

2.3. Segmentation of the lateral ventricles

Prior methods for ventricular segmentation have used semi-automated, automated (Chou et al., 2008), and single-atlas or multi-atlas methods (Chou et al., 2009). Here we chose to

segment the ventricles with a modified multi-atlas approach described previously (Gutman et al., 2013) and tested in a preliminary analysis (Madsen et al., 2013) that we have expanded upon here. Our segmentation approach yields more accurate results by using a group-wise surface registration to existing templates in addition to surface-based template. Segmentation of the lateral ventricles in each subject was performed using a validated method (Chou et al., 2008). Ventricular surfaces were then extracted from these segmentations and an inverse-consistent fluid registration with a mutual information fidelity term aligned a set of hand-labeled ventricular templates to each scan (Leow et al., 2007) (N=536). The template surfaces were registered as a group using medial-spherical registration and the template that best fits the new boundary was selected for each individual subject (Gutman et al., 2013), allowing more flexible segmentation, particularly for outliers.

2.3. Segmentation of cortical GM

Cortical reconstructions and segmentations were obtained to measure cortical GM thickness at each surface point, using the FreeSurfer image analysis package (v5.0.0), which is documented and freely downloadable online (http://surfer.nmr.mgh.harvard.edu/). Technical details have been described previously (Dale et al., 1999, Fischl and Dale, 2000, Fischl et al., 2002, Fischl et al., 1999a, Fischl et al., 1999b, Fischl et al., 2004, Han et al., 2006). Briefly, the processing pipeline involves removing non-brain tissue, intensity normalization, tessellation of the cortical GM/WM boundary, automated topology correction and surface deformation along intensity gradients to optimally define the cortical surface, alignment of cortical anatomy across individuals via registration to a spherical atlas using individual cortical folding patterns, segmentation of total cortical GM volume for the left and right hemispheres, and creation of 3D

maps of GM thickness at each cortical surface point in the left and right hemispheres for each subject (N=677). Processed images are in an isotropic space of 256 voxels along each axis (x, y, and z) with a final voxel size of 1 mm^3.

2.4. Statistical analysis: associations with volumes

Statistical tests using left and right ventricular volumes to predict total cortical GM volumes were conducted in R (http://www.r-project.org/, R Development Core Team, 2008). We tested general linear models (GLMs) with outcome variables of either ventricular volume at baseline (N=834), percent change in ventricular volume (relative to baseline volume) after one year (N=677), percent change in ventricular volume after two years (N=536), or total baseline cortical GM volume (N=677) in the left and right hemispheres separately. Dependent variables included age, sex, years of education, MMSE score, and diagnosis (i.e., healthy elderly control, MCI, or AD). We also tested GLMs with outcome variables of total and percent change in cortical GM volume at one-year (N=646) and two-year (N=507) follow-ups, using dependent variables of baseline ventricular volumes, age, sex, and diagnosis. Diagnosis was coded using indicator variables for each of the AD and MCI groups, with healthy controls as the reference group. We also ran similar GLMs in each diagnostic group separately and tested for associations between total baseline cortical GM volumes and ventricular volume measures, controlling for the appropriate covariates in the left and right hemispheres. Education was not a significant predictor of ventricular or cortical GM measures in these models, so it was not included as a covariate in subsequent analyses.

2.5. Statistical Analysis: cortical surface maps

Statistical tests were conducted at each point on the left and right cortical surface using the general linear model (GLM) analysis tools in FreeSurfer (mri_glmfit, v5.0.0). Prior to analysis, a smoothing kernel of size 25 mm (full width at half maximum) was applied to each subject's 3D cortical surface map of GM thickness. We chose a large smoothing kernel because the regions of brain atrophy seen in normal aging and in AD are relatively large (Buckner et al., 2005a, Serra et al., 2010).

Based on the results of the GLMs using ventricular volume measures and total cortical GM volumes, we tested a series of GLMs for percent change in ventricular volume on baseline cortical GM thickness after: (1) controlling for effects of sex, age, and diagnosis (AD, MCI, or healthy elderly controls) in all individuals (one-year interval: N=677; two-year interval: N=536), (2) controlling for sex and age in AD, MCI, and control groups, separately (one-year: AD N=142, MCI N=335, Control N=200; two-year: AD N=109, MCI N=251, Control N=176), and (3) controlling for sex and age, in matched groups of N=100 AD, MCI and controls, separately to equalize statistical power. We also tested percent change in ventricular volume for relationships with one-year and two-year changes in cortical GM thickness after controlling for effects of sex, age, and diagnosis. Analyses were run separately for the left and right hemispheres, testing for associations of percent change in left lateral ventricles with left baseline cortical GM thickness at each surface point; and similarly for the right ventricle and right cortical surface. To control the rate of false positives, we enforced a standard false discovery rate (FDR) correction (Benjamini and Hochberg, 1995) for multiple statistical comparisons across all surface

vertices on the entire left and right cortical surfaces, using the conventionally accepted false positive rate of 5% (q=0.05).

3. Results

3.1 Study population characteristics

Characteristics of the study population are shown in **Table 1**. Mean age was not significantly different across groups ($p > 0.05$), although the MCI group appeared to have a somewhat higher proportion of men than other groups did. We included age and sex as covariates in all models to adjust for these confounds. The expected trend of poorer MMSE scores, lower total cortical GM volumes and higher ventricular volumes at baseline, and greater percent change in ventricular volumes was observed across the groups, with AD being worst, MCI being intermediate, and controls showing the 'healthiest' values for these measurements. Total GM volumes at baseline were 7.41% lower in AD and 1.77% lower in MCI compared to controls, while ventricular volumes at baseline were 50.6% larger in AD and 18.5% larger in MCI compared to controls, after averaging the left and right hemisphere values. The greater deviation in ventricle volumes compared to total GM volumes across the diagnostic groups suggests that lateral ventricle volume is a more sensitive measure. Rates of ventricular expansion also differed between groups, with average percent change between baseline and one-year and baseline and two-years showing a successive increase from controls to MCI to AD. As expected, the ventricles expanded by about twice as much over the two-year interval than they did over the one-year interval, for each of the AD, MCI, and control groups. (**Figure 1**).

Table 1. Demographic characteristics of the *N*=677 individuals analyzed in the study.

	AD	MCI	Controls	All Individuals
Sample Size (*n*)	142	335	200	677
Sex (women/men)	67/75	124/211	95/105	286/391
Age (years)	75.49 ± 7.39	74.84 ± 7.22	75.97 ± 5.07	75.31 ± 6.71
MMSE (baseline)	23.39 ± 1.92	27.01 ± 1.77	29.13 ± 1.02	26.87 ± 2.59
Lateral **ventricular volume (baseline)**				
Left:	28,594 ± 13,261	22,472 ± 12,254	18,817 ± 10,205	25,043 ± 12,188
Right:	26,455 ± 11,916	20,836 ± 11,080	17,719 ± 8,945	22,668 ± 10,955
(one-year percent change)				
Left:	9.44 ± 6.20	6.52 ± 6.37	3.86 ± 3.93	6.35 ± 6.04
Right:	9.52 ± 6.53	6.52 ± 6.15	3.83 ± 4.15	6.35 ± 6.05
(two-year percent change)	*N*=109	*N*=251	*N*=176	*N*=536
Left:	19.91 ± 11.57	13.47 ± 10.26	8.68 ± 6.26	13.21 ± 10.24
Right:	19.25 ± 12.84	12.74 ± 10.29	7.49 ± 6.24	12.34 ± 10.63

Table 1. Selected demographic information (mean ± standard deviation). Note the claimed precision overstates the accuracy with which these values can be reliably measured (which is no more than 3 significant figures), but we did not round them in case the values are useful for other studies.

Figure 1. Baseline volumes for ventricles and cortical GM and rates of ventricular expansion across groups.

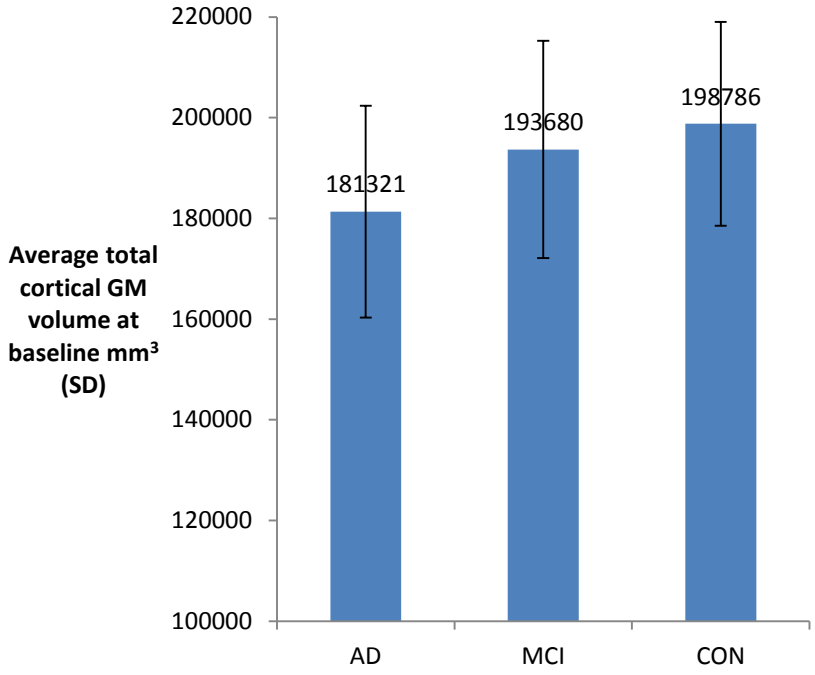

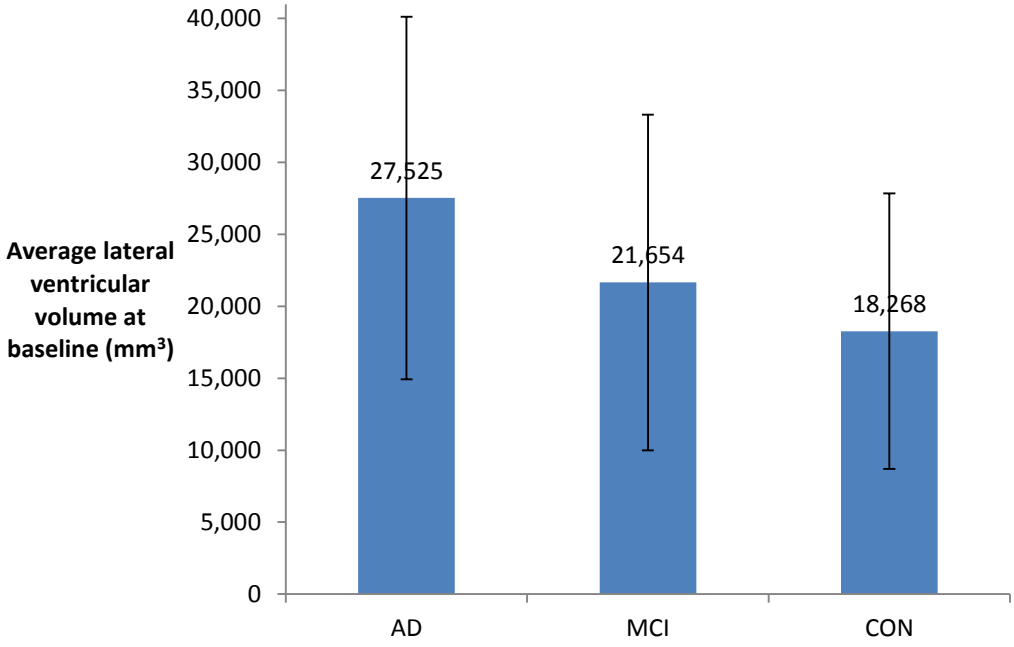

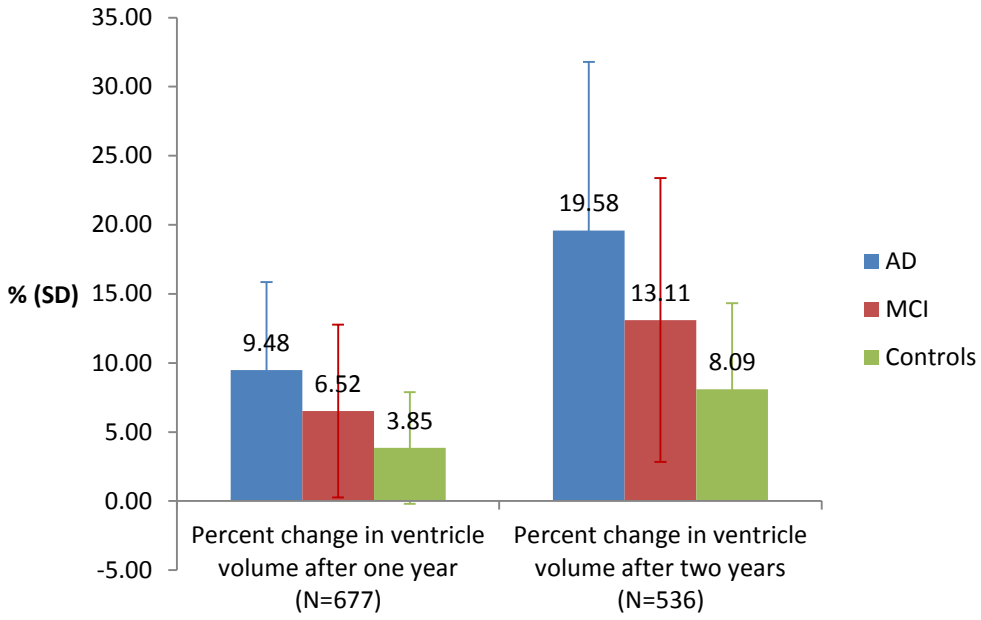

Figure 1. Total cortical GM and ventricular volume at baseline averaged across left and right hemispheres for AD, MCI, and control groups. Percent change in ventricular volume compared to baseline after one- and two-year follow-up intervals averaged across left and right hemispheres for AD, MCI, and control groups. As expected, the amount of expansion (since baseline) roughly doubles from the one-year to two-year interval. Without controlling for confounding factors, and perhaps surprisingly, the standard deviations in these measures were large enough that neither the baseline nor percent change measures were significantly different between any pair of groups. Error bars are standard deviation.

3.2. Associations between cortical GM profiles and ventricular volumes

The AD, MCI, and control groups differed significantly in total cortical GM volumes at baseline (AD: $p<2\text{x}10^{-16}$; MCI: $p<2\text{x}10^{-16}$, averaged for left and right with controls as the reference group) and in one-year and two-year percent difference in ventricular volumes (for one-year, AD: $p<2\text{x}10^{-16}$; MCI: $p=6.25\text{x}10^{-7}$; for two years, AD: $p<2\text{x}10^{-16}$; MCI: $p=5.17\text{x}10^{-7}$), after controlling for age and sex. It is noteworthy that the rate measures were significantly difference between diagnostic groups, whereas baseline ventricular volumes were not, which depend on many factors unrelated to the disease (e.g., neurodevelopmental differences).

In these models, AD was associated, on average, with a 17,650 mm^3 reduction in total cortical GM volume and amounts of ventricular expansion that were 5.55% greater over the one-year interval and 11.39% greater across the two-year interval compared to controls, on average. MCI was associated with an 8,580 mm^3 average reduction in total cortical GM volume and amounts of ventricular expansion that were 2.53% greater for the one-year interval and 4.73% greater across the two-year interval compared to controls, on average.

Lower total GM volumes at baseline were significantly associated with higher two-year (p=0.004), but not one-year (p=0.207), percent changes in ventricular volumes, averaged for the left and right hemispheres in the whole sample after controlling for age, sex, and diagnosis. Percent change in total GM volume at one-year (p=0.012), but not two-years (p=0.170), is significantly associated with baseline ventricular volumes, in the whole sample after controlling for age, sex, and diagnosis. Percent change in total GM volume is significantly associated with percent change in ventricular volume at one-year (p=2.44×10^{-9}) and two-year (p=4.45×10^{-12}) intervals, in the whole sample after controlling for age, sex, and diagnosis. Considering each group separately, in AD we found that lower total GM volumes at baseline were significantly associated with higher one-year (p=0.022) and two-year (p=0.043) percent expansion in lateral ventricular volume in the left, but not right hemisphere. In MCI, lower total GM volumes at baseline were significantly associated with higher ventricular expansion after two years (left: p= 0.046, right: p=0.004), but not after one year. In controls, total GM volume at baseline was not associated with ventricular volume expansion in either interval or hemisphere.

3.2. Mapping ventricular expansion onto cortical GM thickness

In the full sample, we found that **(Figure 2A and 2B)** percent change in ventricular volumes over one-year (N=677) and two-year (N=536) intervals was significantly associated with baseline cortical GM thickness in temporal, inferior and anterior frontal, inferior parietal, and lateral occipital regions, after controlling for age, sex, and diagnosis. The significant regions were somewhat more expansive, in the same areas, for the two-year percent change compared to the one-year percent change in ventricular volume. As expected, no areas of significant positive associations were found. If we expect that ventricular change is approximately linear over time, these two sets of maps should be identical; however the map for change over a longer interval may have greater signal-to-noise-ratio, increasing the power to detect significant associations. All results presented here passed a hemispheric FDR correction at q=0.05.

In the full sample, we also found that percent change in ventricular volumes over one-year (N=646) was significantly associated with cortical GM thickness at one-year follow-up **(Figure 2C)** and that percent change in ventricular volumes over two-year (N=507) was significantly associated with cortical GM thickness at two-year follow-up **(Figure 2D)** in expansion regions covering most of the cortical surface, except for the primary sensorimotor strip and medial occipital regions, after controlling for age, sex, and diagnosis. The significant regions were somewhat more expansive, in the same areas, for the two-year to the one-year maps. As expected, no areas of significant positive associations were found. All results presented here passed a hemispheric FDR correction at q=0.05.

Figure 2. Ventricular expansion mapped onto cortical GM at baseline and at follow-up in the elderly.

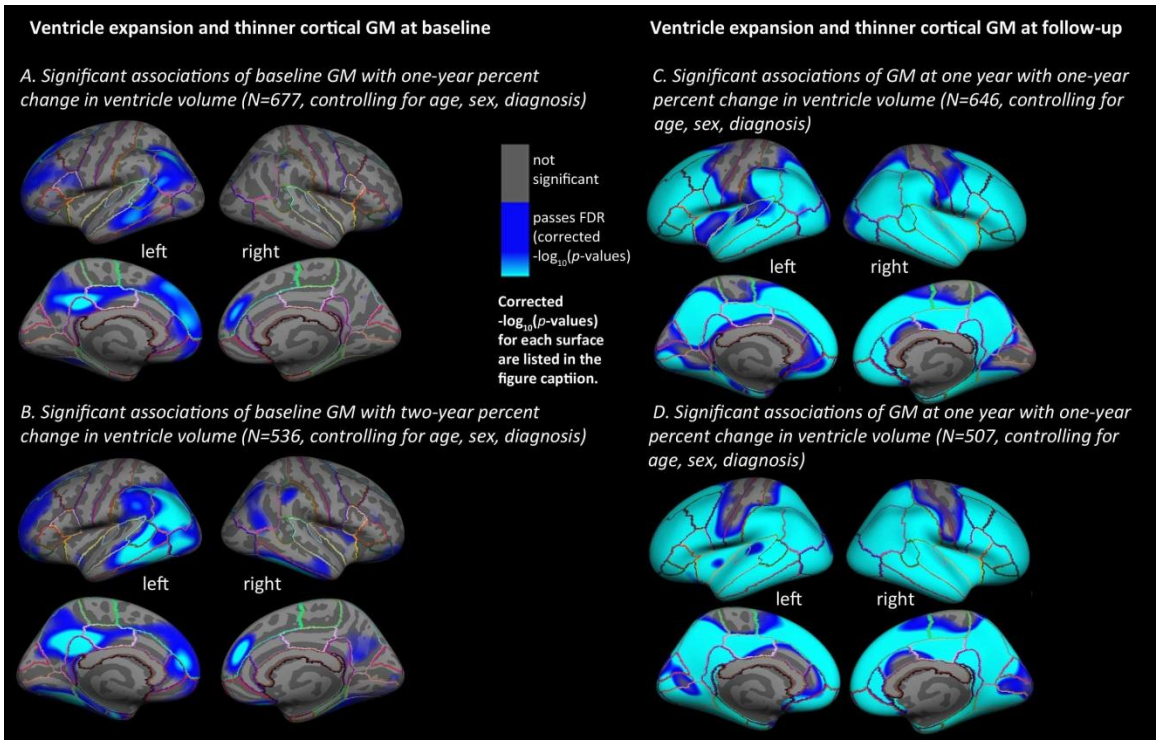

Figure 2. Hemispheric 3D maps in the left panel (**A,B**) show significant negative associations in the entire sample between cortical GM thickness at baseline and one-year (**A**, *N*=677) and two-year (**B**, *N*=536) percent change in ventricular volume in all individuals regardless of cognitive status (AD, MCI, or healthy elderly) (**A,** one-year percent change, left: -$\log_{10}$(*p*-values)=1.77-4.03, right: -$\log_{10}$(*p*-values)=2.61-4.87; **B,** two-year change, left: -$\log_{10}$(*p*-values)=1.62-3.88, right: -$\log_{10}$(*p*-values)=1.98-4.24, corrected, controlling for age, sex, diagnosis). The right panel **(C,D)** shows associations in the entire sample between cortical GM thickness at one-year follow-up and one-year percent change in ventricular volume (**C**, *N*=646) and between cortical GM thickness at two-year follow-up and two-year percent change in ventricular volume (**C**, *N*=507) (**C,** one-year percent change, left: -$\log_{10}$(*p*-values)=1.409-3.667, right: -$\log_{10}$(*p*-values)=1.392-3.650; **D,** two-year change, left: -$\log_{10}$(*p*-values)=1.387-3.644, right: -$\log_{10}$(*p*-values)=1.367-3.624, corrected, controlling for age, sex, diagnosis). The reported *t*-statistic values correspond to the significance threshold that controls the FDR. Results were corrected for multiple comparisons by thresholding at a *q*=0.05 false discovery rate (FDR) threshold across the entire brain surface. Blue areas represent areas where corrected *p*-values passed the significance threshold for a negative relationship between longitudinal ventricular enlargement and cortical thickness values (as hypothesized, higher rates of ventricular enlargement were associated with thinner cortical GM at baseline).

3.3. Mapping ventricular expansion onto cortical GM in AD, MCI, and healthy elderly

Considering each diagnostic group separately, the one-year and two-year percent changes in ventricular volume were significantly associated with baseline cortical GM thickness in MCI only (**Figure 3**), but with no detectable effect in AD or in healthy elderly controls. The MCI group has the largest sample size (N=335 for one-year and N=251 for two-year intervals) compared to the AD (N=142 for one-year and N=109 for two-year intervals) and control groups (N=200 for one-year and N=176 for two-year intervals), suggesting that the lower power could have contributed to the lack of results in AD and controls (this point is addressed in the **section 3.4**). In MCI, small regions of thinner baseline cortical GM - in the bilateral superior frontal and inferior parietal gyri, left precuneus and isthmus of the cingulate, and right supramarginal gyri - were significantly associated with one-year percent change in ventricular volume (left: $-\log_{10}(p\text{-values})$=2.58-4.84, right: $-\log_{10}(p\text{-values})$=3.15-5.41, corrected, controlling for age, sex). The maps associating baseline cortical GM with two-year percent change in ventricular volume in MCI were much more expansive, with significant relationships detected in the bilateral superior, middle, and inferior temporal, lateral occipital, inferior and some superior parietal, supramarginal, rostral inferior, middle, and superior frontal gyri, the precuneus, posterior cingulate, medial orbitofrontal, entorhinal, parahippocampal, fusiform, and lingual gyri (left: $-\log_{10}(p\text{-values})$=1.71-3.97, right: -log10(p-values)=1.79-4.04, corrected, controlling for age, sex), which matches the well-known pattern of AD-related pathology (**Figure 4**). No significant

associations were found in the AD or healthy control groups. As expected, no areas of significant positive associations were found for any group.

Figure 3. Mapping ventricular expansion onto cortical GM thickness in MCI.

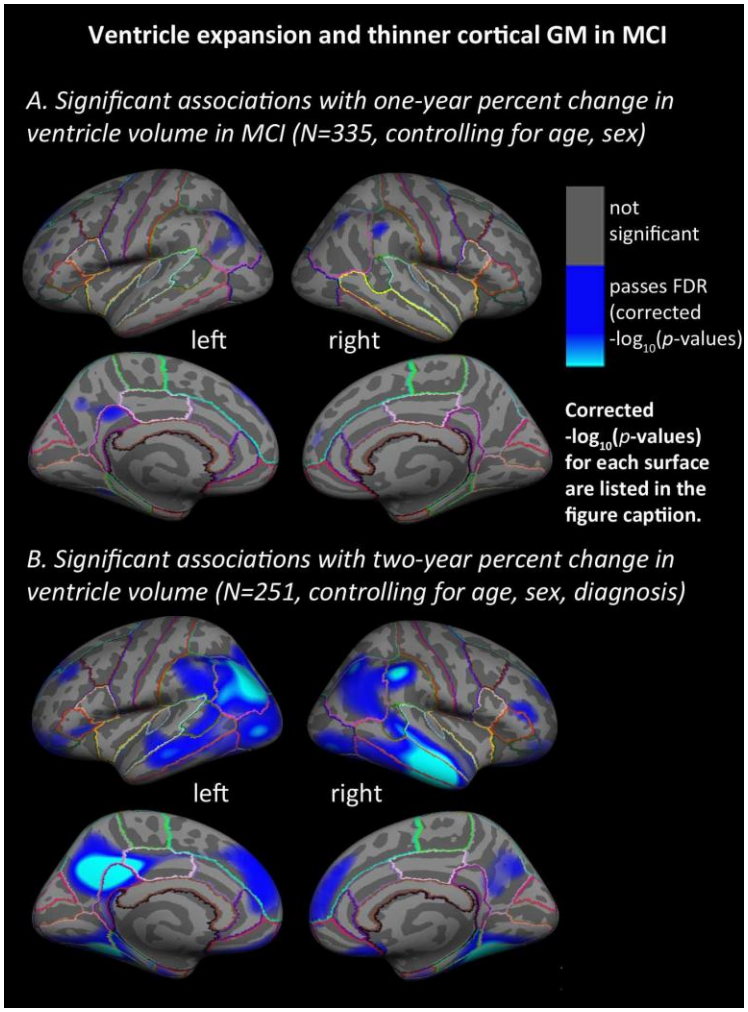

Figure 3. Hemispheric 3D maps show significant negative associations in MCI between cortical GM thickness at baseline and one-year (A, *N*=335) and two-year (B, *N*=251) percent change in ventricular volume after controlling for age, sex (one-year percent change, left: $-\log_{10}(p\text{-values})$=2.58-4.84, right: $-\log_{10}(p\text{-values})$=3.15-5.41, two-year percent change, left: $-\log_{10}(p\text{-values})$=1.71-3.97, right: $-\log_{10}(p\text{-values})$=1.79-4.04, FDR corrected as described in Figure 2). No significant results were found for AD or healthy controls separately.

Figure 4. Canonical progression of MCI and AD pathology.

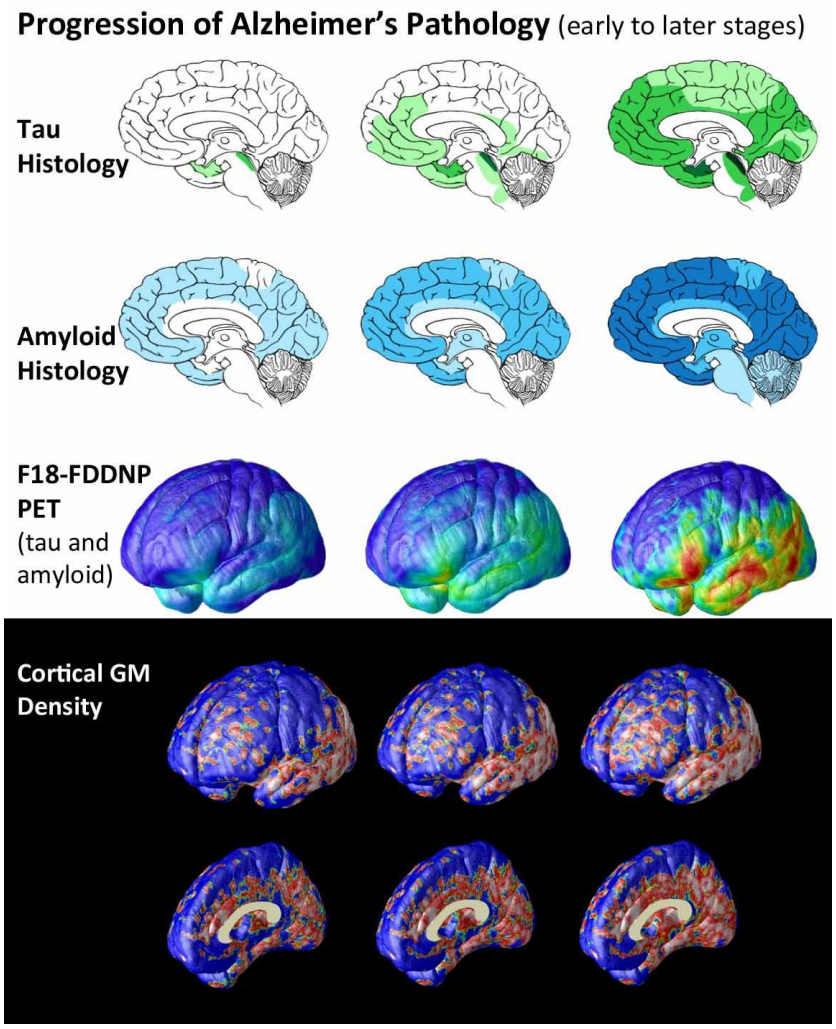

Figure 4. For purposes of comparison, here we show images of the canonical progression of AD pathology (adapted from (Braak and Braak, 1991, Braskie et al., 2010, Thompson et al., 2003) developed from elderly samples that do not overlap with the subjects in this study. Our maps of associations between longitudinal change in ventricular volumes and baseline GM density follow a very similar pattern, with significant associations in areas affected by AD pathology and no relationship detected in areas that are relatively spared by the disease (e.g., in the primary sensorimotor strips).

3.4. Power analysis, equal sized samples of N=100

We felt it was important to determine if significant results were found only in MCI, which had a larger N compared to the AD and control groups, due to differences in power related to the available sample sizes. After limiting the samples to equal-sized subsets of size N=100 (the approximate size of the smallest group) that were matched for age and sex, the data was re-analyzed for AD, MCI, and healthy elderly controls. Significant negative associations were found in MCI for two-year percent change in left ventricular volume related to baseline cortical GM thickness in left superior temporal, supramarginal, inferior and superior parietal, lateral occipital, fusiform, precuneus, posterior cingulate, and small regions in the superior frontal gyri (left: $-\log_{10}(p\text{-values})$=2.05-4.31, controlling for age, sex). No significant results were found in AD or controls at either time interval or in the one-year interval for MCI using the smaller and equally sized samples. No significant positive associations were found in any group.

Figure 5. Significant associations in equally sized samples of *N*=100.

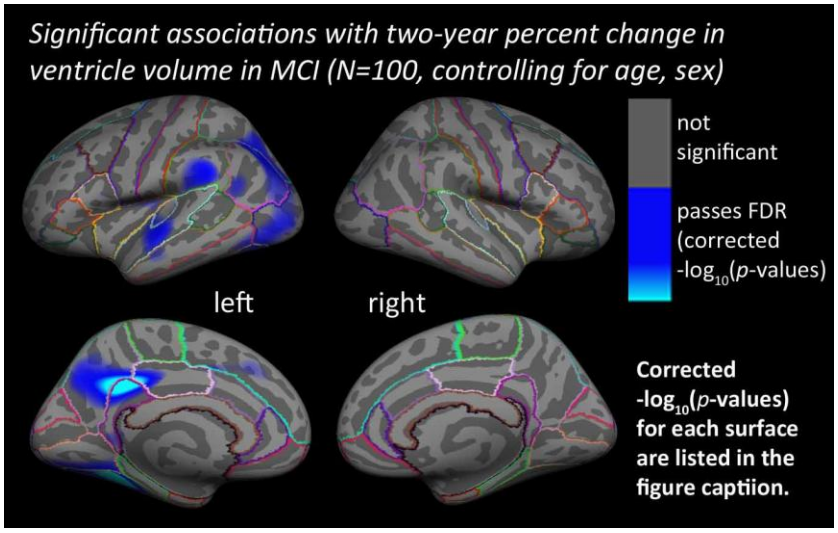

Figure 5. Hemispheric 3D maps show significant negative associations found in MCI in matched *N*=100 subsets for two-year percent change in ventricular volume and baseline cortical GM thickness (two-year change, left: $-\log_{10}(p\text{-values})$=2.05-4.31, right: not significant; controlling for age, sex, FDR corrected as described in Figure 1). Other maps were not significant.

4. Discussion

Our results add to the current literature that identifies changes in ventricular enlargement as a robust biomarker of AD. We make a novel contribution to the field, by showing how longitudinal changes in ventricular volume relate to specific patterns of thinner cortical GM in early stages of this neurodegenerative disorder. These results allow us to make connections between possible atrophy in functionally important cortical areas, and more obvious changes in ventricular segmentations. Ventricular measures are among the most reliable and robust MRI measures for tracking the progression of AD, but are naturally limited in terms of making specific inferences about brain structure and function. Since cortical regions can be challenging or time-consuming to segment in elderly brains, combining information about the cortical

architecture and ventricular enlargement gives us a better understanding of early stages of neurodegenerative disease.

Interestingly, the pattern of significant associations in MCI matches the well-known pattern of progressive cortical atrophy in AD (see, e.g. Figure 6 in (Thompson et al., 2003)) and in MCI to AD conversion (see, e.g. Figures 2-4 in (Whitwell et al., 2007)), pathological amyloid plaque and tau neurofibrillary tangle deposition, metabolic disruption, and functional disconnectivity (see, e.g., Figure 6 in (Buckner et al., 2005b)) characteristic of AD progression (**Figure 4**). Primary sensorimotor areas that may not experience heavy disease burden did not show significant associations in our MCI sample or in the whole sample. These are also relatively difficult cortical areas for measuring GM thickness as the extensive myelination can lead to poor tissue contrast on standard anatomical MRI. When diagnostic groups of the same sample size were studied, in an attempt to equalize statistical power to detect associations, longitudinal ventricular expansion was most strongly associated with thinner cortical GM in the early stages of disease progression, rather than in healthy elderly or in more severely impaired individuals.

In healthy elderly people, the lateral ventricles expand approximately linearly with age, and the changes are accompanied by a progressive decrease in total brain volume (Blatter et al., 1995). Enlarged ventricles are commonly observed even in very healthy elderly individuals (Longstreth, 1998). In cross-sectional studies, average ventricular volumes are largest in AD and MCI compared to healthy elderly controls (in AD, roughly 60% larger than in MCI and roughly 4 times larger than in controls) (Nestor et al., 2008). However, this measure is not ideal for diagnostic classification, as cross-sectional ventricular volumes overlap substantially between

elderly controls and AD subjects (AD: 20-146 cm^3, CON: 11-82 cm^3) (Wang et al., 2002). This makes it vital to consider longitudinal patterns and rates of ventricular expansion. Interestingly, ventricular volumes are larger in AD compared to healthy centenarians, who did not differ from healthy 80-90 year old elderly individuals in one study (Gong, 2011). This suggests that the accelerated expansion of ventricular volumes in AD does eventually result in cross-sectional differences that are large enough to distinguish from normal aging.

Expansion of the lateral ventricles reflects the accumulation of brain tissue reductions globally, throughout multiple brain regions, in which rates of change may be too subtle or more challenging to detect directly. In normal aging, rates of ventricular enlargement accelerate around age sixty, then continue at a stable pace at least into the late nineties (Jernigan et al., 2001, Walhovd et al., 2005). In healthy older adults, the annual increase of 3-13% (approximately 1500 mm^3) in ventricular volume represents a change of less than 0.5% in total brain volume and is much greater than the <1-3% volume reduction seen in the hippocampus (Fjell et al., 2009b, Resnick et al., 2000, Resnick et al., 2003, Ridha et al., 2008, Zhang et al., 2010). Perhaps because this measure is so powerful, many studies have concluded that ventricular measures are more strongly associated than temporal lobe structures with hallmark features of dementia such as baseline cognition, change in global clinical scores and dementia ratings over time, and plaque and tangle accumulation (Fjell et al., 2009a, Jack et al., 2004, Ridha et al., 2008, Silbert et al., 2003).

Due to the overlap in ventricular volumes among diagnostic groups, accelerated *rates* of brain atrophy may be better indicators of MCI and AD. Rates of ventricular enlargement distinguish AD from healthy elderly controls, even when cross-sectional ventricular volumes

overlap between the two groups (Wang et al., 2002). The most extreme acceleration in the rate of ventricular expansion may occur in MCI and at the point of conversion from MCI to AD (Apostolova et al., 2012, Carmichael et al., 2007a, Jack et al., 2008, Ridha et al., 2008), while accumulated total volumes and expansion rates are most extreme later in the disease (Wahlund et al., 1993). Faster rates of ventricular expansion also independently predict cognitive decline (Adak et al., 2004), and are more predictive than other MRI measures in detecting early conversion to AD (Fleisher et al., 2008). In fact, for each standard deviation increase in ventricular volume expansion, the risk for conversion to AD increases by around 1.7% (Jack et al., 2005).

It would also be interesting to apply the reverse approach - i.e., mapping cortical GM measures (average and change in GM thickness in regions of interest, for example) onto 3D ventricular shapes, to see exactly which areas of the ventricles are most strongly associated with cortical thickness changes. In their study, Ferrarini et al., 2006, reported that 22% of the ventricular surface was "significantly different" between AD and healthy elderly, although this number will vary depending on sample size. Even so, the frontal and temporal horns are most sensitive to AD progression in this study and others (Apostolova et al., 2012, Thompson et al., 2004). If significant associations are found between cortical GM and ventricular shape at later stages of AD, we might expect to see expansion of the frontal horns of the lateral ventricle associated with thinner frontal GM, which is typically affected later in the disease.

BIBLIOGRAPHY:

Adak, S., Illouz, K., Gorman, W., Tandon, R., Zimmerman, E.A., Guariglia, R., Moore, M.M., Kaye, J.A. 2004. Predicting the rate of cognitive decline in aging and early Alzheimer disease. Neurology 63(1), 108-14.

Annweiler, C., Montero-Odasso, M., Hachinski, V., Seshadri, S., Bartha, R., Beauchet, O. 2013. Vitamin D concentration and lateral cerebral ventricle volume in older adults. Mol Nutr Food Res 57(2), 267-76. doi:10.1002/mnfr.201200418.

Apostolova, L.G., Green, A.E., Babakchanian, S., Hwang, K.S., Chou, Y.Y., Toga, A.W., Thompson, P.M. 2012. Hippocampal atrophy and ventricular enlargement in normal aging, mild cognitive impairment (MCI), and Alzheimer Disease. Alzheimer Dis Assoc Disord 26(1), 17-27. doi:10.1097/WAD.0b013e3182163b62.

Benjamini, Y., Hochberg, Y. 1995. Controlling the False Discovery Rate - a Practical and Powerful Approach to Multiple Testing. J Roy Stat Soc B Met 57(1), 289-300.

Blatter, D.D., Bigler, E.D., Gale, S.D., Johnson, S.C., Anderson, C.V., Burnett, B.M., Parker, N., Kurth, S., Horn, S.D. 1995. Quantitative volumetric analysis of brain MR: normative database spanning 5 decades of life. AJNR Am J Neuroradiol 16(2), 241-51.

Bourne, S.K., Conrad, A., Konrad, P.E., Neimat, J.S., Davis, T.L. 2012. Ventricular width and complicated recovery following deep brain stimulation surgery. Stereotact Funct Neurosurg 90(3), 167-72. doi:10.1159/000338094.

Braak, H., Braak, E. 1991. Neuropathological stageing of Alzheimer-related changes. Acta Neuropathol 82(4), 239-59.

Braskie, M.N., Klunder, A.D., Hayashi, K.M., Protas, H., Kepe, V., Miller, K.J., Huang, S.C., Barrio, J.R., Ercoli, L.M., Siddarth, P., Satyamurthy, N., Liu, J., Toga, A.W., Bookheimer, S.Y., Small, G.W., Thompson, P.M. 2010. Plaque and tangle imaging and cognition in normal aging and Alzheimer's disease. Neurobiol Aging 31(10), 1669-78. doi:10.1016/j.neurobiolaging.2008.09.012.

Buckner, R.L., Snyder, A.Z., Shannon, B.J., LaRossa, G., Sachs, R., Fotenos, A.F., Sheline, Y.I., Klunk, W.E., Mathis, C.A., Morris, J.C., Mintun, M.A. 2005a. Molecular, structural, and functional characterization of Alzheimer's disease: Evidence for a relationship between

default activity, amyloid, and memory. J Neurosci 25(34), 7709-17. doi:Doi 10.1523/Jneurosci.2177-05.2005.

Buckner, R.L., Snyder, A.Z., Shannon, B.J., LaRossa, G., Sachs, R., Fotenos, A.F., Sheline, Y.I., Klunk, W.E., Mathis, C.A., Morris, J.C., Mintun, M.A. 2005b. Molecular, structural, and functional characterization of Alzheimer's disease: evidence for a relationship between default activity, amyloid, and memory. J Neurosci 25(34), 7709-17. doi:10.1523/JNEUROSCI.2177-05.2005.

Carmichael, O.T., Kuller, L.H., Lopez, O.L., Thompson, P.M., Dutton, R.A., Lu, A., Lee, S.E., Lee, J.Y., Aizenstein, H.J., Meltzer, C.C., Liu, Y., Toga, A.W., Becker, J.T. 2007a. Cerebral ventricular changes associated with transitions between normal cognitive function, mild cognitive impairment, and dementia. Alzheimer Dis Assoc Disord 21(1), 14-24. doi:10.1097/WAD.0b013e318032d2b1.

Carmichael, O.T., Kuller, L.H., Lopez, O.L., Thompson, P.M., Dutton, R.A., Lu, A., Lee, S.E., Lee, J.Y., Aizenstein, H.J., Meltzer, C.C., Liu, Y., Toga, A.W., Becker, J.T. 2007b. Ventricular volume and dementia progression in the Cardiovascular Health Study. Neurobiol Aging 28(3), 389-97. doi:10.1016/j.neurobiolaging.2006.01.006.

Cavedo, E., Galluzzi, S., Pievani, M., Boccardi, M., Frisoni, G.B. 2012. Norms for imaging markers of brain reserve. J Alzheimers Dis 31(3), 623-33. doi:10.3233/JAD-2012-111817.

Chou, Y.Y., Lepore, N., Avedissian, C., Madsen, S.K., Parikshak, N., Hua, X., Shaw, L.M., Trojanowski, J.Q., Weiner, M.W., Toga, A.W., Thompson, P.M., Initia, A.D.N. 2009. Mapping correlations between ventricular expansion and CSF amyloid and tau biomarkers in 240 subjects with Alzheimer's disease, mild cognitive impairment and elderly controls. Neuroimage 46(2), 394-410. doi:DOI 10.1016/j.neuroimage.2009.02.015.

Chou, Y.Y., Lepore, N., de Zubicaray, G.I., Cannichael, O.T., Becker, J.T., Toga, A.W., Thompson, P.M. 2008. Automated ventricular mapping alignment reveals genetic effects with multi-atlas fluid image in Alzheimer's disease. Neuroimage 40(2), 615-30. doi:DOI 10.1016/j.neuroimage.2007.11.047.

Chou, Y.Y., Lepore, N., Saharan, P., Madsen, S.K., Hua, X., Jack, C.R., Shaw, L.M., Trojanowski, J.Q., Weiner, M.W., Toga, A.W., Thompson, P.M., Initi, A.s.D.N. 2010. Ventricular maps in 804 ADNI subjects: correlations with CSF biomarkers and clinical

decline. Neurobiol Aging 31(8), 1386-400. doi:DOI 10.1016/j.neurobiolaging.2010.05.001.

Chou, Y.Y., Lepore, N., de Zubicaray, G.I., Rose, S.E., Carmichael, O.T., Becker, J.T., Toga, A.W., Thompson, P.M. 2007. Automated 3D mapping and shape analysis of the lateral ventricles via fluid registration of multiple surface-based atlases. 2007 4th IEEE International Symposium on Biomedical Imaging: Macro to Nano 1288-91.

Coffey, C.E., Ratcliff, G., Saxton, J.A., Bryan, R.N., Fried, L.P., Lucke, J.E. 2001. Cognitive correlates of human brain aging: A quantitative magnetic resonance imaging investigation. J Neuropsych Clin N 13(4), 471-85. doi:DOI 10.1176/appi.neuropsych.13.4.471.

Dale, A.M., Fischl, B., Sereno, M.I. 1999. Cortical surface-based analysis - I. Segmentation and surface reconstruction. Neuroimage 9(2), 179-94. doi:DOI 10.1006/nimg.1998.0395.

Feng, L., Isaac, V., Sim, S., Ng, T.P., Krishnan, K.R.R., Chee, M.W.L. 2013. Associations Between Elevated Homocysteine, Cognitive Impairment, and Reduced White Matter Volume in Healthy Old Adults. Am J Geriat Psychiat 21(2), 164-72. doi:DOI 10.1016/j.jagp.2012.10.017.

Ferrarini, L., Palm, W.M., Olofsen, H., van Buchem, M.A., Reiber, J.H., Admiraal-Behloul, F. 2006. Shape differences of the brain ventricles in Alzheimer's disease. Neuroimage 32(3), 1060-9. doi:10.1016/j.neuroimage.2006.05.048.

Ferrarini, L., Palm, W.M., Olofsen, H., van der Landen, R., van Buchem, M.A., Reiber, J.H., Admiraal-Behloul, F. 2008. Ventricular shape biomarkers for Alzheimer's disease in clinical MR images. Magn Reson Med 59(2), 260-7. doi:10.1002/mrm.21471.

Fischl, B., Dale, A.M. 2000. Measuring the thickness of the human cerebral cortex from magnetic resonance images. P Natl Acad Sci USA 97(20), 11050-5. doi:DOI 10.1073/pnas.200033797.

Fischl, B., Salat, D.H., Busa, E., Albert, M., Dieterich, M., Haselgrove, C., van der Kouwe, A., Killiany, R., Kennedy, D., Klaveness, S., Montillo, A., Makris, N., Rosen, B., Dale, A.M. 2002. Whole brain segmentation: Automated labeling of neuroanatomical structures in the human brain. Neuron 33(3), 341-55. doi:Doi 10.1016/S0896-6273(02)00569-X.

Fischl, B., Sereno, M.I., Dale, A.M. 1999a. Cortical surface-based analysis. II: Inflation, flattening, and a surface-based coordinate system. Neuroimage 9(2), 195-207. doi:10.1006/nimg.1998.0396.

Fischl, B., Sereno, M.I., Tootell, R.B., Dale, A.M. 1999b. High-resolution intersubject averaging and a coordinate system for the cortical surface. Hum Brain Mapp 8(4), 272-84.

Fischl, B., van der Kouwe, A., Destrieux, C., Halgren, E., Segonne, F., Salat, D.H., Busa, E., Seidman, L.J., Goldstein, J., Kennedy, D., Caviness, V., Makris, N., Rosen, B., Dale, A.M. 2004. Automatically parcellating the human cerebral cortex. Cereb Cortex 14(1), 11-22. doi:DOI 10.1093/cercor/bhg087.

Fjell, A.M., Amlien, I.K., Westlye, L.T., Walhovd, K.B. 2009a. Mini-Mental State Examination Is Sensitive to Brain Atrophy in Alzheimer's Disease. Dement Geriatr Cogn 28(3), 252-8. doi:Doi 10.1159/000241878.

Fjell, A.M., Walhovd, K.B., Fennema-Notestine, C., McEvoy, L.K., Hagler, D.J., Holland, D., Brewer, J.B., Dale, A.M. 2009b. One-year brain atrophy evident in healthy aging. J Neurosci 29(48), 15223-31. doi:10.1523/JNEUROSCI.3252-09.2009.

Fleisher, A.S., Sun, S., Taylor, C., Ward, C.P., Gamst, A.C., Petersen, R.C., Jack, C.R., Aisen, P.S., Thal, L.J., Study, A.s.D.C. 2008. Volumetric MRI vs clinical predictors of Alzheimer disease in mild cognitive impairment. Neurology 70(3), 191-9. doi:DOI 10.1212/01.wnl.0000287091.57376.65.

Folstein, M.F., Folstein, S.E., McHugh, P.R. 1975. "Mini-mental state". A practical method for grading the cognitive state of patients for the clinician. J Psychiatr Res 12(3), 189-98.

Frisoni, G.B., Geroldi, C., Beltramello, A., Bianchetti, A., Binetti, G., Bordiga, G., DeCarli, C., Laakso, M.P., Soininen, H., Testa, C., Zanetti, O., Trabucchi, M. 2002. Radial width of the temporal horn: A sensitive measure in Alzheimer disease. Am J Neuroradiol 23(1), 35-47.

Gong, Z., Lu, J., Chen, J., Wang, Y., Yuan, Y., Zhang, T., Guo, L., Miller, L.S., and the Georgia Centenarian Study. 2011. Ventricle Shape Analysis for Centenarians, Elderly Subjects, MCI and AD Patients. MBIA, 84-92.

Gutman, B.A., Hua, X., Rajagopalan, P., Chou, Y.Y., Wang, Y., Yanovsky, I., Toga, A.W., Jack, C.R., Jr., Weiner, M.W., Thompson, P.M. 2013. Maximizing power to track Alzheimer's disease and MCI progression by LDA-based weighting of longitudinal ventricular surface features. Neuroimage 70, 386-401. doi:10.1016/j.neuroimage.2012.12.052.

Han, X., Jovicich, J., Salat, D., van der Kouwe, A., Quinn, B., Czanner, S., Busa, E., Pacheco, J., Albert, M., Killiany, R., Maguire, P., Rosas, D., Makris, N., Dale, A., Dickerson, B., Fischl, B. 2006. Reliability of MRI-derived measurements of human cerebral cortical thickness: The effects of field strength, scanner upgrade and manufacturer. Neuroimage 32(1), 180-94. doi:DOI 10.1016/j.neuroimage.2006.02.051.

Hua, X., Hibar, D.P., Ching, C.R., Boyle, C.P., Rajagopalan, P., Gutman, B.A., Leow, A.D., Toga, A.W., Jack, C.R., Jr., Harvey, D., Weiner, M.W., Thompson, P.M. 2013. Unbiased tensor-based morphometry: improved robustness and sample size estimates for Alzheimer's disease clinical trials. Neuroimage 66, 648-61. doi:10.1016/j.neuroimage.2012.10.086.

Isaac, V., Sim, S., Zheng, H., Zagorodnov, V., Tai, E.S., Chee, M. 2011. Adverse associations between visceral adiposity, brain structure, and cognitive performance in healthy elderly. Front Aging Neurosci 3. doi:Artn 12

Jack, Weigand, S.D., Shiung, M.M., Przybelski, S.A., O'Brien, P.C., Gunter, J.L., Knopman, D.S., Boeve, B.F., Smith, G.E., Petersen, R.C. 2008. Atrophy rates accelerate in amnestic mild cognitive impairment. Neurology 70(19), 1740-52.

Jack, C.R., Jr., Bernstein, M.A., Fox, N.C., Thompson, P., Alexander, G., Harvey, D., Borowski, B., Britson, P.J., J, L.W., Ward, C., Dale, A.M., Felmlee, J.P., Gunter, J.L., Hill, D.L., Killiany, R., Schuff, N., Fox-Bosetti, S., Lin, C., Studholme, C., DeCarli, C.S., Krueger, G., Ward, H.A., Metzger, G.J., Scott, K.T., Mallozzi, R., Blezek, D., Levy, J., Debbins, J.P., Fleisher, A.S., Albert, M., Green, R., Bartzokis, G., Glover, G., Mugler, J., Weiner, M.W. 2008. The Alzheimer's Disease Neuroimaging Initiative (ADNI): MRI methods. J Magn Reson Imaging 27(4), 685-91. doi:10.1002/jmri.21049.

Jack, C.R., Jr., Shiung, M.M., Gunter, J.L., O'Brien, P.C., Weigand, S.D., Knopman, D.S., Boeve, B.F., Ivnik, R.J., Smith, G.E., Cha, R.H., Tangalos, E.G., Petersen, R.C. 2004. Comparison of different MRI brain atrophy rate measures with clinical disease progression in AD. Neurology 62(4), 591-600.

Jack, C.R., Jr., Shiung, M.M., Weigand, S.D., O'Brien, P.C., Gunter, J.L., Boeve, B.F., Knopman, D.S., Smith, G.E., Ivnik, R.J., Tangalos, E.G., Petersen, R.C. 2005. Brain atrophy rates predict subsequent clinical conversion in normal elderly and amnestic MCI. Neurology 65(8), 1227-31. doi:10.1212/01.wnl.0000180958.22678.91.

Jernigan, T.L., Archibald, S.L., Fennema-Notestine, C., Gamst, A.C., Stout, J.C., Bonner, J., Hesselink, J.R. 2001. Effects of age on tissues and regions of the cerebrum and cerebellum. Neurobiol Aging 22(4), 581-94. doi:Doi 10.1016/S0197-4580(01)00217-2.

Kline, R.P., Pirraglia, E., Cheng, H., De Santi, S., Li, Y., Haile, M., de Leon, M.J., Bekker, A. 2012. Surgery and brain atrophy in cognitively normal elderly subjects and subjects diagnosed with mild cognitive impairment. Anesthesiology 116(3), 603-12. doi:10.1097/ALN.0b013e318246ec0b.

Leow, A.D., Yanovsky, I., Chiang, M.C., Lee, A.D., Klunder, A.D., Lu, A., Becker, J.T., Davis, S.W., Toga, A.W., Thompson, P.M. 2007. Statistical properties of Jacobian maps and the realization of unbiased large-deformation nonlinear image registration. Ieee T Med Imaging 26(6), 822-32. doi:Doi 10.1109/Tmi.2007.892646.

Longstreth, W.T.J. 1998. Brain abnormalities in the elderly: frequency and predictors in the United States (the Cardiovascular Health Study). J Neural Transm-Supp (53), 9-16.

Madsen, S.K., Gutman, B. A., Joshi, S. H., Toga, A. W., Jack, C. R. Jr., Weiner, M. W., Thompson, P. M., for the Alzheimer's Disease Neuroimaging Initiative (ADNI). 2013. Mapping dynamic changes in ventricular volume onto the cortical surface in normal aging, MCI, and Alzheimer's disease. The 16th International Conference on Medical Imaging Computing and Computer Assisted Intervention.

Mueller, S.G., Weiner, M.W., Thal, L.J., Petersen, R.C., Jack, C.R., Jagust, W., Trojanowski, J.Q., Toga, A.W., Beckett, L. 2005. Ways toward an early diagnosis in Alzheimer's disease: the Alzheimer's Disease Neuroimaging Initiative (ADNI). Alzheimers Dement 1(1), 55-66. doi:10.1016/j.jalz.2005.06.003.

Murphy, E.A., Holland, D., Donohue, M., McEvoy, L.K., Hagler, D.J., Dale, A.M., Brewer, J.B., Neuroimaging, A.s.D. 2010. Six-month atrophy in MTL structures is associated with subsequent memory decline in elderly controls. Neuroimage 53(4), 1310-7. doi:DOI 10.1016/j.neuroimage.2010.07.016.

Nestor, S.M., Rupsingh, R., Borrie, M., Smith, M., Accomazzi, V., Wells, J.L., Fogarty, J., Bartha, R., Initi, A.s.D.N. 2008. Ventricular enlargement as a possible measure of

Alzheimers disease progression validated using the Alzheimers disease neuroimaging initiative database. Brain 131, 2443-54. doi:Doi 10.1093/Brain/Awn146.

Olesen, P.J., Guo, X., Gustafson, D., Borjesson-Hanson, A., Sacuiu, S., Eckerstrom, C., Bigler, E.D., Skoog, I. 2011. A population-based study on the influence of brain atrophy on 20-year survival after age 85. Neurology 76(10), 879-86. doi:10.1212/WNL.0b013e31820f2e26.

Perlman, D. 2007. Cortical Thickness: Practicalities and Comparisons. University of Wisconsin Statistics 692 project.

Qiu, A., Fennema-Notestine, C., Dale, A.M., Miller, M.I. 2009. Regional shape abnormalities in mild cognitive impairment and Alzheimer's disease. Neuroimage 45(3), 656-61.

Resnick, S.M., Goldszal, A.F., Davatzikos, C., Golski, S., Kraut, M.A., Metter, E.J., Bryan, R.N., Zonderman, A.B. 2000. One-year age changes in MRI brain volumes in older adults. Cereb Cortex 10(5), 464-72. doi:DOI 10.1093/cercor/10.5.464.

Resnick, S.M., Pham, D.L., Kraut, M.A., Zonderman, A.B., Davatzikos, C. 2003. Longitudinal magnetic resonance imaging studies of older adults: a shrinking brain. J Neurosci 23(8), 3295-301.

Ridha, B.H., Anderson, V.M., Barnes, J., Boyes, R.G., Price, S.L., Rossor, M.N., Whitwell, J.L., Jenkins, L., Black, R.S., Grundman, M., Fox, N.C. 2008. Volumetric MRI and cognitive measures in Alzheimer disease : comparison of markers of progression. J Neurol 255(4), 567-74. doi:10.1007/s00415-008-0750-9.

Sanchez-Benavides, G., Gomez-Anson, B., Sainz, A., Vives, Y., Delfino, M., Pena-Casanova, J. 2010. Manual validation of FreeSurfer's automated hippocampal segmentation in normal aging, mild cognitive impairment, and Alzheimer Disease subjects. Psychiat Res-Neuroim 181(3), 219-25. doi:DOI 10.1016/j.pscychresns.2009.10.011.

Schott, J.M., Price, S.L., Frost, C., Whitwell, J.L., Rossor, M.N., Fox, N.C. 2005. Measuring atrophy in Alzheimer disease: a serial MRI study over 6 and 12 months. Neurology 65(1), 119-24. doi:10.1212/01.wnl.0000167542.89697.0f.

Serra, L., Cercignani, M., Lenzi, D., Perri, R., Fadda, L., Caltagirone, C., Macaluso, E., Bozzali, M. 2010. Grey and White Matter Changes at Different Stages of Alzheimer's Disease. J Alzheimers Dis 19(1), 147-59. doi:Doi 10.3233/Jad-2010-1223.

Silbert, L.C., Quinn, J.F., Moore, M.M., Corbridge, E., Ball, M.J., Murdoch, G., Sexton, G., Kaye, J.A. 2003. Changes in premorbid brain volume predict Alzheimer's disease pathology. Neurology 61(4), 487-92.

Team, R.D.C. 2008. R: A language and environment for statistical computing. R Foundation for Statistical Computing, Vienna, Austria.

Thompson, P.M., Hayashi, K.M., de Zubicaray, G., Janke, A.L., Rose, S.E., Semple, J., Herman, D., Hong, M.S., Dittmer, S.S., Doddrell, D.M., Toga, A.W. 2003. Dynamics of gray matter loss in Alzheimer's disease. J Neurosci 23(3), 994-1005.

Thompson, P.M., Hayashi, K.M., de Zubicaray, G.I., Janke, A.L., Rose, S.E., Semple, J., Hong, M.S., Herman, D.H., Gravano, D., Doddrell, D.M., Toga, A.W. 2004. Mapping hippocampal and ventricular change in Alzheimer disease. Neuroimage 22(4), 1754-66. doi:DOI 10.1016/j.neuroimage.2004.03.040.

Wahlund, L.O., Andersson-Lundman, G., Basun, H., Almkvist, O., Bjorksten, K.S., Saaf, J., Wetterberg, L. 1993. Cognitive functions and brain structures: a quantitative study of CSF volumes on Alzheimer patients and healthy control subjects. Magn Reson Imaging 11(2), 169-74.

Walhovd, K.B., Fjell, A.M., Reinvang, I., Lundervold, A., Dale, A.M., Eilertsen, D.E., Quinn, B.T., Salat, D., Makris, N., Fischl, B. 2005. Effects of age on volumes of cortex, white matter and subcortical structures. Neurobiol Aging 26(9), 1261-70. doi:DOI 10.1016/j.neurobiolaging.2005.05.020.

Wang, D., Chalk, J.B., Rose, S.E., de Zubicaray, G., Cowin, G., Galloway, G.J., Barnes, D., Spooner, D., Doddrell, D.M., Semple, J. 2002. MR image-based measurement of rates of change in volumes of brain structures. Part II: application to a study of Alzheimer's disease and normal aging. Magn Reson Imaging 20(1), 41-8.

Whitwell, J.L., Przybelski, S.A., Weigand, S.D., Knopman, D.S., Boeve, B.F., Petersen, R.C., Jack, C.R. 2007. 3D maps from multiple MRI illustrate changing atrophy patterns as subjects progress from mild cognitive impairment to Alzheimer's disease. Brain 130, 1777-86. doi:Doi 10.1093/Brain/Awml12.

Wyman, B.T., Harvey, D.J., Crawford, K., Bernstein, M.A., Carmichael, O., Cole, P.E., Crane, P.K., Decarli, C., Fox, N.C., Gunter, J.L., Hill, D., Killiany, R.J., Pachai, C., Schwarz, A.J., Schuff, N., Senjem, M.L., Suhy, J., Thompson, P.M., Weiner, M., Jack, C.R., Jr. 2012. Standardization of analysis sets for reporting results from ADNI MRI data. Alzheimers Dement. doi:10.1016/j.jalz.2012.06.004.

Zhang, Y., Qiu, C., Lindberg, O., Bronge, L., Aspelin, P., Backman, L., Fratiglioni, L., Wahlund, L.O. 2010. Acceleration of hippocampal atrophy in a non-demented elderly population: the SNAC-K study. Int Psychogeriatr 22(1), 14-25. doi:10.1017/S1041610209991396.

CHAPTER 3

Brain imaging of modifiable risk factors for dementia

3.1 Thyroid hormones and structural brain differences in non-demented elderly

This section is adapted from the following paper.

Madsen, S.K., Liang, L., Boyle, C. A., Rajagopalan, P., Cappola, A. R., Becker, J. T., Lopez, O. L., Thompson, P. M. (2013). Thyroid hormones are related to future differences in brain tissue in 495 healthy euthyroid elderly. in preparation for submission July 2013.

Thyroid Hormones are related to Future Differences in Brain Tissue in 495 Healthy Euthyroid Elderly

Sarah K. Madsen, B.S.[a], Letty Liang, B.S. [a], Christina Boyle, B.S. [a], Priya Rajagopalan, M.B.B.S., M.P.H[a]., Anne R. Cappola, M.D., Sc.M. [b], James T. Becker, Ph.D.[c], Oscar L. Lopez, M.D. [d], Paul M. Thompson, Ph.D. [a]

a. Imaging Genetics Center, Laboratory of Neuro Imaging, Department of Neurology, UCLA
b. Department of Medicine, University of Pennsylvania
c. Department of Psychiatry, University of Pittsburgh Medical Center
d. Department of Neurology, University of Pittsburgh Medical Center

Will submit in July 2013

Abstract:

Alterations in levels of thyroid hormones, even within the normal range, are associated with cognitive deficits increased risk for dementia in the elderly, which have higher rates of subclinical deviations in thyroid hormone levels. Thyroid hormones have known interactions with beta amyloid pathology, effect cardiovascular function, and can alter working memory. Understand how thyroid hormone levels are related to structural brain integrity in the elderly, may present an opportunity to improve cognition or decrease dementia risk. Using data from the Cardiovascular Health Study (CHS), we investigated the relationship between thyroid hormone levels and future differences in regional brain tissue volumes in 485 cognitively normal euthyroid elderly individuals. We excluded individuals taking thyroid medication or with clinical thyroid dysfunction, and controlled for thyroid antibody positivity. Higher levels of free T4 were significantly related to brain tissue contraction in bilateral frontal cortex, pre- and postcentral gyri, right supramarginal cortex, right middle temporal white matter, left precuneus, and right lateral occipital white matter. Higher levels of free T4 were also associated with brain tissue expansion in left lateral occipital gray matter, bilateral lingual gyrus, and left occipital pole, right heschl's gyrus, and the right transverse cistern. These areas include those implicated in traditional Alzheimer's disease pathology, as well as, areas that relate to symptoms of thyroid dysfunction.

Keywords:

MRI; elderly; thyroid hormones; thyroxine; fT4; thyrotropin; TSH; triiodothyronine; fT3l; euthyroid; non-demented; tensor based morphometry; brain

Introduction:

The thyroid hormone system plays a crucial role in mediating metabolism throughout life and in nervous system development. There is evidence that the thyroid hormone system changes in old age [1] [2] [3], perhaps as the body loses its ability to produce or respond to thyroid hormones or as the set-point for thyroid hormone levels changes based on different metabolic demands [4] [5]. Several studies have linked thyroid dysfunction to cognitive impairment and to increased risk for Alzheimer's disease and mild cognitive impairment [6][7]. This is true even for alterations in thyroid hormone levels that are well within clinically acceptable levels. Since current treatment options for Alzheimer's dementia are sparse and the expected number of demented elderly is set to expand, it's of huge clinical importance to identify ways to reduce dementia risk in the elderly. Understanding more about how thyroid hormone levels are related to the brain in healthy elderly individuals, could lead to better guidelines for reducing dementia risk by more careful modulation of thyroid hormone levels using existing treatment options, if continued research deems this appropriate

Rates of subclinical thyroid dysfunction increase with age [8], from 0.4% to 3.5% for subclinical hypothyroidism and from 1.9% to 7.8% for subclinical hyperthyroidism in individuals under vs. over the age of 65 years old [2]. Others have found even higher rates of subclinical hypothyroidism (up to 20% [9]) among elderly populations. Rates of undiagnosed thyroid dysfunction are also high among the elderly [10] [11]. Thyroid conditions are more common in women and this holds true for the elderly population [11] [12].

Alterations of thyroid hormone levels in both directions have been linked to several aspects of general prognosis and specifically to cognitive health in the elderly. Subclinical hypothyroidism is related to longevity and lower levels of thyroid hormones are found in close

relatives of [13]. Higher levels of fT4 are associated with poorer long-term survival rates in hospitalized elderly [14] and reduced levels of T4 and T3 are associated with a transient post-operative cognitive impairment in the elderly [15]. While some cross-sectional studies of subclinically hypothyroidism in the elderly have found no or very subtle differences in cognition (as measured by the MMSE) [16] [17] [18], other studies show deficits in memory (especially delayed retrieval of verbal information) and cognition [19] [20] [21], that may improve with L-T4 treatment [22]. Lower levels of T4 in elderly women are also associated with greater risk for cognitive decline in one longitudinal study [23]. Subclinical hyperthyroidism in the elderly has also been linked to worse cognition in elderly individuals without dementia [2] [24] [2]. Higher levels of fT4 within the normal range are associated with worse MMSE scores [24] and less independence in daily activities in mild-moderate Alzheimer's dementia [25]. Subclinically higher levels of T3 are associated with worse memory, visuospatial, and executive function in mild cognitive impairment [26] and with worse executive function, but not memory in cognitively normal elderly [27]. Interestingly, even though levels of TSH are used to categorize individuals within subclinical and clinical thyroid dysfunction, several studies found that T3 or T4 were associated with cognition, but not TSH levels themselves [23] [25] [26] [15] [25], suggesting that T3 and T4 may be more sensitive markers.

Links between overt thyroid disorder and dementia are not strong (possibly because overt thyroid conditions are more likely to be identified and treated); however several lines of evidence link subclinical alterations in thyroid hormone levels to risk for dementia in the elderly. The prevalence of over thyroid disorders in the elderly with dementia is not higher than in cognitively normal elderly [28] [29], and the incidence of dementia is not higher in overt thyroid dysfunction [30]. Also, levels of thyroid hormones may not be statistically different between demented and

non-demented elderly [31] [32] [33] [5]. However, cross-sectional [34] and longitudinal studies have found that subclinical hyperthyroidism is associated with increased risk for dementia (possibly by up to more than three-fold [35]). Higher fT4 is associated with increased risk for developing dementia [36] [37] and with greater loads of amyloid and tau pathology at autopsy in elderly euthyroid men [37]. In cognitively normal elderly women, both higher and lower levels of TSH are associated with increased risk of developing Alzheimer's disease [38] and subclinically lower TSH increased risk for Alzheimer's disease [39]. Subclinically lower levels of TSH [40], T3 [41] [40] [42], and fT4 [40] have been found in patients with Alzheimer's disease.

Several structural brain imaging studies on thyroid hormones have been conducted on whole brain volume and in specific regions of interest [33] [44] [45] [46].Studies of functional activations [47] [48] and cerebral blood perfusion [49] [50] [51] have also been performed. Ours is the first study to look at structural differences in the whole brain on a voxel-wise level in a large cohort of elderly euthyroid individuals. Since CHS collected extensive clinical information, we were also able to exclude individuals who were taking thyroid hormone medications and to control for the possible confounding effects of thyroid hormone antibody positivity.

We analyzed associations between thyroid hormone levels and tissue volume differences at each voxel in the brain for 485 non-demented euthyroid elderly individuals in the Cardiovascular Health Study (CHS). Thyroid hormone measures were taken in 1992-3 and in 1996-7, while brain MRIs were acquired at a follow-up assessment in 1998. This data enables us to relate thyroid hormone measures to future differences in brain anatomy. We found that higher levels of free T4 (fT4) at the first time point were significantly associated with later brain tissue contraction in areas implicated in working memory and higher-order cognition (bilateral

superior, inferior, middle frontal gyri, medial frontal cortex), primary somatosensory and motor functions (pre- and postcentral gyri), language (right supramarginal gyrus) and age-related memory loss (right temporal white matter). Higher levels of fT4 were also associated with future brain tissue expansion in visual (left lateral occipital and occipital pole, bilateral lingual gyrus) and auditory (right heschl's gyrus) regions. Regional brain volumes were not significantly associated with levels of thyroid stimulating hormone (TSH) or total triiodothyronine (T3) levels at either tine point, or with fT4 levels taken in 1996-7.

Materials and Methods:

Subjects:

We analyzed data from cognitively normal elderly individuals in the Cardiovascular Health Study (CHS). Data was collected at four sites across the US and each subject received blood tests for thyroid hormone levels in 1992-1993 and in 1995-1996 and a brain MRI scan in 1998. Demographics are described in **Table 1**. Subjects were excluded if their TSH levels exceeded the clinical norms [52, 53] (clinically hyperthyroid (>20.01 mU/L), N=7 excluded; clinically hypothyroid (<0.44 mU/L,) N=2 excluded; N=119 excluded because thyroid hormone data for 1992-1993 was missing) or if they were taking thyroid medication at any time point within the study (N=98 excluded). Our sample included only euthyroid elderly individuals without dementia (N=498 total for TSH, N=494 for T3, N=495 for fT4). We also controlled for thyroid antibody positivity (N=55 positive, N=432 negative, N=11 unknown), excluding subjects whose antibody status was unknown (N= 487 total analyzed for TSH, N=484 total for T3, N=185 total for fT4, see **Table 1** for demographics). In a follow-up analysis, we looked separately at groups of individuals who were borderline hyperthyroid (N=189 for TSH, N=188 for T3 and

fT4), subclinically hyperthyroid (N=230 for TSH, N=227 for T3, N=228 for fT4), or borderline and hypothyroid together (N=79 for TSH, T3, and fT4, combined due to lower total number of subjects). These distinctions were made following accepted guidelines, with the borderline group being closer to normal and the subclinical group being closer to clinically different levels [52, 53].

Table 1	All Euthyroid Healthy Elderly	Excluding Antibody Positivity
Subjects (*n*)	498	487
Age (years)	77.6 ± 3.8	77.57 ± 3.87
Sex	281F, 217M	274F, 231M
Education (years)	13.3 ± 2.7	13.34 ± 2.71
Scan Site	11 WHU 160 UCD 123 JHU 204 UP	11 WHU 155 UCD 122 JHU 199 UP
TSH (uIU/mL)	2.71 ± 2.09 (*n*=498)	2.73 ± 2.11 (*n*=487)
Total T3 (nmol/L)	1.81 ± 0.33 (*n*=494)	1.81 ± 0.33 (*n*=484)
Free T4 (ng/dL)	1.19 ± 0.17 (*n*=495)	1.19 ± 0.17 (*n*=485)
Antibody positivity (positive/negative)	55/432 (*n*=487)	55/432 (*n*=487)

Table 1. Demographic Information

Demographic information for our study population is shown (mean ± standard deviation). The four scan sites are Wake Forest University (WFU), University of California at Davis (UCD), John Hopkins University (JHU), and University of Pittsburgh (UP).

Thyroid Hormone Levels:

All subjects included in our study received blood serum tests for levels of TSH (uIU/mL), total T3 (nmol/L), free T4 (ng/dL), and thyroid hormone antibody positivity (positive or

negative). We grouped subjects into tertiles based on their thyroid hormone levels. Due to the relatively small magnitude and range of values for the thyroid hormone levels (as is expected in this measurement), the thyroid hormone values for several subjects fell directly on the threshold distinguishing the bins. To follow a consistent rule, we assigned these subjects to the higher bin (for example, if a subject had a free T4 level of 1.1100, which was the cutoff between the first and second tertiles, this subject was assigned to the second tertile). This explains why there are not an equal number of subjects in each tertile.

Since our data includes MRI scans obtained several years after the measurement of thyroid hormone levels, we thought it was important to assess the stability of thyroid hormone levels across the two time points (1992-1993 and 1996-1997). We calculated the mean and standard deviation of TSH and fT4 levels at each time point and performed two-way paired *t*-tests to compare each measure across this interval. T3 was only available at the first time point (1992-1993), so we were not able to assess stability of this measure in our data. These calculations were performed in our sample of euthyroid elderly, excluding subjects who were taking thyroid medication or who tested positive for thyroid hormone antibodies.

MRI Acquisition and Preprocessing:

All MRI scans were acquired on a 1.5 T GE Signa scanner (GE Medical Systems, Milwaukee, WI, LX Version) at four sites (Wake Forest University (WFU), University of California at Davis (UCD), John Hopkins University (JHU), and University of Pittsburgh (UP)). A whole brain 3D volumetric spoiled gradient recalled acquisition (SPGR) was obtained for each subject (TE/TR = 5*25 msec, slip angle = 40^0, NEX = 1, slice thickness = 1.5 mm/0 mm

interslice gap). Images were acquired with an in-plane acquisition matrix of 256 x 256 x 256 image elements, 250 x 250 mm^2 field of view, and an in-plane voxel size of 0.98 mm.

Each subjects' brain scan was corrected for intensity inhomogeneity (N3, [54, 55]) and linearly registered to the International Consortium for Brain Mapping (ICBM [56]) standard brain template. A nine- parameter registration was used to account for global position and scale differences across individuals, including head size, which has been found to outperform six-parameter registration in multi-centers studies such as CHS [57, 58]. Registered images were re-sampled into an isotropic voxels (220 voxels in each *x*, *y*, *z* axis) with a final voxel size of 1 mm^3.

Tensor Based Morphometry (TBM):

A minimal deformation template (MDT) was created from 40 cognitively normal CHS subjects after preprocessing and registration. This "average brain template" enables automated image registration, reduces statistical bias, and optimizes the detection of statistically significant effects [57], which can be interpreted as deviations from an "average normal" brain in our sample. The subjects selected for the template are chosen to create an unbiased representation of our sample, with equal number of men and women (N=20 each). There is no significant difference in age or thyroid hormone levels between our sample and the MDT (p>0.05 for age and for TSH, T3, and fT4 at 1992-1993 and 1996-1997).

After preprocessing, all scans were nonlinearly aligned to the study-specific MDT template, resulting in a common coordinate system. We plotted the Jacobian determinant for each subject, which is the local expansion or contraction factor of the 3D elastic warping transform. 3D Jacobian maps show relative volume differences between each individual subject

and the common MDT template. For each individual, this represents the relative expansion or contraction at each brain voxel compared to the population average. For example, in a dementia study, you would expect to find relative contraction in brain regions that experience tissue loss, along with expansion in regions such as the lateral ventricles, which expand in dementia.

Sixty subjects with processed brain MRI data were excluded because demographic and clinical data was not available for these subjects. Thirty-seven subjects were excluded due to poor MRI quality.

Statistics: Relating Thyroid Hormone Levels to Brain Tissue Volumes

Statistical tests were performed using the general linear model (GLM) at each voxel. Brain volume differences are the dependent *Y* variable. We tested a series of GLM models for each thyroid hormone measure separately (TSH, T3, and fT4 in tertiles) at two time points (1992-1993 and 1996-1997) using the MRI brain data collected in 1998. We controlled for the effects of age, sex, years of education, and scanner site. We then tested GLM models after controlling for the presence of thyroid hormone antibodies (positive or negative), in addition to controlling for age, sex, years of education, scanner site. For significant tests, we created average jacobian maps for the first and third tertile of the thyroid hormone measure, and then computed an average difference map to visualize the magnitude of brain tissue differences.

We also tested GLM models for each thyroid hormone measure separately (TSH, T3, and fT4 in tertiles) in subsets of the sample, looking separately at groups who were subclinically hyperthyroid (*N*=230), borderline hyperthyroid (*N*=189), and borderline and subclinical hypothyroid combined (these last two groups were run together because the sample sizes were

small alone, *N*=18 for borderline hypothyroid, *N*=61 for subclinical hypothyroid, *N*=79 together). We controlled for the effects of age, sex, years of education, and scanner site.

Results:

Thyroid Variable characteristics and stability

We calculated the following tertiles based on thyroid hormone levels for the first time point (TSH: 0.006-0.942, 0.943-1.069, 1.070-75.770; T3: 0.762-1.652, 1.653-1.929, 1.930-3.970; fT4: 0.348-1.109, 1.110-1.259, 1.260-1.780) in the whole sample. Demographic information for the fT4 tertiles in 1992-1993 are shown in **Table 2** because this variable was significantly associated with brain volumes (TSH and T3 tertiles were also analyzed, but were not significant).

Table 2	First tertile of Free T4	Second tertile of Free T4	Third tertile of Free T4
Subjects (*n*)	157	173	165
Age (years)	77.08 ± 2.83	77.91 ± 2.83	77.65 ± 2.53
Sex	99F, 58M	90F, 83M	91F, 74M
Education (years)	13.54 ± 3.62	13.30 ± 3.76	13.19 ± 4.09
Scan Site	4 WHU 53 UCD 45 JHU 55 UP	2 WHU 58 UCD 35 JHU 78 UP	5 WHU 47 UCD 43 JHU 70 UP
TSH (uIU/mL)	3.60 ± 2.79 (*n*=157)	2.36 ± 1.69 (*n*=173)	2.25 ± 1.30 (*n*=165)
Total T3 (nmol/L)	1.77 ± 0.32 (*n*=156)	1.81 ± 0.35 (*n*=173)	1.85 ± 0.32 (*n*=165)
Free T4 (ng/dL)	1.00 ± 0.08 (*n*=157)	1.18 ± 0.04 (*n*=173)	1.37 ± 0.09 (*n*=165)
Antibody positivity (positive/negative)	31/124 (*n*=155)	10/157 (*n*=167)	14/149 (*n*=163)

Table 2. Demographic Information for free T4 tertiles

Demographic information for our study population is shown for free T4 tertiles (mean ± standard deviation). The four scan sites are Wake Forest University (WFU), University of California at Davis (UCD), John Hopkins University (JHU), and University of Pittsburgh (UP). We present this data because we found significant associations between free T4 tertiles and brain tissue differences in our sample (TSH and T3 tertiles were not significant). Due to the relatively small magnitude and range of values for the thyroid hormone levels (as is expected in this measurement), the thyroid hormone values for several subjects fell directly on the threshold distinguishing the bins. In these cases, we assigned these subjects to the higher bin to follow a consistent rule (for example, if a subject had a free T4 level of 1.1100, which was the cutoff between the first and second tertiles, this subject was assigned to the second tertile). This explains why there are not an equal number of subjects in each tertile.

In our analysis of thyroid hormone stability over time, we found that TSH was stable across the 3-5 year interval between the two time points (p=0.17, N=487 in 1992-1993, N=481 in 1996-1997). On average, fT4 levels were significantly lower (by 0.1327 ng/dL) at the later time point compared to the first time point (p=0.01, N=485 in 1992-1993, N=68 in 1996-1997). At the

later time point, a much smaller number of subjects had fT4 data available and only 35 subjects overlapped between the two time points. The later time points consisted predominantly of subclinical hypothyroid individuals (*N*=42 subclinical hypothyroid, *N*=6 borderline hypothyroid, *N*=6 borderline hyperthyroid, *N*=3 subclinical hyperthyroid), whereas the earlier time point included a large proportion of borderline and subclinical hyperthyroid individuals (*N*=61 subclinical hypothyroid, *N*=0 borderline hypothyroid, *N*=201 borderline hyperthyroid, *N*=223 subclinical hyperthyroid). These differences in the sample characteristics may explain why we found significant associations for the first, but not second time point, in the TBM analysis.

Associations with Brain Tissue Volumes

All results presented in the following sections are for the associations between thyroid hormone levels measured in 1992-1993 and brain MRI scans collected in 1998. No significant associations were found between TSH or T3 levels and regional brain tissue volumes, either at the 1992-1993 or 1996-1997 time points. No significant associations were found for fT4 at the 1996-1997 time point. All results presented below are for fT4 levels measured in 1992-1993.

Free T4 Levels and Brain Tissue Volumes in Euthyroid Elderly Individuals

As shown in **Figure 1**, higher levels of fT4 are associated with future brain tissue contraction in left superior frontal gyrus, bilateral middle frontal gyrus, left pre- and post-central gyrus, right post-central and supramarginal gyrus, left precuneus, right lateral occipital white matter, and bilateral anterior lobe of the cerebellum (negative association). In maps comparing averages of the first and third tertile of fT4, we see relative tissue contraction of approximately

5% for frontal regions, 5-7% for pre- and post-central gyrus and supramarginal cortex, 4-5% for the left precuneus, 5% for right lateral occipital white matter, and 1-4% for cerebellum.

Higher levels of free T4 were associated with future brain tissue expansion in left lateral occipital cortex, and left lingual gyrus and occipital pole (positive association). We also see relative tissue expansion in the third tertile compared to the first tertile of fT4 in the range of 2-6% for left occipital regions.

We controlled for age, sex, years of education, and scan site. Results were corrected for multiple comparisons by thresholding at the standard p=0.05 false discovery rate (FDR) across the entire brain.

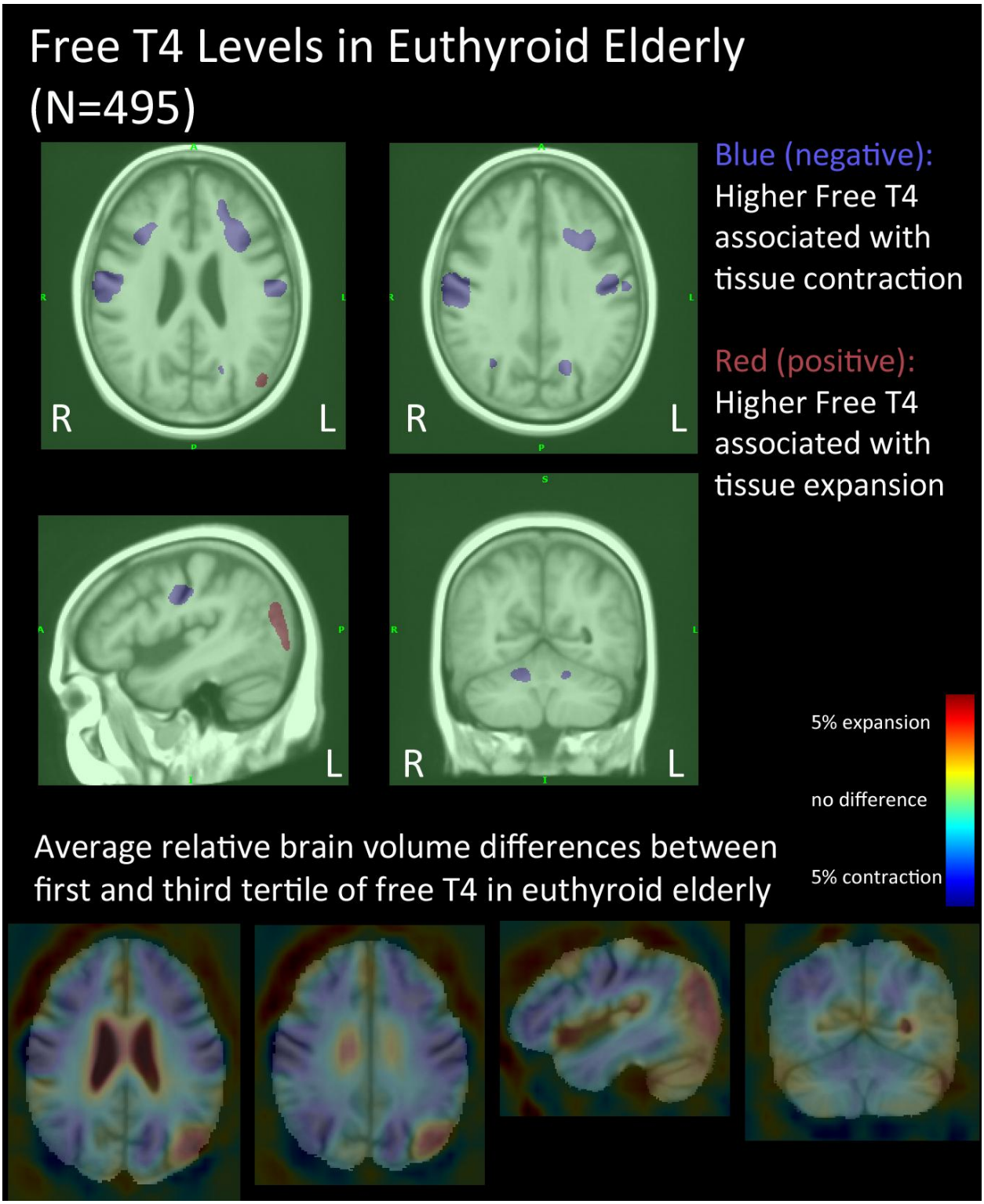

Figure 1. Significant associations between fT4 levels and regional brain tissue volumes

Top Panel: Whole-brain maps show were significant associations were found between levels of fT4 and future regional brain tissue volumes in N=495 non-demented euthyroid elderly adults in the CHS study who were not taking thyroid medication, after controlling for age, sex, years of education, and scan site. Blue represents areas where there is a significant negative relationship between fT4 levels and future brain volume differences (i.e. higher levels of fT4 are associated with tissue contraction). Red represents areas where there is a significant positive relationship between fT4 levels and later brain volume differences (i.e. higher levels of fT4 are associated with tissue expansion). Results were corrected for multiple comparisons by thresholding at the standard p=0.05 false discovery rate (FDR) across the entire brain.

Bottom Panel: Whole-brain maps show differences in Jacobian determinants between the group averages for the first and third tertile of fT4 levels (third tertiles mean map – first tertile mean map). Light to dark blue represents areas with up to 5% relative tissue contraction in the third tertile of fT4 compared to the first tertile of fT4, on average. Yellow to red represents areas with up to 5% relative expansion in the first tertile compared to the third tertile of fT4, on average. Green represents no difference, on average.

Free T4 Levels and Brain Tissue Volumes in Euthyroid Elderly Individuals, controlling for thyroid antibody positivity

As shown in **Figure 2**, after adding thyroid antibody positivity as an additional covariate of non-interest, the maps of significant associations showed similar patterns that covered a larger extent and also included several regions that were not found in the previous map.

Higher levels of free T4 were associated with future brain tissue contraction in bilateral superior, middle, and frontal cortex, bilateral frontal pole, bilateral medial frontal cortex, bilateral pre- and post-central cortex, right supramarginal cortex, right middle temporal white matter, left precuneus, and right lateral occipital white matter (negative association). Results in the bilateral inferior frontal gyrus, bilateral frontal pole, bilateral middle frontal gyrus, right precentral gyrus (before only a very small result here in the sulcus), and right temporal white matter were not found in the previous map that did not control for thyroid antibody positivity.

Higher levels of free T4 were associated with future brain tissue expansion in left lateral occipital gray matter, bilateral lingual gyrus, left occipital pole, right heschl's gyrus, and the right transverse cistern (positive association). Results in the right lingual gyrus, right heschl's gyrus, and right transverse cistern were not found in the previous map that did not control for thyroid antibody positivity.

We controlled for age, sex, years of education, scan site, and the presence of thyroid hormone antibodies (positive or negative). Results were corrected for multiple comparisons by thresholding at the standard p=0.05 false discovery rate (FDR) across the entire brain.

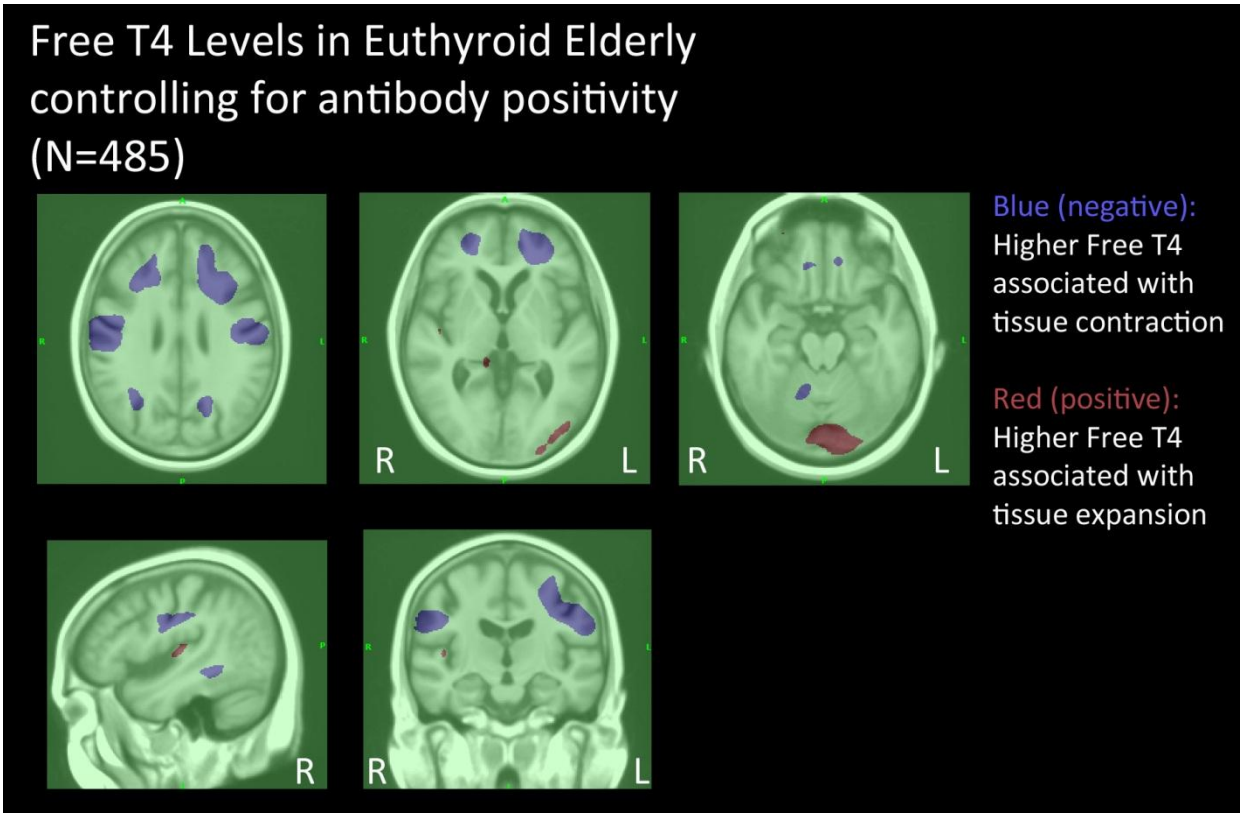

Figure 2. Significant associations between fT4 levels and regional brain tissue volumes become more pronounced after controlling for thyroid antibody positivity

Whole-brain maps show were significant associations were found between levels of fT4 and future regional brain tissue volumes in N=485 non-demented euthyroid elderly adults in the CHS study who were not taking thyroid medication, after controlling for age, sex, years of education, scan site, and the presence of thyroid hormone antibodies (positive or negative). Blue represents areas where there is a significant negative relationship between fT4 levels and later brain volume differences (i.e. higher levels of fT4 are associated with tissue contraction). Red represents areas where there is a significant positive relationship between fT4 levels and later brain volume differences (i.e. higher levels of fT4 are associated with tissue expansion). Results were corrected for multiple comparisons by thresholding at the standard p=0.05 false discovery rate (FDR) across the entire brain.

Free T4 Levels and Brain Tissue Volumes in Elderly Individuals with Subclinical Hyperthyroidism

As shown in **Figure 3**, we also performed the analysis in a subgroup of the sample with subclinical hyperthyroidism. The previous maps were of all euthyroid elderly individuals in the study and included those with subclinical hypothyroidism, borderline hypothyroidism, subclinical hyperthyroidism, or subclinical hyperthyroidism. In all samples, we excluded individuals who with clinical thyroid dysfunction or who were taking thyroid medication.

Higher levels of fT4 were associated with future brain tissue contraction in left orbitofrontal cortex, right postcentral and supramarginal gyrus, and left precuneus. The left precuneus and right postcentral and supramarginal gyrus were also found in the full sample (which included borderline and subclinical hypothyroidism and hyperthyroidism). In this map we also found a small region in left orbitofrontal cortex in which tissue contraction was related to higher levels of free T4, which was not seen in the full euthyroid sample (either with or without the additional covariate for thyroid antibody positivity). No areas of significant positive associations were found in the subclinically hyperthyroid group.

We controlled for age, sex, years of education, and scan site. Results were corrected for multiple comparisons by thresholding at the standard p=0.05 false discovery rate (FDR) across the entire brain.

No significant results were found for thyroid hormone variables in the other groups (borderline hyperthyroid or in subclinical and borderline hypothyroid combined).

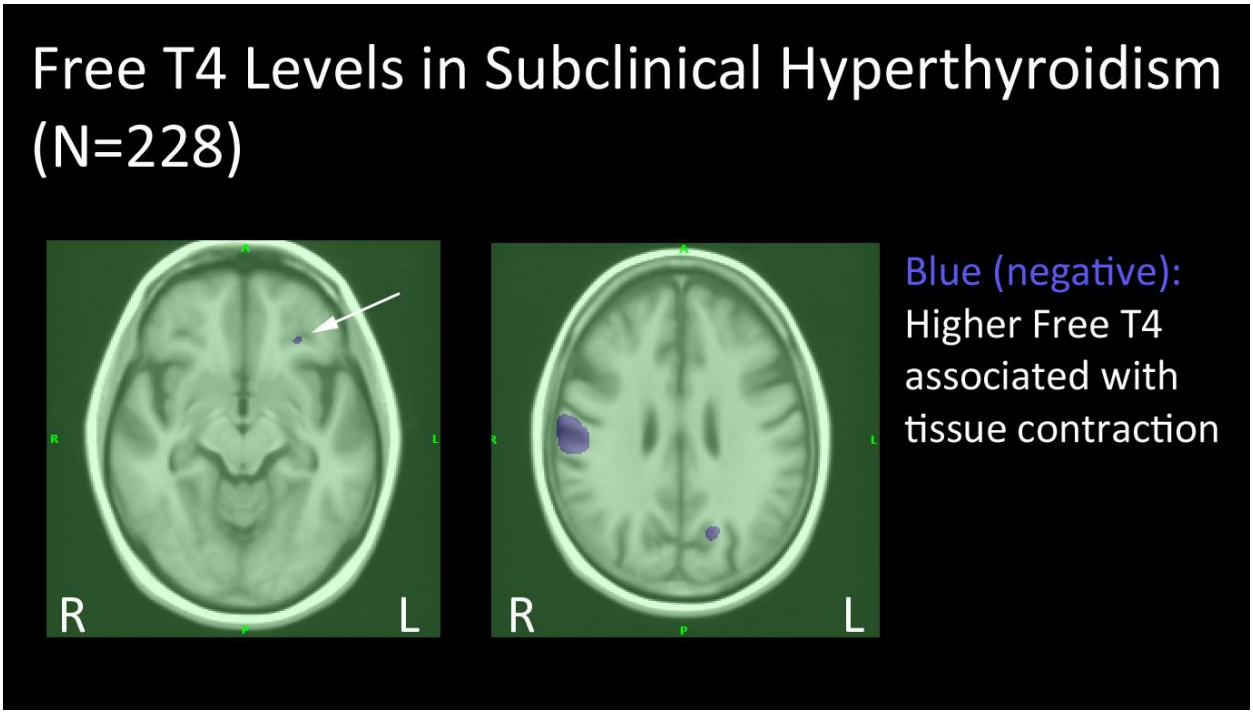

Figure 3. Significant associations between fT4 levels and regional brain tissue volumes in Subclinical Hyperthyroidism

Whole-brain maps show were significant associations were found between levels of fT4 and future regional brain tissue volumes in a N=228 subclinically hyperthyroid sample of the non-demented euthyroid elderly adults in the CHS study who were not taking thyroid medication, after controlling for age, sex, years of education, and scan site. Blue represents areas where there is a significant negative relationship between fT4 levels and later brain volume differences (i.e. higher levels of fT4 are associated with tissue contraction). No significant positive relationships between fT4 levels and later brain volume differences (i.e. higher levels of fT4 are associated with tissue expansion) were found. Results were corrected for multiple comparisons by thresholding at the standard p=0.05 false discovery rate (FDR) across the entire brain.

Discussion:

We found that subclinical fT4 levels at the first time point were significantly associated with future regional brain tissue differences in euthyroid elderly adults without dementia. Higher levels of fT4 were associated with relative tissue contraction in bilateral frontal, bilateral primary

motor and sensory areas (pre-and post-central gyri), and higher order visual regions (left precuneus). Higher levels of fT4 were associated with relative brain tissue expansion in primary visual areas (left lateral occipital and occipital pole). These effects were independent of the effects of age, sex, education, and scan site in this multicenter study. Adding in thyroid hormone antibody positivity as a regressor of non-interest resulted in similar maps with a larger extent, and included additional significant positive associations in bilateral frontal gyri and right temporal white matter and negative associations in right visual (lingual gyrus) and auditory regions (heschl's gyrus). We believe that the negative associations may be driven mainly by the subclinically hyperthyroid group, which showed significant negative associations with fT4 and left orbitofrontal cortex, right postcentral and supramarginal, and left precuneus when analyzed, even with reduced power due to the lower sample size. Also, fT4 levels as the later time point, which was predominantly subclinically hypothyroid, were not significantly associated with any differences in brain volumes.

Overall, we found that fT4 levels, within clinically normal levels, were associated with structural brain differences in areas underling visual memory (lingual gyrus), visuospatial processing (precuneus), age-related memory decline (temporal white matter), and primary visual (occipital) and auditory (heschl's gyrus) processing. Dementia is accompanied by deficits in visuospatial and language abilities, in addition to memory and executive function deficits. Thyroid hormone dysfunction is associated with sensorimotor disturbances (fatigue in hypothyroid and tremor in hyperthyroid, with muscle weakness occurring in both), which is a domain that is generally preserved in dementia. Left lateral occipital GM volume differences have also been linked with two thyroid hormone transporter gene variants [59]. This suggests

that the patterns we are seeing include a combination of thyroid hormone and dementia-related brain differences.

The measures of thyroid hormone levels were stable across individuals from the first to the second time point (3-5 years apart), suggesting that it is informative to test for associations between thyroid hormone measures taken at one time point and brain MRI scans obtained later. This study provides unique information about how thyroid hormone levels in non-demented euthyroid elderly relate to future differences in brain structure.

The lack of significant results for TSH may make sense, as other studies have found that subclinical TSH levels are useful to classify individuals by thyroid hormone status, but TSH levels themselves are not always associated with clinical scores or dementia risk [23] [25] [26] [15] [25] . It's not clear why T3 levels were not significantly associated with brain volumes in our study, although other studies have found association in fT4, but not T3 [14] [33]. The majority of active thyroid hormone in the brain is converted locally in brain tissue from the more stable fT4 in the blood stream [61], so it's possible that fT4 levels are more indicative of true thyroid hormone available in the brain.

In previous structural brain imaging studies, subclinically higher levels of fT4 have been associated with lower hippocampal and amygdala volumes in healthy euthyroid elderly (no findings for TSH or T3) [33]. Subclinically higher TSH have been associated with the presence of severe brain atrophy and infarct-like lesions (assessed visually with a binary rating scale) in elderly euthyroid men, but not women [45]. We did not find any associations with TSH in our sample, which included both men and women. It's possible that a strong gender effect is present, which would be interesting to explore in future analysis that are split by gender. In development, resistance to thyroid hormones is associated with structural abnormalities in areas that we found

to be significantly related to fT4 levels in the elderly [46]. Males with developmental thyroid hormone resistance are more likely to be missing gyri in the parietal bank of the Sylvian fissure (where we found relative brain volume contraction with higher free T4 levels) and to have multiple transverse gyri in heschl's gyrus (where we found relative brain volume expansion with higher free T4 levels, after controlling for thyroid antibody positivity).

In functional MRI studies, subclinical and clinical hypothyroidism in adults is associated with impaired performance on a working memory task and is accompanied by alterations in brain activity within the frontoparietal network [47]. After treatment to normalize thyroid hormone levels, the activation patterns also normalized. Our results found relative brain tissue contraction with higher fT4 in these fronto-parietal areas. In a study that investigated the neural correlates of motor weakness symptoms in thyroid dysfunction, increased activation in areas including primary and supplementary somatosensory and motor areas, auditory regions, the inferior temporal lobe, and cerebellum were found in both hypo- and hyperthyroid adults performing a finger-taping task [48]. Our results show structural differences in these somatosensory, motor, and auditory areas.

Clinical hypothyroidism in adults is associated with reduced cerebral blood flow to areas including right parieto-occipital gyri, precuneus, lingual gyrus, and pre- and post-central gyri [49] [50].Our study found significant relationships between fT4 levels and brain volumes in these regions. These areas are implicated in attention, motor speed, memory, and visuospatial processing, which are aspects of cognitive that are hindered when thyroid hormone levels are altered.

There is evidence to suggest that alterations in thyroid hormone levels in adulthood can actually cause differences in blood flow and in brain structure, although these studies were either small or performed in animal models. Transiently induced hypothyroidism after thyroidectomy causes decreased blood flow in parietal and occipital region, which normalized with thyroid hormone replacement in about half of the sixteen participants [51]. One study in adult rats, found that experimentally lowering T3 (but not T4) caused a reduction in WM, GM, total brain, and hippocampal volumes, along with producing abnormal clusters of neurons in the corpus callosum [60]. A small study (N=11) of middle-aged adults found that lowering fT4 levels from hyperthyroid to normal levels over a span of several months reduced total brain volume and increased ventricle volume [44], suggesting that it may be possible for brain changes to occur in the short-term, possibly in addition to long-term changes [44]. More evidence is needed in this area, since these claims are somewhat dramatic.

Future work will analyze men and women separately to improve our understanding of the gender differences in thyroid dysfunction and brain anatomy, which may explain some of the discrepant findings in the existing literature. In addition, we will investigate how depression scores and obesity are involved in the relationship between thyroid hormones and brain differences. It would also be interesting to consider how trends may differ across different age groups, perhaps between elderly individuals younger and older than 80 years old.

BIBLIOGRAPHY:

1. Lamberts, S.W.J., *The endocrinology of aging and the brain.* Archives of Neurology, 2002. **59**(11): p. 1709-1711.

2. Ceresini, G., et al., *Thyroid Function Abnormalities and Cognitive Impairment in Elderly People: Results of the Invecchiare in Chianti Study.* Journal of the American Geriatrics Society, 2009. **57**(1): p. 89-93.

3. Feart, C., et al., *Aging affects the retinoic acid and the triiodothyronine nuclear receptor mRNA expression in human peripheral blood mononuclcar cells.* European Journal of Endocrinology, 2005. **152**(3): p. 449-458.

4. Bremner, A.P., et al., *Age-Related Changes in Thyroid Function: A Longitudinal Study of a Community-Based Cohort.* Journal of Clinical Endocrinology & Metabolism, 2012. **97**(5): p. 1554-1562.

5. Annerbo, S., M. Kivipelto, and J. Lokk, *A Prospective Study on the Development of Alzheimer's Disease with Regard to Thyroid-Stimulating Hormone and Homocysteine.* Dementia and Geriatric Cognitive Disorders, 2009. **28**(3): p. 275-280.

6. Krysiak, R., B. Marek, and B. Okopien, *[Subclinical hyperthyroidism]*. Endokrynologia Polska, 2007. **58**(6): p. 536-42.

7. Breteler, M.M., et al., *Medical history and the risk of Alzheimer's disease: a collaborative re-analysis of case-control studies. EURODEM Risk Factors Research Group.* International journal of epidemiology, 1991. **20 Suppl 2**: p. S36-42.

8. Bagchi, N., T.R. Brown, and R.F. Parish, *Thyroid-Dysfunction in Adults over Age 55 Years - a Study in an Urban United-States Community.* Archives of Internal Medicine, 1990. **150**(4): p. 785-787.

9. Roberts, L.M., et al., *Is subclinical thyroid dysfunction in the elderly associated with depression or cognitive dysfunction?* Annals of Internal Medicine, 2006. **145**(8): p. 573-581.

10. Atkinson, R.L., et al., *Occult Thyroid Disease in an Elderly Hospitalized Population.* Journals of Gerontology, 1978. **33**(3): p. 372-376.

11. Bahemuka, M. and H.M. Hodkinson, *Screening for Hypothyroidism in Elderly Inpatients.* British Medical Journal, 1975. **2**(5971): p. 601-603.

12. Drinka, P.J. and W.E. Nolten, *Prevalence of Previously Undiagnosed Hypothyroidism in Residents of a Midwestern Nursing-Home.* Southern Medical Journal, 1990. **83**(11): p. 1259-&.

13. Corsonello, A., et al., *A cross-section analysis of FT3 age-related changes in a group of old and oldest-old subjects, including centenarians' relatives, shows that a down-regulated thyroid function has a familial component and is related to longevity.* Age and ageing, 2010. **39**(6): p. 723-727.

14. De Alfieri, W., et al., *Thyroid Hormones as Predictors of Short- and Long-term Mortality in Very Old Hospitalized Patients.* J Gerontol A Biol Sci Med Sci, 2013.

15. Mafrica, F. and V. Fodale, *Thyroid function, Alzheimer's disease and postoperative cognitive dysfunction: A tale of dangerous liaisons?* Journal of Alzheimers Disease, 2008. **14**(1): p. 95-105.

16. Jorde, R., et al., *Neuropsychological function and symptoms in subjects with subclinical hypothyroidism and the effect of thyroxine treatment.* Journal of Clinical Endocrinology & Metabolism, 2006. **91**(1): p. 145-153.

17. Parle, J., et al., *A Randomized Controlled Trial of the Effect of Thyroxine Replacement on Cognitive Function in Community-Living Elderly Subjects with Subclinical Hypothyroidism: The Birmingham Elderly Thyroid Study.* Journal of Clinical Endocrinology & Metabolism, 2010. **95**(8): p. 3623-3632.

18. Roberts, L.M., et al., *Is subclinical thyroid dysfunction in the elderly associated with depression or cognitive dysfunction?* Annals of Internal Medicine, 2006. **145**(8): p. 573-81.

19. Burmeister, L.A., et al., *Hypothyroidism and cognition: Preliminary evidence for a specific defect in memory.* Thyroid, 2001. **11**(12): p. 1177-1185.

20. Cook, S.E., et al., *Memory impairment in elderly individuals with a mildly elevated serum TSH: The role of processing resources, depression and cerebrovascular disease.* Aging Neuropsychology and Cognition, 2002. **9**(3): p. 175-183.

21. Osterweil, D., et al., *Cognitive Function in Nondemented Older Adults with Hypothyroidism.* Journal of the American Geriatrics Society, 1992. **40**(4): p. 325-335.

22. Jaeschke, R., et al., *Does treatment with L-thyroxine influence health status in middle-aged and older adults with subclinical hypothyroidism?* Journal of General Internal Medicine, 1996. **11**(12): p. 744-749.

23. Volpato, S., et al., *Serum thyroxine level and cognitive decline in euthyroid older women.* Neurology, 2002. **58**(7): p. 1055-1061.

24. Stuerenburg, H.J., S. Arlt, and T. Mueller-Thomsen, *Free thyroxine, cognitive decline and depression in Alzheimer's disease.* Neuroendocrinology Letters, 2006. **27**(4): p. 535-537.

25. Patterson, M., J. Lonie, and J.M. Starr, *Thyroid function, cognition, functional independence and behavioural and psychological symptoms of dementia in Alzheimer's disease.* International Journal of Geriatric Psychiatry, 2010. **25**(11): p. 1196-1197.

26. Quinlan, P., et al., *Thyroid Hormones Are Associated with Poorer Cognition in Mild Cognitive Impairment.* Dementia and Geriatric Cognitive Disorders, 2010. **30**(3): p. 205-211.

27. Grigorova, M. and B.B. Sherwin, *Thyroid hormones and cognitive functioning in healthy, euthyroid women: A correlational study.* Hormones and Behavior, 2012. **61**(4): p. 617-622.

28. Barclay, L.L., et al., *Risk Factors in Alzheimer's Disease.* Alzheimer's and Parkinson's Disease, 1986. **29**: p. 141-146.

29. Lopez, O., et al., *Prevalence of Thyroid Abnormalities Is Not Increased in Alzheimers-Disease.* Neurobiology of Aging, 1989. **10**(3): p. 247-251.

30. Yoshimasu, F., et al., *The association between Alzheimer's disease and thyroid disease in Rochester, Minnesota.* Neurology, 1991. **41**(11): p. 1745-7.

31. Etgen, T., H. Bickel, and H. Forstl, *Metabolic and endocrine factors in mild cognitive impairment.* Ageing Research Reviews, 2010. **9**(3): p. 280-288.

32. Miller, J.W., et al., *Homocysteine, vitamin B-6, and vascular disease in AD patients.* Neurology, 2002. **58**(10): p. 1471-1475.

33. de Jong, F.J., et al., *Thyroid hormones, dementia, and atrophy of the medial temporal lobe.* The Journal of clinical endocrinology and metabolism, 2006. **91**(7): p. 2569-73.

34. Ganguli, M., et al., *Association between dementia and elevated TSH: a community-based study.* Biological Psychiatry, 1996. **40**(8): p. 714-25.

35. Kalmijn, S., et al., *Subclinical hyperthyroidism and the risk of dementia. The Rotterdam study.* Clinical Endocrinology, 2000. **53**(6): p. 733-737.

36. Yeap, B.B., et al., *Higher Free Thyroxine Levels Predict Increased Incidence of Dementia in Older Men: The Health In Men Study.* Journal of Clinical Endocrinology & Metabolism, 2012. **97**(12): p. E2230-E2237.

37. de Jong, F.J., et al., *Thyroid function, the risk of dementia and neuropathologic changes: The Honolulu-Asia Aging Study*. Neurobiology of Aging, 2009. **30**(4): p. 600-606.

38. Tan, Z.S., et al., *Thyroid function and the risk of Alzheimer disease: The Framingham Study.* Archives of Internal Medicine, 2008. **168**(14): p. 1514-1520.

39. van Osch, L.A.D.M., et al., *Low thyroid-stimulating hormone as an independent risk factor for Alzheimer disease.* Neurology, 2004. **62**(11): p. 1967-1971.

40. Li, Y.H., et al., *Hypothalamic-Pituitary-Thyroid Axis in Patients With Alzheimer Disease (AD).* Journal of Investigative Medicine, 2013. **61**(3): p. 578-581.

41. Thomas, D.R., et al., *Thyroid Status in Senile Dementia of the Alzheimer Type (Sdat).* Acta Psychiatrica Scandinavica, 1987. **76**(2): p. 158-163.

42. Faldt, R., et al., *Prevalence of thyroid hormone abnormalities in elderly patients with symptoms of organic brain disease.* Aging-Clinical and Experimental Research, 1996. **8**(5): p. 347-353.

43. Haupt, M. and A. Kurz, *Reversibility of Dementia in Hypothyroidism.* Journal of Neurology, 1993. **240**(6): p. 333-335.

44. Oatridge, A., et al., *Changes in brain size with treatment in patients with hyper- or hypothyroidism.* American Journal of Neuroradiology, 2002. **23**(9): p. 1539-1544.

45. Reitz, C., et al., *Relation of plasma thyroid-stimulating hormone levels to vascular lesions and atrophy of the brain in the elderly.* Neuroepidemiology, 2006. **27**(2): p. 89-95.

46. Leonard, C.M., et al., *Magnetic-Resonance-Imaging of Cerebral Anomalies in Subjects with Resistance to Thyroid-Hormone.* American Journal of Medical Genetics, 1995. **60**(3): p. 238-243.

47. Zhu, D.F., et al., *fMRI revealed neural substrate for reversible working memory dysfunction in subclinical hypothyroidism.* Brain, 2006. **129**: p. 2923-2930.

48. Khushu, S., et al., *Cortical activation during finger tapping in thyroid dysfunction: A functional magnetic resonance imaging study.* Journal of Biosciences, 2006. **31**(5): p. 543-550.

49. Krausz, Y., et al., *Regional cerebral blood flow in patients with mild hypothyroidism.* Journal of Nuclear Medicine, 2004. **45**(10): p. 1712-1715.

50. Krausz, Y., et al., *Brain SPECT study of common ground between hypothyroidism and depression.* International Journal of Neuropsychopharmacology, 2007. **10**(1): p. 99-106.

51. Nagamachi, S., et al., *Cerebral blood flow abnormalities induced by transient hypothyroidism after thyroidectomy - Analysis by Tc-99m-HMPAO and SPM96.* Annals of Nuclear Medicine, 2004. **18**(6): p. 469-477.

52. Cappola, A.R., et al., *Thyroid status, cardiovascular risk, and mortality in older adults.* Jama-Journal of the American Medical Association, 2006. **295**(9): p. 1033-1041.

53. Lekakis, J., et al., *Flow-mediated, endothelium-dependent vasodilatation is impaired in subjects with hypothyroidism, borderline hypothyroidism, and high-normal serum thyrotropin (TSH) values.* Thyroid, 1997. **7**(3): p. 411-414.

54. Sled, J.G., A.P. Zijdenbos, and A.C. Evans, *A nonparametric method for automatic correction of intensity nonuniformity in MRI data.* Ieee Transactions on Medical Imaging, 1998. **17**(1): p. 87-97.

55. Boyes, R.G., et al., *Intensity non-uniformity correction using N3 on 3-T scanners with mutichannel phased array coils.* Neuroimage, 2008. **39**(4): p. 1752-1762.

56. Mazziotta, J., et al., *A probabilistic atlas and reference system for the human brain: International Consortium for Brain Mapping (ICBM).* Philosophical Transactions of the Royal Society B-Biological Sciences, 2001. **356**(1412): p. 1293-1322.

57. Hua, X., et al., *Optimizing power to track brain degeneration in Alzheimer's disease and mild cognitive impairment with tensor-based morphometry: an ADNI study of 515 subjects.* Neuroimage, 2009. **48**(4): p. 668-81.

58. Paling, S.M., et al., *The application of serial MRI analysis techniques to the study of cerebral atrophy in late-onset dementia.* Medical image analysis, 2004. **8**(1): p. 69-79.

59. Dixson, L., et al., *Thyroid hormone transporter genes and grey matter changes in patients with major depressive disorder and healthy controls.* Psychoneuroendocrinology, 2011. **36**(6): p. 929-934.

60. Powell, M.H., et al., *Magnetic resonance imaging and volumetric analysis: Novel tools to study the effects of thyroid hormone disruption on white matter development*. Neurotoxicology, 2012. **33**(5): p. 1322-1329.

61. Schreiber, G. *The evolutionary and integrative roles of transthyretin in thyroid hormone homeostasis*. Journal of Endocrinology, 2002. **175**(1): p. 61-73.

3.2 Higher homocysteine is associated with thinner cortical gray matter

This section is adapted from the following paper.

Madsen S. K., Rajagopalan, P., Joshi, S.H., Toga, A.W., Thompson, P.M. & the Alzheimer's Disease Neuroimaging Initiative (ADNI) (2013). Elevated homocysteine is associated with thinner cortical gray matter in 803 ADNI subjects, *Neurobiology of Aging*, under review May 1 2013.

Higher homocysteine associated with thinner cortical gray matter in 803 ADNI subjects

Sarah K. Madsen B.S.[a], Priya Rajagopalan M.B.B.S, M.P.H. [a], Shantanu H. Joshi Ph.D. [a],

Arthur W. Toga Ph.D. [a], Paul M. Thompson Ph.D.[a,b]

& the Alzheimer's Disease Neuroimaging Initiative (ADNI)*

[a]Imaging Genetics Center, Laboratory of Neuro Imaging, Dept. of Neurology, UCLA
[b]Dept. of Psychiatry, Semel Institute, UCLA

Submitted to *Neurobiology of Aging*

June 6, 2013

*Data used in the preparation of this article were obtained from the Alzheimer's Disease Neuroimaging Initiative database (www.loni.ucla.edu/ADNI). As such, many investigators within the ADNI contributed to the design and implementation of ADNI and/or provided data but most did not participate in analysis or writing of this report. For a complete listing of ADNI investigators, please see: http://adni.loni.ucla.edu/wp-content/uploads/how_to_apply/ADNI_Authorship_List.pdf

Abstract

A substantial proportion of our risk for dementia in old age is associated with lifestyle factors (diet, exercise, and cardiovascular health) that are modifiable, at least in principle. One such risk factor – high homocysteine levels in the blood – is known to increase risk for Alzheimer's disease and vascular disorders. Here we set out to understand how homocysteine levels relate to 3D surface-based maps of cortical gray matter distribution (thickness, volume, surface area) computed from brain MRI in 803 elderly subjects from the Alzheimer's Disease Neuroimaging Initiative (ADNI) dataset. Individuals with higher serum levels of homocysteine had lower gray matter thickness in bilateral frontal, parietal, occipital and right temporal regions; and lower gray matter volumes in left frontal, parietal, temporal, and occipital regions, after controlling for diagnosis, age, and sex and correcting for multiple comparisons. These regional differences in gray matter structure may be useful biomarkers to assess the effectiveness of interventions, such as vitamin B supplements, that aim to prevent homocysteine-related brain atrophy by normalizing homocysteine levels.

Keywords

Alzheimer's disease; MRI; cortical; gray matter; atrophy; thickness; volume; surface area; brain structure; homocysteine; folate; vitamin B; ADNI

1. Introduction

The quest to avert the societal crisis of Alzheimer's disease (AD) involves understanding modifiable risk factors for dementia and how they affect the brain. The core pathology of AD (plaques and tangles) is challenging to treat, but there is a multitude of known risk factors that are modifiable (at least in principle), and contribute to dementia risk. Many recent studies have established consistent links between cognition and brain integrity with an individual's physical activity (Erickson et al., 2010), body mass index and its genetic determinants (Ho et al., 2010, Kerwin et al., 2011, Kerwin et al., 2010, Raji et al., 2010), blood levels of the stress-related hormone cortisol (Rajagopalan, 2013), the fat-mass related hormone leptin (Rajagopalan et al., 2013b), and biomarkers of kidney health, such as creatinine and cystatin C (Rajagopalan et al., 2013a). One factor in the blood that is perhaps less studied, in terms of detailed mapping of the brain's cortex, is homocysteine; although recent evidence has connected it to both brain atrophy and dementia risk (Rajagopalan et al., 2011).

An abnormally high level of homocysteine in the blood is a major cardiovascular risk factor (Bostom et al., 1999, Bots et al., 1997, Perry et al., 1995, Selhub et al., 1995) and there is mounting evidence that poor cardiovascular health is associated with brain atrophy and increased risk for developing Alzheimer's dementia (Breteler, 2000, Gustafson et al., 2004, Leritz et al., 2011, Muqtadar et al., 2012, Oulhaj et al., 2010, Salat et al., 2012, Swan et al., 1998). Deaths from cardiovascular events in the elderly (Bostom et al., 1999, Bots et al., 1997), coronary heart disease (Bostom et al., 1999), carotid atherosclerosis (Selhub et al., 1995), and stroke (Perry et al., 1995) are all more common in individuals with elevated homocysteine levels. High blood levels of homocysteine are also a known risk factor for the development of poor cognition and

dementia, including Alzheimer's disease (Lehmann et al., 1999, Morris et al., 2001, Riggs et al., 1996). In fact, the adjusted relative risk of dementia is 40% higher for every standard deviation increase in homocysteine (log transformed, as is standard) (Seshadri et al., 2002).

Mechanistically, elevated homocysteine levels promote neurotoxicity by altering synaptic function (Lipton et al., 1997) and inducing DNA damage in neurons (Kruman et al., 2000). The neurotoxic effects could explain the association between elevated homocysteine levels and dementia risk (Seshadri et al., 2002), white matter (WM) deterioration (Rajagopalan et al., 2011), and, as evaluated in the current study, altered profiles of cortical gray matter (GM) thickness and volume. In clinical studies, the reduction in cortical GM, along with previously reported WM deficits, may serve as a neuro-structural biomarker to help localize and identify regional brain atrophy associated with elevated homocysteine. Together, both GM and WM measures can also quantitatively assess the effects of interventions, such as vitamin B supplements, which normalize homocysteine levels (Clarke et al., 2005) and therefore may be expected to slow or prevent homocysteine-related cognitive decline (de Jager et al., 2012) and brain atrophy.

The link between homocysteine and dementia, along with the known mechanisms for homocysteine induced neurotoxicity, suggest that elevated homocysteine levels in the elderly might also be associated with brain atrophy detectable on MRI. Our previous study of 732 elderly Caucasians from the Alzheimer's Disease Neuroimaging Initiative (ADNI) cohort found that higher levels of homocysteine were significantly associated with lower regional WM volumes in large frontal and parietal regions (Rajagopalan et al., 2011). That study used whole-brain tensor-based morphometry (TBM) to show statistically significantly lower GM and WM associated with higher levels of homocysteine after controlling for the effects of sex, age, and

dementia diagnosis (AD or MCI) and correcting for multiple comparisons (false discovery rate). That analysis showed significant homocysteine effects in the smaller sample of MCI individuals separately (N=356), suggesting that homocysteine-related WM atrophy may be detectable early in the disease; although the lack of significant results in the separate AD or control groups could also be attributed to poorer statistical power (healthy controls, N=203; AD, N=173).

Importantly, the areas where WM volumes were lower in individuals with higher homocysteine levels appear to correspond with cortical GM regions that degenerate in AD (Apostolova et al., 2007b, Pievani et al., 2009, Salat et al., 1999, Serra et al., 2010, Thompson et al., 2003, Toga and Thompson, 2013). While the TBM method (used in Rajagopalan et al. 2011) is very sensitive to differences in subcortical WM and GM structures in the brain (Hua et al., 2013, Leow et al., 2005), it is not optimized for detecting effects on the thin strip of GM that makes up the cortical mantle. In TBM studies, it is challenging to perform accurate cortical morphometry, even with very large sample sizes, without the use of explicit cortical surface models that adapt to the geometry of the highly folded cortical surface. Without such models, a 3D volumetric nonlinear registration is not usually able to reliably register the cortical folds since it lacks of a reliable feature set to accurately match this complex geometry. With this in mind, we decided to use a surface-based morphometry approach for the current study, as cortical mapping has been informative in many studies of aging and AD (Apostolova et al., 2007a, Apostolova et al., 2007b, Apostolova and Thompson, 2007, Frisoni et al., 2009, Prestia et al., 2010, Thompson et al., 2003). To examine associations between homocysteine levels and cortical GM more precisely, and to accurately localize the associated cortical regions, we analyzed cortical GM thickness, volume, and surface area, in the ADNI sample of N=803 elderly individuals.

We hypothesized that lower cortical GM measures in frontal, parietal, and temporal regions – areas implicated in AD studies using MRI – would be significantly associated with higher levels of homocysteine, even after controlling for age, sex, and diagnosis. We were especially interested in knowing whether the homocysteine-associated atrophy pattern was essentially uniform across the brain, or whether it was detectable primarily in areas traditionally considered to be vulnerable to AD-related cortical thinning.

2. Methods

2.1. Study population

We analyzed brain MRI scans from 803 elderly individuals (AD: N=186, MCI: N=392, healthy elderly controls: N=225) who received a 1.5T anatomical brain MRI scan, blood draw, and neuropsychological battery as part of the ADNI study. Our subject sample included only subjects listed in the standard set of baseline scans obtained during the ADNI1 phase of data collection, which was created to promote rigor and meaningful comparability across the large number of ADNI studies (Wyman et al., 2012). Fourteen subjects from the standard set were excluded in our study because they did have homocysteine data (six subjects) or their cortical GM surfaces did not pass QC (eight subjects).

ADNI was launched in 2004 by the National Institute of Health, the Food and Drug Administration, private pharmaceutical companies, and non-profit organizations to identify and evaluate biomarkers of AD for use in multisite studies. All ADNI data are publicly available at adni.loni.ucla.edu. The study was conducted according to the Good Clinical Practice guidelines,

the Declaration of Helsinki, and the US 21 CFR Part 50–Protection of Human Subjects, and Part 56–Institutional Review Boards. Written informed consent was obtained from all participants in advance.

Blood serum samples were collected before breakfast on the morning of the baseline MRI scans, after an overnight fast in order to avoid inaccuracies due to recent consumption of certain foods. Total homocysteine levels were measured in a sample of blood plasma taken from each subject using a validated enzyme immunoassay (Shaw, 2008).

All individuals also underwent a thorough clinical and cognitive evaluation close to the time of the MRI scan acquisition, including a diagnosis of probable AD, MCI, or cognitively normal. A diagnosis of MCI is made for participants who have reported a subjective memory concern without impairment in other cognitive domains and no signs of dementia. A diagnosis of probable AD was made for subjects who met the NINCDS/ADRDA criteria. Inclusion and exclusion criteria are detailed in the ADNI protocol (Mueller et al., 2005).

We analyzed all N=803 ADNI individuals who had plasma homocysteine levels assessed at the time of their baseline MRI scans. All MRI scans underwent quality control after processing with the FreeSurfer software (v5.0.0) (Fischl and Dale, 2000, Perry, 1995) for cortical GM extraction (Table 1) by visually inspecting the cortical surfaces from multiple points of view. Only subjects that passed quality control were included in the study. A one-way ANOVA and separate one-tailed two-sample t-tests with unequal variance were used to statistically compare homocysteine levels across AD, MCI, and healthy elderly control groups (using p=0.05 as a significance criterion).

Table 1. Demographic characteristics of N=803 individuals analyzed in this study.

	AD	MCI	Controls	All Individuals
Sample Size (*n*)	186	392	225	803
Sex (women/men)	89/97	141/251	108/117	338/465
Age (years)	75.45 ± 6.84	75.39 ± 7.60	75.33 ± 7.67	75.30 ± 6.84
Plasma Homocysteine (μM)	10.77 ± 3.32 *	10.62 ± 2.82 *	9.94 ± 2.80	10.46 ± 2.95

Table 1: Selected demographic information for the study participants (mean ± standard deviation). An asterisk denotes a significant difference relative to the control group (see also **Figure 1**).

2.2. Image acquisition and processing

High-resolution structural brain MRI scans were acquired on 1.5T scanners from General Electric (Milwaukee, Wisconsin, USA), Siemens (Germany), or Philips (The Netherlands) with a standardized MRI protocol (Jack et al., 2008). Each scan involved a three-dimensional sagittal magnetization-prepared rapid gradient-echo sequence with the following parameters: repetition time (2400ms), flip angle (8°), inversion time (1000 ms), 24-cm field of view, a 192×192×166 acquisition matrix, a voxel size of 1.25×1.25×1.2 mm3, later reconstructed to 1 mm isotropic voxels.

2.3. FreeSurfer cortical GM analysis

Cortical reconstruction and GM segmentation was performed with the FreeSurfer image analysis suite (v5.0.0), which is documented and freely available for download online (http://surfer.nmr.mgh.harvard.edu/). Technical details of these procedures have been described previously (Dale et al., 1999, Fischl and Dale, 2000, Fischl et al., 2002, Fischl et al., 1999a, Fischl et al., 1999b, Fischl et al., 2004, Han et al., 2006). Briefly, the processing includes motion correction and averaging of each subject's volumetric T1-weighted MRI brain image, removal of non-brain tissue, intensity normalization, tessellation of cortical GM/WM boundary, automated topology correction and surface deformation along intensity gradients to optimally define cortical surface borders, registration to a spherical atlas using individual cortical folding patterns to align cortical anatomy across subjects, and creation of 3D maps of GM (as measured with thickness, volume, and surface area) at each point on the cortical surface. After processing, images are in an isotropic space of 256 voxels along each axis (*x*, *y*, and *z*) with a final voxel size of 1 mm^3. GM thickness was calculated as the average of the distance from the GM/cerebrospinal fluid boundary to the GM/WM surface, and vice versa, at each vertex on the cortical surface. The GM surface area at each vertex was defined as the average of the areas of triangles that include that vertex (clearly, "surface area" is not defined at a point, but this measure is proportional to the area of a cortical region, when averaged over that region). The GM volume was obtained by multiplying the GM thickness by the area of the surface layer equidistant between the inner and outer cortical surfaces.

2.4. Statistical Analysis

Statistical tests were conducted using the general linear model (GLM) analysis tools in FreeSurfer (mri_glmfit, v5.0.0). Smoothing was applied separately to each subject's 3D cortical surface map for GM thickness, volume, and surface area (kernel radius= 25 mm full width half maximum). We chose a large smoothing kernel based on the past literature showing that the size of regions affected by brain atrophy in this population is generally quite expansive (Buckner et al., 2005, Serra et al., 2010).

We tested a series of three step-wise GLM models for total homocysteine levels on cortical GM: (1) controlling for effects of sex and age in all subjects; (2) controlling for effects of sex, age, and diagnosis (probable AD, MCI, or healthy elderly control) in all subjects; and (3) controlling for sex and age in AD, MCI and healthy elderly control groups, separately. To control for false positives, we enforced a standard false discovery rate (FDR) correction (Benjamini and Hochberg, 1995, Genovese et al., 2002) for multiple statistical comparisons across voxels in the entire left and right brain surfaces, using the conventionally accepted false positive rate of 5% (q=0.05).

3. Results

3.1. Homocysteine levels across AD, MCI, and healthy elderly controls

A one-way ANOVA showed that homocysteine levels were significantly different across the AD, MCI, and healthy elderly controls (p=0.006, F=5.08, dof=2). Separate one-tailed two sample t-tests with unequal variance showed that AD (p=0.004) and MCI (p=0.002) groups each

had significantly higher levels of homocysteine compared to healthy elderly controls (AD: 10.77 ± 3.32 μM, MCI: 10.62 ± 2.82 μM, healthy elderly controls: 9.94 ± 2.80 μM), as expected. Homocysteine levels did not differ significantly between the AD and MCI groups (p=0.295).

3.2. Homocysteine and cortical GM thickness

In the entire sample, higher levels of serum homocysteine were significantly associated with thinner GM in large bilateral regions including frontal, parietal, temporal, and occipital cortex (**Figure 2A**), after controlling for age and sex. Results were similar, although not identical, between the left and right hemispheres. Adding diagnosis (AD, MCI, or control) to the regressors of non-interest, produced a map showing significant associations between higher levels of homocysteine and thinner cortical GM in the bilateral superior frontal gyrus, paracentral gyrus, precuneus, precentral gyrus, postcentral gyrus, and superior parietal cortex, along with right entorhinal, cuneus, pericalcarine cortex, middle temporal gyrus, superior temporal gyrus, inferior parietal cortex, pars opercularis, and caudal middle frontal gyrus (**Figure 2B**). No significant associations were found between homocysteine levels and cortical GM thickness in the AD, MCI, or healthy elderly control groups separately, after controlling for age and sex. All surface-based statistical results underwent correction for multiple comparisons using FDR (5% false positive rate, q=0.05). No areas of significant positive associations between higher homocysteine and greater cortical GM thickness were found.

Figure 2. Homocysteine and cortical GM thickness.

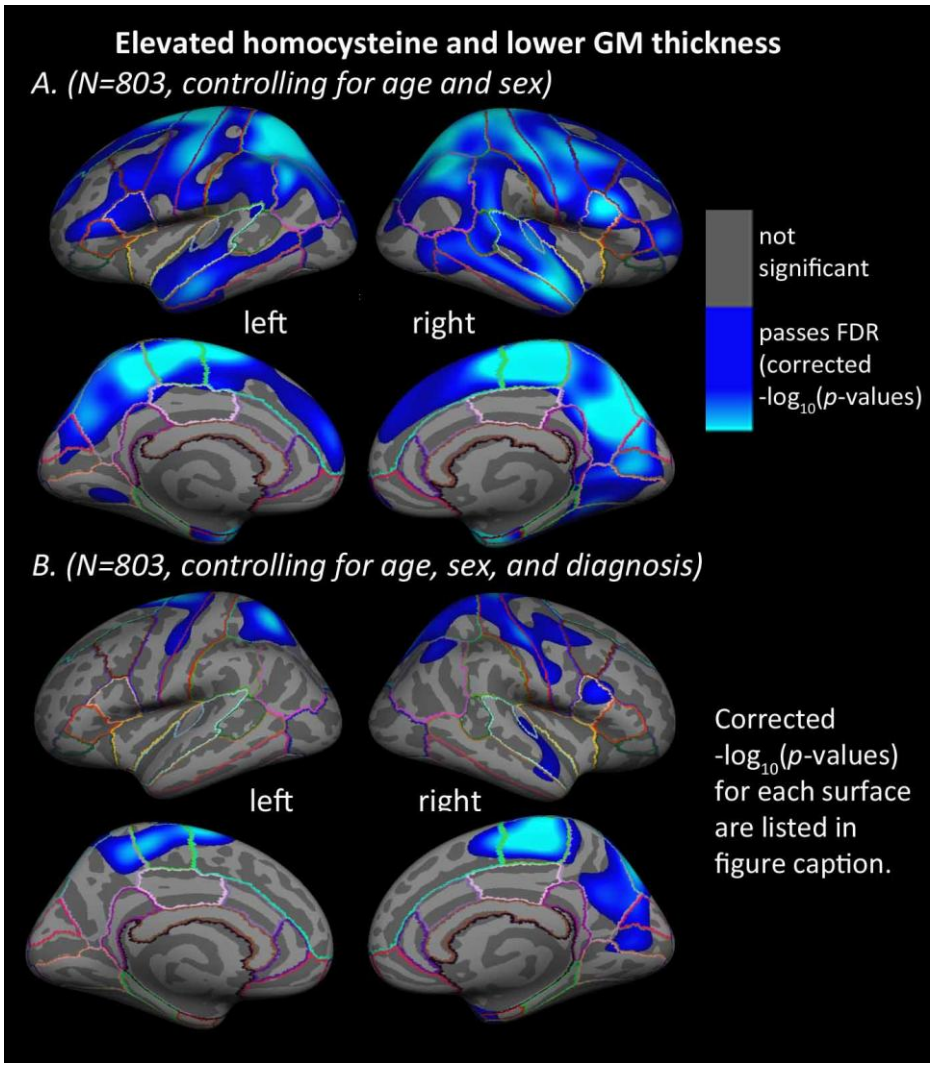

Figure 2: Whole-brain 3D maps show significant associations between homocysteine levels in the blood and cortical gray matter (GM) thickness in the left and right hemispheres for all *N*=803 subjects, (A) after controlling for age and sex (left: $-\log_{10}(p\text{-value})=1.597\text{-}3.855$, right: $-\log_{10}(p\text{-value})=1.499\text{-}3.757$, FDR corrected), and (B) after controlling for age, sex, and diagnosis (AD, MCI, or healthy elderly) (left: $-\log_{10}(p\text{-value})=2.321\text{-}4.579$, right: $-\log_{10}(p\text{-value})=1.996\text{-}4.253$, FDR corrected at $q=0.05$). Results were corrected for multiple comparisons by thresholding at a $p=0.05$ false discovery rate (FDR) threshold across the entire brain hemisphere. Blue areas represent points on the cortical surface where *p*-values passed the corrected significance threshold for a negative relationship between homocysteine levels and cortical thickness values (higher levels of homocysteine associated with lower cortical GM thickness). No areas of significant positive associations were found, in a post hoc test, after appropriate FDR correction.

3.3. Homocysteine and cortical GM volume

In the entire sample, higher levels of serum homocysteine were significantly associated with lower cortical GM volumes in large bilateral regions including frontal, parietal, temporal, and occipital lobes after controlling for age and sex (**Figure 3A**). Results were similar, but not identical, between the left and right hemispheres and covered a slightly smaller area of the brain surface compared to the cortical thickness results. Adding diagnosis (AD, MCI, or control) to the regressors of non-interest, produced a map showing significant associations between higher levels of homocysteine and lower cortical GM volumes in the left superior frontal gyrus, paracentral gyrus, precuneus, superior temporal gyrus, superior precentral gyrus, inferior postcentral gyrus, supramarginal gyrus and superior and inferior parietal cortex (no significant regions were found in the right hemisphere for cortical GM volume) (**Figure 3B**). No significant associations were found between homocysteine levels and cortical GM volumes in the AD, MCI, or healthy elderly control groups separately, after controlling for age and sex. All vertex-wise statistical results on the surfaces were corrected for multiple comparisons using standard FDR (5% false positive rate, q=0.05). No areas of significant positive associations between homocysteine and cortical GM volume were found.

Figure 3. Homocysteine levels are related to regional cortical GM volumes.

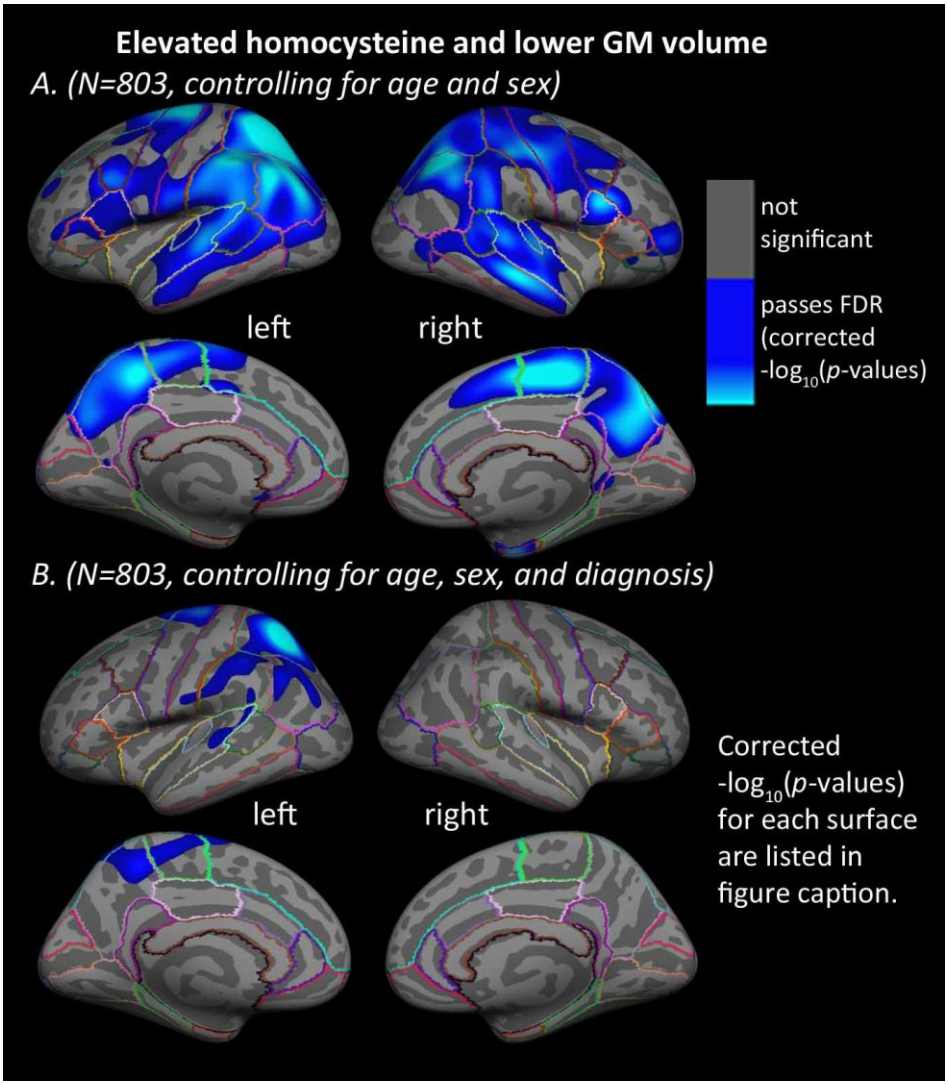

Figure 3: Whole brain 3D maps of significant associations between homocysteine levels and regional cortical gray matter (GM) volumes in the left and right hemispheres of all *N*=803 subjects, (A) after controlling for age and sex (left: $-\log_{10}(p\text{-value})$=1.673-3.930, right: $-\log_{10}(p\text{-value})$=1.663-3.920, FDR corrected) and (B) after controlling for age, sex, and diagnosis (AD, MCI, or healthy elderly) (left: $-\log_{10}(p\text{-value})$=2.204-4.462, right: not significant, FDR corrected). Results were corrected for multiple comparisons by thresholding at a p=0.05 false discovery rate (FDR) threshold across the entire brain surface. Blue areas represent points on the cortical surface where *p*-values passed the corrected significance threshold for a negative relationship between homocysteine levels and cortical GM volumes (higher levels of homocysteine associated with lower cortical GM volumes). No areas of significant positive associations were found.

3.4. Homocysteine and cortical GM surface area

In the entire sample, higher levels of serum homocysteine were significantly associated with lower cortical GM surface areas in left superior temporal, supramarginal, and inferior parietal cortices after controlling for age and sex (**Figure 4**). No significant regions were found in the right hemisphere for cortical GM surface area. Adding diagnosis (AD, MCI, or control) to the regressors of non-interest did not produce any regions of significant association. No significant associations were found between homocysteine levels and cortical GM surface area in the AD, MCI, or healthy elderly control groups separately, after controlling for age and sex. All results presented passed correction for multiple comparisons using FDR (5% false positive rate, q=0.05). No areas of significant positive associations between homocysteine and cortical GM surface area were found.

Figure 4. Homocysteine and cortical GM surface area.

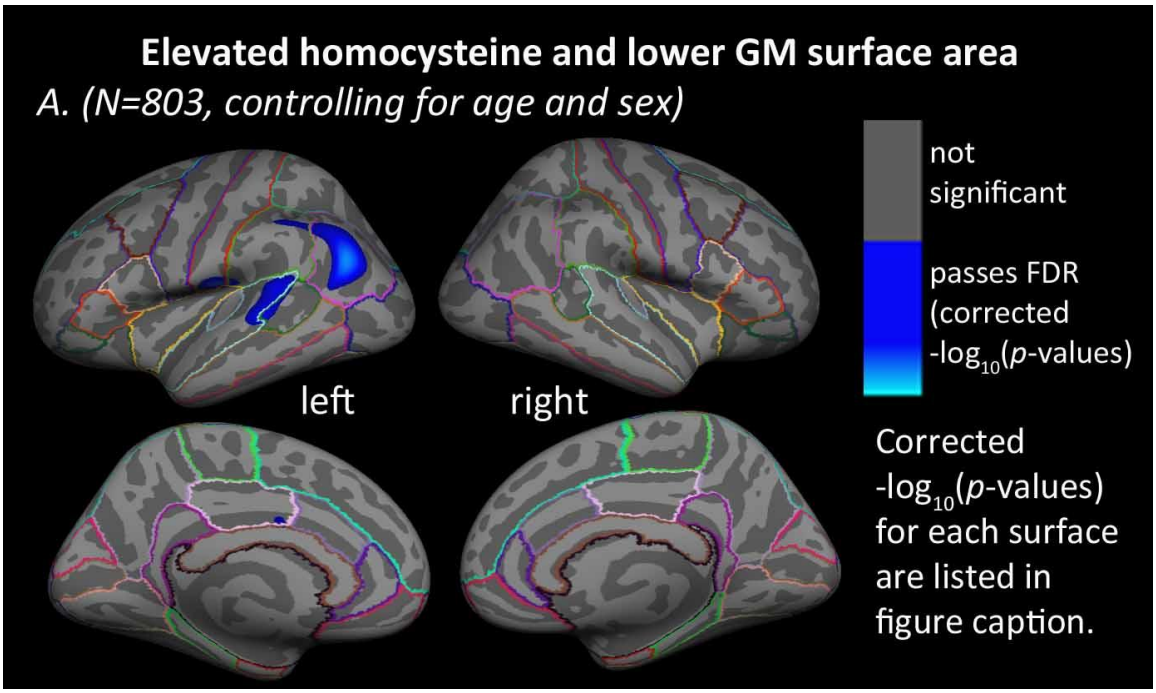

Figure 4: Whole brain 3D maps of significant associations between homocysteine levels and cortical gray matter (GM) surface area in the left and right hemispheres of all N=803 subjects, (A) after controlling for age and sex (left: $-log_{10}(p\text{-}value)$=2.763-5.021, right: not significant, FDR corrected) and (B) after controlling for age, sex, and diagnosis (AD, MCI, or healthy elderly) (left and right: not significant, FDR corrected). Results were corrected for multiple comparisons by thresholding at a p=0.05 false discovery rate (FDR) threshold across the entire brain surface. Blue areas represent points on the cortical surface where t-values passed the corrected significance threshold for a negative relationship between homocysteine levels and cortical GM surface area (higher levels of homocysteine associated with lower cortical GM surface area). No areas of significant positive associations were found.

4. Discussion

Our results show that elevated levels of homocysteine are associated with regional GM reductions in the cortex of elderly individuals, irrespective of age, sex, and dementia diagnosis. As expected, AD and MCI groups had significantly elevated homocysteine levels compared to healthy elderly controls. The lack of significant difference between AD and MCI groups may

suggest that while elevated homocysteine levels at any point in time confer an increased risk for dementia (Seshadri et al., 2002), they may not worsen substantially after the MCI stage. A longitudinal investigation of homocysteine levels taken at multiple time points is needed before we can make this statement conclusively. To our knowledge, no such longitudinal report exists for cortical GM, which would be a helpful contribution to the field.

This new cortical mapping study complements prior studies associating high levels of homocysteine with WM atrophy rate, baseline volume and atrophy rate of the hippocampus (Firbank et al., 2010), lower tissue volumes in frontal and parietal WM (Rajagopalan et al., 2011), longitudinal ventricular volume enlargement in elderly individuals with arteriosclerotic disease (Jochemsen et al., 2012), lower whole brain GM volume in non-demented elderly (Whalley et al., 2003) in humans and with lower GM volume and density in prefrontal cortices and striatum in rhesus monkeys (Willette et al., 2012). Our prior study in an almost entirely overlapping subject population – but with a different method, TBM – found WM tissue contraction (Rajagopalan et al., 2011) in areas that structurally connect the GM regions we see here in the cortex.

Cortical GM structures underlie a wide range of cognitive functions and are also susceptible to age- and disease-related degeneration (Dickerson et al., 2009a, Dickerson et al., 2009b, Thompson et al., 2004, Wolk et al., 2010). Our results show relative reductions in cortical GM in regions that have already been consistently implicated in AD by a convergence of molecular, structural, and functional neuroimaging data, specifically posterior cortical regions including the posterior cingulate, retrosplenial, and lateral parietal cortex - as clearly outlined in Figure 6 of (Buckner et al., 2005). Broadly, these areas are implicated in memory networks (Sperling et al.,

2010) and default mode network activity (Wu et al., 2011) and are susceptible to amyloid deposition, cortical atrophy, and metabolic disruption in AD (Alexander et al., 2012, Reiman and Jagust, 2012, Wolf et al., 2013). It makes sense that we would see these areas in our study of homocysteine-relate brain differences, because elevated homocysteine levels are associated with increased risk for AD and cognitive decline similar to AD.

As with other studies of ADNI and other large cohorts, the relatively large sample size of N=803 makes this a statistically well-powered study. We were able to perform a GLM analysis of homocysteine levels on GM thickness, volume, and surface area at each point on the cortical surface, after controlling for confounding factors. A prior study using more global measures such as total brain, ventricular, and cortical volume (Jochemsen et al., 2012) did not detect significant associations between homocysteine and regional GM measures, even in a large sample of N=663. The detailed 3D pattern of cortical GM atrophy we identified here is an important signature of homocysteine-related brain atrophy that may be missed by more global summary statistics. One prior study, that assessed GM at each voxel in the brains of adults with cardiovascular disease, found widespread regions of lower GM volume associated with higher homocysteine; even so, only small subcortical areas and no cortical GM regions remained significant after controlling for age, sex, and other measures of health status (Ford et al., 2012). This study was relatively large, with N=150; however, our results suggest that cortical studies of homocysteine effects on the brain may require even larger sample sizes, especially to control for the many confounding factors known to affect brain structure.

A large sample size is beneficial for cortical GM studies, as effect sizes tend to be small (cortical thickness differences between AD and elderly controls may range up to 0.20 mm)

(Becker et al., 2011, McGinnis et al., 2011). Measurements may also be noisy due to the complexity of the cortical surface, especially in atrophied elderly brains. Sample size estimates suggest that 50 subjects per group are needed to detect a 0.25 mm group difference (Pardoe et al., 2012), which would be considered a large degree of cortical atrophy. In a study such as ours, where associations with blood measures are subtle, a large sample size may be crucial. This may explain why we found significant associations between homocysteine levels and cortical GM in this large sample, but several prior studies of smaller datasets using different segmentation methods, did not find significant cortical associations.

One difference between the cortical GM results presented here and our previous TBM study is that significant relationships were found in frontoparietal WM for the MCI group, whereas we did not find any significant associations for cortical GM in the MCI group, considered separately. We may have lacked power to detect cortical differences in this region (N=392 MCI for this analysis), or they may not be present.

Higher levels of homocysteine and lower levels of folate and B vitamins are found in people with Alzheimer's disease (AD) (Clarke et al., 1998). As a result, there has been much interest in testing dietary vitamin B supplements (including folate) that reduce homocysteine to normal levels (Clarke et al., 2005) and to see if this can thereby prevent or limit the related negative cardiovascular and neurological effects. A meta-analysis failed to show that homocysteine lowering interventions were effective against preventing cardiovascular events (Marti-Carvajal et al., 2013), but the results for alleviating dementia have been more supportive. A randomized, double-blind controlled trial was performed with a high dose of folate and vitamin B supplements, given over the course of two years, to MCI individuals over the age of 70 years (de

Jager et al., 2012, Smith et al., 2010). Treatment slowed the accelerated brain atrophy and cognitive decline that is typically seen at this stage of the disease. Another study found that adults with greater intake of B vitamins (B6 and B12) had greater GM volumes in medial and lateral frontal, parietal, and temporal cortical regions (Erickson et al., 2008). This readily accessible treatment therefore has the potential, at least in principle, to reduce risk for cognitive impairment and dementia associated with high homocysteine levels. To understand treatment effects, we also need to better understand the specific neural correlates of homocysteine levels.

Elevated homocysteine levels are neurotoxic and are linked with cardiovascular dysfunction, cognitive decline, increased dementia risk, and brain atrophy. This large study identifies a detailed 3D pattern of lower cortical GM thickness, volume, and surface area associated with elevated homocysteine in the elderly. This cortical signature, along with lower subcortical brain volumes, may offer a more comprehensive set of biomarkers to identify brain atrophy associated with high levels of homocysteine. This has important clinical implications in trials of homocysteine lowering interventions such as folate and B vitamins. These cortical and subcortical biomarkers could be useful to assess the effectiveness of interventions that aim to prevent or slow homocysteine-related brain degeneration and dementia.

BIBLIOGRAPHY:

Alexander, G.E., Bergfield, K.L., Chen, K.W., Reiman, E.M., Hanson, K.D., Lin, L., Bandy, D., Caselli, R.J., Moeller, J.R. 2012. Gray matter network associated with risk for Alzheimer's disease in young to middle-aged adults. Neurobiol Aging 33(12), 2723-32. doi:DOI 10.1016/j.neurobiolaging.2012.01.014.

Apostolova, L.G., Akopyan, G.G., Partiali, N., Steiner, C.A., Dutton, R.A., Hayashi, K.M., Dinov, I.D., Toga, A.W., Cummings, J.L., Thompson, P.M. 2007a. Structural correlates of apathy in Alzheimer's disease. Dement Geriatr Cogn 24(2), 91-7. doi:10.1159/000103914.

Apostolova, L.G., Steiner, C.A., Akopyan, G.G., Dutton, R.A., Hayashi, K.M., Toga, A.W., Cummings, J.L., Thompson, P.M. 2007b. Three-dimensional gray matter atrophy mapping in mild cognitive impairment and mild Alzheimer disease. Arch Neurol-Chicago 64(10), 1489-95. doi:DOI 10.1001/archneur.64.10.1489.

Apostolova, L.G., Thompson, P.M. 2007. Brain mapping as a tool to study neurodegeneration. Neurotherapeutics 4(3), 387-400. doi:DOI 10.1016/j.nurt.2007.05.009.

Becker, J.A., Hedden, T., Carmasin, J., Maye, J., Rentz, D.M., Putcha, D., Fischl, B., Greve, D.N., Marshall, G.A., Salloway, S., Marks, D., Buckner, R.L., Sperling, R.A., Johnson, K.A. 2011. Amyloid-beta associated cortical thinning in clinically normal elderly. Ann Neurol 69(6), 1032-42. doi:10.1002/ana.22333.

Benjamini, Y., Hochberg, Y. 1995. Controlling the False Discovery Rate - a Practical and Powerful Approach to Multiple Testing. J Roy Stat Soc B Met 57(1), 289-300.

Bostom, A.G., Silbershatz, H., Rosenberg, I.H., Selhub, J., D'Agostino, R.B., Wolf, P.A., Jacques, P.F., Wilson, P.W.F. 1999. Nonfasting plasma total homocysteine levels and all-cause and cardiovascular disease mortality in elderly Framingham men and women. Arch Intern Med 159(10), 1077-80. doi:DOI 10.1001/archinte.159.10.1077.

Bots, M.L., Launer, L.J., Lindemans, J., Hofman, A., Grobbee, D.E. 1997. Homocysteine, atherosclerosis and prevalent cardiovascular disease in the elderly: The Rotterdam Study. J Intern Med 242(4), 339-47. doi:DOI 10.1046/j.1365-2796.1997.00239.x.

Breteler, M.M.B. 2000. Vascular risk factors for Alzheimer's disease: An epidemiologic perspective. Neurobiol Aging 21(2), 153-60. doi:Doi 10.1016/S0197-4580(99)00110-4.

Buckner, R.L., Snyder, A.Z., Shannon, B.J., LaRossa, G., Sachs, R., Fotenos, A.F., Sheline, Y.I., Klunk, W.E., Mathis, C.A., Morris, J.C., Mintun, M.A. 2005. Molecular, structural, and functional characterization of Alzheimer's disease: Evidence for a relationship between default activity, amyloid, and memory. J Neurosci 25(34), 7709-17. doi:Doi 10.1523/Jneurosci.2177-05.2005.

Clarke, R., Frost, C., Sherliker, P., Lewington, S., Collins, R., Brattstrom, L., Brouwer, I., van Dusseldorp, M., Steegers-Theunissen, R.P.M., Cuskelly, G., Ward, M., McNulty, H., Scott, J., den Heijer, M., Blom, H., van der Put, N., Shorah, C.J., Malinow, M.R., McMahon, M., Tobert, J., Kush, D., Joosten, E., Riezier, R., Pietrzik, K., Dierkes, J., Bronstrup, A., Jacques, P., Mason, J., Rosenberg, I., Thambyrajah, J., Landray, M., Townend, J., Wheeler, D., Ubbink, J., van Oort, F., Melse-Boonstra, A., Verhoef, P., Woodside, J.V., Yarnell, J., Young, I.S., Evans, A.E., Wald, D., Law, M., Wald, N., C, H.L.T. 2005. Dose-dependent effects of folic acid on blood concentrations of homocysteine: a meta-analysis of the randomized trials. Am J Clin Nutr 82(4), 806-12.

Clarke, R., Smith, A.D., Jobst, K.A., Refsum, H., Sutton, L., Ueland, P.M. 1998. Folate, vitamin B-12, and serum total homocysteine levels in confirmed Alzheimer disease. Arch Neurol-Chicago 55(11), 1449-55. doi:DOI 10.1001/archneur.55.11.1449.

Dale, A.M., Fischl, B., Sereno, M.I. 1999. Cortical surface-based analysis - I. Segmentation and surface reconstruction. Neuroimage 9(2), 179-94. doi:DOI 10.1006/nimg.1998.0395.

de Jager, C.A., Oulhaj, A., Jacoby, R., Refsum, H., Smith, A.D. 2012. Cognitive and clinical outcomes of homocysteine-lowering B-vitamin treatment in mild cognitive impairment: a randomized controlled trial. Int J Geriatr Psychiatry 27(6), 592-600. doi:10.1002/gps.2758.

Dickerson, B.C., Bakkour, A., Salat, D.H., Feczko, E., Pacheco, J., Greve, D.N., Grodstein, F., Wright, C.I., Blacker, D., Rosas, H.D., Sperling, R.A., Atri, A., Growdon, J.H., Hyman, B.T., Morris, J.C., Fischl, B., Buckner, R.L. 2009a. The cortical signature of Alzheimer's disease: regionally specific cortical thinning relates to symptom severity in very mild to mild AD dementia and is detectable in asymptomatic amyloid-positive individuals. Cereb Cortex 19(3), 497-510. doi:10.1093/cercor/bhn113.

Dickerson, B.C., Feczko, E., Augustinack, J.C., Pacheco, J., Morris, J.C., Fischl, B., Buckner, R.L. 2009b. Differential effects of aging and Alzheimer's disease on medial temporal lobe cortical thickness and surface area. Neurobiol Aging 30(3), 432-40. doi:10.1016/j.neurobiolaging.2007.07.022.

Erickson, K.I., Raji, C.A., Lopez, O.L., Becker, J.T., Rosano, C., Newman, A.B., Gach, H.M., Thompson, P.M., Ho, A.J., Kuller, L.H. 2010. Physical activity predicts gray matter volume in late adulthood The Cardiovascular Health Study. Neurology 75(16), 1415-22.

Erickson, K.I., Suever, B.L., Prakash, R.S., Colcombe, S.J., McAuley, E., Kramer, A.F. 2008. Greater intake of vitamins B6 and B12 spares gray matter in healthy elderly: A voxel-based morphometry study. Brain Res 1199, 20-6. doi:DOI 10.1016/j.brainres.2008.01.030.

Firbank, M.J., Narayan, S.K., Saxby, B.K., Ford, G.A., O'Brien, J.T. 2010. Homocysteine is associated with hippocampal and white matter atrophy in older subjects with mild hypertension. Int Psychogeriatr 22(5), 804-11. doi:Doi 10.1017/S1041610210000499.

Fischl, B., Dale, A.M. 2000. Measuring the thickness of the human cerebral cortex from magnetic resonance images. P Natl Acad Sci USA 97(20), 11050-5. doi:DOI 10.1073/pnas.200033797.

Fischl, B., Salat, D.H., Busa, E., Albert, M., Dieterich, M., Haselgrove, C., van der Kouwe, A., Killiany, R., Kennedy, D., Klaveness, S., Montillo, A., Makris, N., Rosen, B., Dale, A.M. 2002. Whole brain segmentation: automated labeling of neuroanatomical structures in the human brain. Neuron 33(3), 341-55.

Fischl, B., Sereno, M.I., Dale, A.M. 1999a. Cortical surface-based analysis. II: Inflation, flattening, and a surface-based coordinate system. Neuroimage 9(2), 195-207. doi:10.1006/nimg.1998.0396.

Fischl, B., Sereno, M.I., Tootell, R.B., Dale, A.M. 1999b. High-resolution intersubject averaging and a coordinate system for the cortical surface. Hum Brain Mapp 8(4), 272-84.

Fischl, B., van der Kouwe, A., Destrieux, C., Halgren, E., Segonne, F., Salat, D.H., Busa, E., Seidman, L.J., Goldstein, J., Kennedy, D., Caviness, V., Makris, N., Rosen, B., Dale, A.M. 2004. Automatically parcellating the human cerebral cortex. Cereb Cortex 14(1), 11-22.

Ford, A.H., Garrido, G.J., Beer, C., Lautenschlager, N.T., Arnolda, L., Flicker, L., Almeida, O.P. 2012. Homocysteine, grey matter and cognitive function in adults with cardiovascular disease. Plos One 7(3), e33345. doi:10.1371/journal.pone.0033345.

Frisoni, G.B., Prestia, A., Rasser, P.E., Bonetti, M., Thompson, P.M. 2009. In vivo mapping of incremental cortical atrophy from incipient to overt Alzheimer's disease. J Neurol 256(6), 916-24. doi:10.1007/s00415-009-5040-7.

Genovese, C.R., Lazar, N.A., Nichols, T. 2002. Thresholding of statistical maps in functional neuroimaging using the false discovery rate. Neuroimage 15(4), 870-8. doi:DOI 10.1006/nimg.2001.1037.

Gustafson, D., Lissner, L., Bengtsson, C., Bjorkelund, C., Skoog, I. 2004. A 24-year follow-up of body mass index and cerebral atrophy. Neurology 63(10), 1876-81.

Han, X., Jovicich, J., Salat, D., van der Kouwe, A., Quinn, B., Czanner, S., Busa, E., Pacheco, J., Albert, M., Killiany, R., Maguire, P., Rosas, D., Makris, N., Dale, A., Dickerson, B., Fischl, B. 2006. Reliability of MRI-derived measurements of human cerebral cortical thickness: the effects of field strength, scanner upgrade and manufacturer. Neuroimage 32(1), 180-94. doi:10.1016/j.neuroimage.2006.02.051.

Ho, A.J., Stein, J.L., Hua, X., Lee, S., Hibar, D.P., Leow, A.D., Dinov, I.D., Toga, A.W., Saykin, A.J., Shen, L., Foroud, T., Pankratz, N., Huentelman, M.J., Craig, D.W., Gerber, J.D., Allen, A.N., Corneveaux, J.J., Stephan, D.A., DeCarli, C.S., DeChairo, B.M., Potkin, S.G., Jack, C.R., Weiner, M.W., Raji, C.A., Lopez, O.L., Becker, J.T., Carmichael, O.T., Thompson, P.M., Neuroimaging, A.s.D. 2010. A commonly carried allele of the obesity-related FTO gene is associated with reduced brain volume in the healthy elderly. P Natl Acad Sci USA 107(18), 8404-9. doi:DOI 10.1073/pnas.0910878107.

Hua, X., Hibar, D.P., Ching, C.R., Boyle, C.P., Rajagopalan, P., Gutman, B.A., Leow, A.D., Toga, A.W., Jack, C.R., Jr., Harvey, D., Weiner, M.W., Thompson, P.M. 2013. Unbiased tensor-based morphometry: improved robustness and sample size estimates for Alzheimer's disease clinical trials. Neuroimage 66, 648-61. doi:10.1016/j.neuroimage.2012.10.086.

Jack, C.R., Jr., Bernstein, M.A., Fox, N.C., Thompson, P., Alexander, G., Harvey, D., Borowski, B., Britson, P.J., J, L.W., Ward, C., Dale, A.M., Felmlee, J.P., Gunter, J.L., Hill, D.L., Killiany, R., Schuff, N., Fox-Bosetti, S., Lin, C., Studholme, C., DeCarli, C.S., Krueger, G., Ward, H.A., Metzger, G.J., Scott, K.T., Mallozzi, R., Blezek, D., Levy, J., Debbins,

J.P., Fleisher, A.S., Albert, M., Green, R., Bartzokis, G., Glover, G., Mugler, J., Weiner, M.W. 2008. The Alzheimer's Disease Neuroimaging Initiative (ADNI): MRI methods. J Magn Reson Imaging 27(4), 685-91. doi:10.1002/jmri.21049.

Jochemsen, H.M., Kloppenborg, R.P., de Groot, L.C., Kampman, E., Mali, W.P., van der Graaf, Y., Geerlings, M.I. 2012. Homocysteine, progression of ventricular enlargement, and cognitive decline. The Second Manifestations of ARTerial disease-Magnetic Resonance study. Alzheimers Dement. doi:10.1016/j.jalz.2011.11.008.

Kerwin, D.R., Gaussoin, S.A., Chlebowski, R.T., Kuller, L.H., Vitolins, M., Coker, L.H., Kotchen, J.M., Nicklas, B.J., Wassertheil-Smoller, S., Hoffmann, R.G., Espeland, M.A., Memory, W.H.I. 2011. Interaction Between Body Mass Index and Central Adiposity and Risk of Incident Cognitive Impairment and Dementia: Results from the Women's Health Initiative Memory Study. J Am Geriatr Soc 59(1), 107-12. doi:DOI 10.1111/j.1532-5415.2010.03219.x.

Kerwin, D.R., Zhang, Y.H., Kotchen, J.M., Espeland, M.A., Van Horn, L., McTigue, K.M., Robinson, J.G., Powell, L., Kooperberg, C., Coker, L.H., Hoffmann, R. 2010. The Cross-Sectional Relationship Between Body Mass Index, Waist-Hip Ratio, and Cognitive Performance in Postmenopausal Women Enrolled in the Women's Health Initiative. J Am Geriatr Soc 58(8), 1427-32. doi:DOI 10.1111/j.1532-5415.2010.02969.x.

Kruman, I.I., Culmsee, C., Chan, S.L., Kruman, Y., Guo, Z.H., Penix, L., Mattson, M.P. 2000. Homocysteine elicits a DNA damage response in neurons that promotes apoptosis and hypersensitivity to excitotoxicity. J Neurosci 20(18), 6920-6.

Lehmann, M., Gottfries, C.G., Regland, B. 1999. Identification of cognitive impairment in the elderly: Homocysteine is an early marker. Dement Geriatr Cogn 10(1), 12-20. doi:Doi 10.1159/000017092.

Leow, A., Huang, S.C., Geng, A., Becker, J., Davis, S., Toga, A., Thompson, P. 2005. Inverse consistent mapping in 3D deformable image registration: Its construction and statistical properties. Lect Notes Comput Sc 3565, 493-503.

Leritz, E.C., Salat, D.H., Williams, V.J., Schnyer, D.M., Rudolph, J.L., Lipsitz, L., Fischl, B., McGlinchey, R.E., Milberg, W.P. 2011. Thickness of the human cerebral cortex is associated with metrics of cerebrovascular health in a normative sample of community dwelling older adults. Neuroimage 54(4), 2659-71. doi:DOI 10.1016/j.neuroimage.2010.10.050.

Lipton, S.A., Kim, W.K., Choi, Y.B., Kumar, S., DEmilia, D.M., Rayudu, P.V., Arnelle, D.R., Stamler, J.S. 1997. Neurotoxicity associated with dual actions of homocysteine at the N-methyl-D-aspartate receptor. P Natl Acad Sci USA 94(11), 5923-8. doi:DOI 10.1073/pnas.94.11.5923.

Marti-Carvajal, A.J., Sola, I., Lathyris, D., Karakitsiou, D.E., Simancas-Racines, D. 2013. Homocysteine-lowering interventions for preventing cardiovascular events. Cochrane Db Syst Rev (1).

McGinnis, S.M., Brickhouse, M., Pascual, B., Dickerson, B.C. 2011. Age-Related Changes in the Thickness of Cortical Zones in Humans. Brain Topogr 24(3-4), 279-91. doi:DOI 10.1007/s10548-011-0198-6.

Morris, M.S., Jacques, P.F., Rosenberg, I.H., Selhub, J. 2001. Hyperhomocysteinemia associated with poor recall in the third National Health and Nutrition Examination Survey. Am J Clin Nutr 73(5), 927-33.

Mueller, S.G., Weiner, M.W., Thal, L.J., Petersen, R.C., Jack, C.R., Jagust, W., Trojanowski, J.Q., Toga, A.W., Beckett, L. 2005. Ways toward an early diagnosis in Alzheimer's disease: the Alzheimer's Disease Neuroimaging Initiative (ADNI). Alzheimers Dement 1(1), 55-66. doi:10.1016/j.jalz.2005.06.003.

Muqtadar, H., Testai, F.D., Gorelick, P.B. 2012. The dementia of cardiac disease. Curr Cardiol Rep 14(6), 732-40. doi:10.1007/s11886-012-0304-8.

Oulhaj, A., Refsum, H., Beaumont, H., Williams, J., King, E., Jacoby, R., Smith, A.D. 2010. Homocysteine as a predictor of cognitive decline in Alzheimer's disease. Int J Geriatr Psychiatry 25(1), 82-90. doi:Doi 10.1002/Gps.2303.

Pardoe, H.R., Abbott, D.F., Jackson, G.D. 2012. Sample size estimates for well-powered cross-sectional cortical thickness studies. Hum Brain Mapp. doi:10.1002/hbm.22120.

Perry, I.J. 1995. Prospective-Study of Serum Total Homocysteine Concentration and Risk of Stroke in Middle-Aged British Men (Vol 346, Pg 1395, 1995). Lancet 346(8990), 1640-.

Perry, I.J., Refsum, H., Morris, R.W., Ebrahim, S.B., Ueland, P.M., Shaper, A.G. 1995. Prospective-Study of Serum Total Homocysteine Concentration and Risk of Stroke in

Middle-Aged British Men. Lancet 346(8987), 1395-8. doi:Doi 10.1016/S0140-6736(95)92407-8.

Pievani, M., Rasser, P.E., Galluzzi, S., Benussi, L., Ghidoni, R., Sabattoli, F., Bonetti, M., Binetti, G., Thompson, P.M., Frisoni, G.B. 2009. Mapping the effect of APOE epsilon 4 on gray matter loss in Alzheimer's disease in vivo. Neuroimage 45(4), 1090-8. doi:DOI 10.1016/j.neuroimage.2009.01.009.

Prestia, A., Drago, V., Rasser, P.E., Bonetti, M., Thompson, P.M., Frisoni, G.B. 2010. Cortical Changes in Incipient Alzheimer's Disease. J Alzheimers Dis 22(4), 1339-49. doi:Doi 10.3233/Jad-2010-101191.

Rajagopalan, P., Gutman, B., Toga, A.W., Jack , C.R.Jr., Weiner, M.W., Thompson, P.M., for the Alzheimer's Disease Neuroimaging Initiative. 2013. Stress hormone, cortisol, is associated with 3D patterns of accelerated brain tissue loss in the elderly.

Rajagopalan, P., Hua, X., Toga, A.W., Jack, C.R., Weiner, M.W., Thompson, P.M., Initia, A.D.N. 2011. Homocysteine effects on brain volumes mapped in 732 elderly individuals. Neuroreport 22(8), 391-5. doi:Doi 10.1097/Wnr.0b013e328346bf85.

Rajagopalan, P., Refsum, H., Hua, X., Toga, A.W., Jack, C.R., Weiner, M.W., Thompson, P.M., Initi, A.s.D.N. 2013a. Mapping creatinine- and cystatin C-related white matter brain deficits in the elderly. Neurobiol Aging 34(4), 1221-30. doi:DOI 10.1016/j.neurobiolaging.2012.10.022.

Rajagopalan, P., Toga, A.W., Jack, C.R., Weiner, M.W., Thompson, P.M., Initi, A.s.D.N. 2013b. Fat-mass-related hormone, plasma leptin, predicts brain volumes in the elderly. Neuroreport 24(2), 58-62. doi:Doi 10.1097/Wnr.0b013e32835c5254.

Raji, C.A., Ho, A.J., Parikshak, N.N., Becker, J.T., Lopez, O.L., Kuller, L.H., Hua, X., Leow, A.D., Toga, A.W., Thompson, P.M. 2010. Brain Structure and Obesity. Hum Brain Mapp 31(3), 353-64. doi:Doi 10.1002/Hbm.20870.

Reiman, E.M., Jagust, W.J. 2012. Brain imaging in the study of Alzheimer's disease. Neuroimage 61(2), 505-16. doi:DOI 10.1016/j.neuroimage.2011.11.075.

Riggs, K.M., Spiro, A., Tucker, K., Rush, D. 1996. Relations of vitamin B-12, vitamin B-6, folate, and homocysteine to cognitive performance in the normative aging study. Am J Clin Nutr 63(3), 306-14.

Salat, D.H., Kaye, J.A., Janowsky, J.S. 1999. Prefrontal gray and white matter volumes in healthy aging and Alzheimer disease. Arch Neurol-Chicago 56(3), 338-44.

Salat, D.H., Williams, V.J., Leritz, E.C., Schnyer, D.M., Rudolph, J.L., Lipsitz, L.A., McGlinchey, R.E., Milberg, W.P. 2012. Inter-individual variation in blood pressure is associated with regional white matter integrity in generally healthy older adults. Neuroimage 59(1), 181-92. doi:DOI 10.1016/j.neuroimage.2011.07.033.

Selhub, J., Jacques, P.F., Bostom, A.G., Dagostino, R.B., Wilson, P.W.F., Belanger, A.J., Oleary, D.H., Wolf, P.A., Schaefer, E.J., Rosenberg, I.H. 1995. Association between Plasma Homocysteine Concentrations and Extracranial Carotid-Artery Stenosis. New Engl J Med 332(5), 286-91. doi:Doi 10.1056/Nejm199502023320502.

Serra, L., Cercignani, M., Lenzi, D., Perri, R., Fadda, L., Caltagirone, C., Macaluso, E., Bozzali, M. 2010. Grey and White Matter Changes at Different Stages of Alzheimer's Disease. J Alzheimers Dis 19(1), 147-59. doi:Doi 10.3233/Jad-2010-1223.

Seshadri, S., Beiser, A., Selhub, J., Jacques, P.F., Rosenberg, I.H., D'Agostino, R.B., Wilson, P.W.F., Wolf, P.A. 2002. Plasma homocysteine as a risk factor for dementia and Alzheimer's disease. New Engl J Med 346(7), 476-83. doi:Doi 10.1056/Nejmoa011613.

Shaw, L.M. 2008. PENN biomarker core of the Alzheimer's disease Neuroimaging Initiative. Neurosignals 16(1), 19-23. doi:10.1159/000109755.

Smith, A.D., Smith, S.M., de Jager, C.A., Whitbread, P., Johnston, C., Agacinski, G., Oulhaj, A., Bradley, K.M., Jacoby, R., Refsum, H. 2010. Homocysteine-Lowering by B Vitamins Slows the Rate of Accelerated Brain Atrophy in Mild Cognitive Impairment: A Randomized Controlled Trial. Plos One 5(9).

Sperling, R.A., Dickerson, B.C., Pihlajamaki, M., Vannini, P., LaViolette, P.S., Vitolo, O.V., Hedden, T., Becker, J.A., Rentz, D.M., Selkoe, D.J., Johnson, K.A. 2010. Functional Alterations in Memory Networks in Early Alzheimer's Disease. Neuromol Med 12(1), 27-43. doi:DOI 10.1007/s12017-009-8109-7.

Swan, G.E., DeCarli, C., Miller, B.L., Reed, T., Wolf, P.A., Jack, L.M., Carmelli, D. 1998. Association of midlife blood pressure to late-life cognitive decline and brain morphology. Neurology 51(4), 986-93.

Thompson, P.M., Hayashi, K.M., de Zubicaray, G., Janke, A.L., Rose, S.E., Semple, J., Herman, D., Hong, M.S., Dittmer, S.S., Doddrell, D.M., Toga, A.W. 2003. Dynamics of gray matter loss in Alzheimer's disease. The Journal of neuroscience : the official journal of the Society for Neuroscience 23(3), 994-1005.

Thompson, P.M., Hayashi, K.M., Sowell, E.R., Gogtay, N., Giedd, J.N., Rapoport, J.L., de Zubicaray, G.I., Janke, A.L., Rose, S.E., Semple, J., Doddrell, D.M., Wang, Y.L., van Erp, T.G.M., Cannon, T.D., Toga, A.W. 2004. Mapping cortical change in Alzheimer's disease, brain development, and schizophrenia. Neuroimage 23, S2-S18. doi:DOI 10.1016/j.neuroimage.2004.07.071.

Toga, A.W., Thompson, P.M. 2013. Connectomics sheds new light on Alzheimer's disease. Biol Psychiatry 73(5), 390-2. doi:10.1016/j.biopsych.2013.01.004.

Whalley, L.J., Staff, R.T., Murray, A.D., Duthie, S.J., Collins, A.R., Lemmon, H.A., Starr, J.M., Deary, I.J. 2003. Plasma vitamin C, cholesterol and homocysteine are associated with grey matter volume determined by MRI in non-demented old people. Neurosci Lett 341(3), 173-6.

Willette, A.A., Gallagher, C., Bendlin, B.B., McLaren, D.G., Kastman, E.K., Canu, E., Kosmatka, K.J., Field, A.S., Alexander, A.L., Colman, R.J., Voytko, M.L.L., Weindruch, R.H., Coe, C.L., Johnson, S.C. 2012. Homocysteine, neural atrophy, and the effect of caloric restriction in rhesus monkeys. Neurobiol Aging 33(4), 670-80. doi:DOI 10.1016/j.neurobiolaging.2010.06.003.

Wolf, A.B., Caselli, R.J., Reiman, E.M., Valla, J. 2013. APOE and neuroenergetics: an emerging paradigm in Alzheimer's disease. Neurobiol Aging 34(4), 1007-17. doi:DOI 10.1016/j.neurobiolaging.2012.10.011.

Wolk, D.A., Dickerson, B.C., Neuroimaging, A.s.D. 2010. Apolipoprotein E (APOE) genotype has dissociable effects on memory and attentional-executive network function in Alzheimer's disease. P Natl Acad Sci USA 107(22), 10256-61. doi:DOI 10.1073/pnas.1001412107.

Wu, X., Li, R., Fleisher, A.S., Reiman, E.M., Guan, X.T., Zhang, Y.M., Chen, K.W., Yao, L. 2011. Altered Default Mode Network Connectivity in Alzheimer's Disease-A Resting Functional MRI and Bayesian Network Study. Hum Brain Mapp 32(11), 1868-81. doi:Doi 10.1002/Hbm.21153.

Wyman, B.T., Harvey, D.J., Crawford, K., Bernstein, M.A., Carmichael, O., Cole, P.E., Crane, P.K., Decarli, C., Fox, N.C., Gunter, J.L., Hill, D., Killiany, R.J., Pachai, C., Schwarz, A.J., Schuff, N., Senjem, M.L., Suhy, J., Thompson, P.M., Weiner, M., Jack, C.R., Jr. 2012. Standardization of analysis sets for reporting results from ADNI MRI data. Alzheimers Dement. doi:10.1016/j.jalz.2012.06.004.

CHAPTER 4

Related works completed during graduate studies

4.1 Review of visual processing in anorexia nervosa and body dysmorphic disorder

This section is adapted from the following paper.

Madsen, S.K., Bohon, C., Feusner, J.D. (2013). Visual processing in anorexia nervosa and body dysmorphic disorder: similarities, differences, and future research directions. *Journal of Psychiatric Research*, available online July 1st, 2013.

Journal of Psychiatric Research xxx (2013) 1–9

Contents lists available at SciVerse ScienceDirect

Journal of Psychiatric Research

journal homepage: www.elsevier.com/locate/psychires

Review

Visual processing in anorexia nervosa and body dysmorphic disorder: Similarities, differences, and future research directions

Sarah K. Madsen [a,*], Cara Bohon [b], Jamie D. Feusner [c]

[a] Imaging Genetics Center, Laboratory of Neuro Imaging, Department of Neurology, University of California, Los Angeles School of Medicine, Los Angeles, CA, USA
[b] Department of Psychiatry and Behavioral Sciences, Stanford University, School of Medicine, Stanford, CA, USA
[c] Department of Psychiatry and Biobehavioral Sciences, University of California, Los Angeles School of Medicine, Los Angeles, CA, USA

ARTICLE INFO

Article history:
Received 15 January 2013
Received in revised form
4 June 2013
Accepted 6 June 2013

Keywords:
Visual processing
Visual perception
Bodies
Faces
Anorexia nervosa
Body dysmorphic disorder

ABSTRACT

Anorexia nervosa (AN) and body dysmorphic disorder (BDD) are psychiatric disorders that involve distortion of the experience of one's physical appearance. In AN, individuals believe that they are overweight, perceive their body as "fat," and are preoccupied with maintaining a low body weight. In BDD, individuals are preoccupied with misperceived defects in physical appearance, most often of the face. Distorted visual perception may contribute to these cardinal symptoms, and may be a common underlying phenotype. This review surveys the current literature on visual processing in AN and BDD, addressing lower- to higher-order stages of visual information processing and perception. We focus on peer-reviewed studies of AN and BDD that address ophthalmologic abnormalities, basic neural processing of visual input, integration of visual input with other systems, neuropsychological tests of visual processing, and representations of whole percepts (such as images of faces, bodies, and other objects). The literature suggests a pattern in both groups of over-attention to detail, reduced processing of global features, and a tendency to focus on symptom-specific details in their own images (body parts in AN, facial features in BDD), with cognitive strategy at least partially mediating the abnormalities. Visuospatial abnormalities were also evident when viewing images of others and for non-appearance related stimuli. Unfortunately no study has directly compared AN and BDD, and most studies were not designed to disentangle disease-related emotional responses from lower-order visual processing. We make recommendations for future studies to improve the understanding of visual processing abnormalities in AN and BDD.

1. Introduction

Anorexia nervosa (AN) and body dysmorphic disorder (BDD) are psychiatric disorders characterized by disturbances in the experience of one's physical appearance. In AN, individuals are preoccupied with body weight and size, often resorting to caloric restriction to maintain a low body weight. They hold often-delusional convictions of being overweight, despite substantial evidence to the contrary. Additionally, they focus on specific body areas that they believe appear "fat," such as the abdominal region, hips, and face. In BDD, individuals are preoccupied with misperceived defects in appearance (Phillips et al., 2010). As a result, they believe that they look deformed or ugly, even though the perceived abnormalities are not noticeable to others or appear minor. They are often concerned with specific details, typically of the face or head (e.g. skin blemishes, hair texture, shape of nose), although any body part may be of concern. As in AN, they also are highly convinced of their perceptions, and 27–60% are classified as currently delusional (Mancuso et al., 2010; Phillips et al., 2006). Both disorders may manifest similar phenomenologic patterns involving hypervigilant attention to details of appearance, which are perceived as flawed, likely contributing to often-delusional distortions in perception.

AN and BDD are associated with substantial psychological distress and functional impairment. Underscoring the broad public health significance of these conditions, the lifetime risk of attempted suicide in BDD is 22–27.5% (Phillips et al., 2005a; Phillips and Diaz, 1997; Veale et al., 1996), and the risk of completed suicide is 30 times that of the general population (Phillips and Menard, 2006). AN is associated with a mortality rate of 5–7% per decade,

* Corresponding author. Neuroscience Interdepartmental Program, Imaging Genetics Center, Laboratory of Neuro Imaging, David Geffen School of Medicine at UCLA, 635 Charles Young Drive South, Suite 225, Los Angeles, CA 90095 7334, USA. Tel.: +1 858 775 9302; fax: +1 310 206 5518.
E-mail addresses: sarah.madsen@loni.ucla.edu, smadsen1@gmail.com (S.K. Madsen).

0022-3956/$ – see front matter © 2013 Elsevier Ltd. All rights reserved.
http://dx.doi.org/10.1016/j.jpsychires.2013.06.003

and an overall standardized mortality higher than any other psychiatric illness (Sullivan, 1995).

In addition to similarities in phenomenology, AN and BDD share a peak onset during adolescence, high risk for chronicity, and have similar comorbidity patterns (although there are higher rates of generalized anxiety disorder in AN and higher rates of panic disorder in BDD) (American Psychiatric Association., 2000; Phillips and Kaye, 2007; Phillips et al., 2005b; Swinbourne and Touyz, 2007). AN and BDD co-occur frequently; up to 32% of BDD patients also have a lifetime comorbid eating disorder (Ruffolo et al., 2006) and 25–39% of those with AN are diagnosed with comorbid BDD (Grant et al., 2002; Rabe-Jablonska Jolanta and Sobow Tomasz, 2000). There is also overlap in specific areas of appearance concerns, e.g. size of abdomen, hips, and thighs (Grant and Phillips, 2004). Approximately 30% of individuals with BDD report significant weight concerns, a characteristic linked to greater symptom severity and morbidity (Kittler et al., 2007). The few studies that have directly compared AN and BDD found similarities on clinical and psychological measures, with both groups exhibiting severe body image symptoms and low self-esteem compared to healthy controls (Hrabosky et al., 2009; Kollei, Brunhoeber, Rauh, de Zwaan, & Martin, 2012; Rosen and Ramirez, 1998). There are also important differences, most notably that the gender distribution is less skewed toward females in BDD (Buhlmann et al., 2010; Koran et al., 2008; Rief et al., 2006).

The similarities in clinical features suggest that AN and BDD may represent overlapping body image disorders (Cororve and Gleaves, 2001). However, BDD is currently categorized as a somatoform disorder in DSM-IV-TR and as a form of hypochondriasis in ICD-10, while AN is categorized as an eating disorder in both systems (American Psychiatric Association, 2000; World Health Organization, 1992). Moreover, BDD is often considered to be on the obsessive-compulsive disorder (OCD) spectrum, due to similar phenomenology, demographics, heredity, course of illness, and response to treatment (Hollander and Wong, 1995; Phillips et al., 2007). (Of note, AN also has some features suggestive of overlap with OCD, including obsessive thoughts and ritualized eating behaviors, high comorbidity of OCD, and a high proportion of first degree relatives with OCD (Phillips et al., 2007).)

Since distorted perception of appearance is a key feature of both AN and BDD, examining visual processing as a phenotype may provide a level of understanding about the relationship between these two disorders, and about the neurobiology behind this phenomenon, which is less likely to be captured by examining individual categorical diagnoses (Insel and Cuthbert, 2009). This has important clinical relevance, as persistent perceptual disturbance is a strong predictor of relapse in AN (Keel et al., 2005). There is a considerable need for understanding the neurobiology of perception in AN and BDD, including any similarities and differences, to help guide the development of rational treatments. To maintain focus on the phenotype of abnormal visual perception of appearance, we did not include other disorders in this review such as OCD or social anxiety disorder; these disorders may also be related to AN and BDD, although perhaps via different overlapping phenotypes (heightened self-consciousness, tendencies for obsessive thoughts and compulsive behaviors, etc.). We have not included other eating disorders, such as bulimia nervosa (BN), for several reasons. Among BN, AN, and BDD there is overlap of certain common clinical features (perceptual distortions, high trait perfectionism, and high comorbid anxiety) (American Psychiatric Association, 2000; Phillips et al., 2005b, 2010; Sutandar-Pinnock et al., 2003; Swinbourne et al., 2007). However, BN has additional characteristics that set it apart from AN and BDD with respect to perception and visual processing. For one, distorted body image perception is required for a diagnosis of AN or BDD, but not for BN (American Psychiatric Association, 2000). While many individuals with BN do have body image disturbances (Jansen et al., 2005; Schneider et al., 2009), this disorder is characterized by a preoccupation with shape and weight, along with body dissatisfaction (even if shape and weight are accurately perceived) (Stice and Agras, 1998). Thus, BN is more heterogeneous when it comes to perceptual distortions, with less consistency than in AN and BDD. Another characteristic that sets BN apart from AN and BDD, in general, is that individuals with BN have higher rates of impulsivity (Claes et al., 2012a; Claes et al., 2012b) and comorbidity with impulse control-related disorders (Fernandez-Aranda et al., 2008). Finally, there is support for the conceptualization of AN and BDD, unlike BN, as including individuals with low insight or delusional beliefs (Hartmann et al., 2013; Konstantakopoulos et al., 2012; Mancuso et al., 2010).

Conscious perception is a complex phenomenon that relies on multiple visual processing systems in the brain, along with tightly linked cognitive and emotional processes that contribute to the subjective perceptual experience (Moutoussis, 2009; Zeki and Bartels, 1999). Visual information is exchanged through functional connections between lower- and higher-order visual areas (occipital, temporal, and parietal), and centers for emotion, cognition, and memory (Lamme and Roelfsema, 2000). This facilitates both bottom-up, perceptually driven visual inputs to emotion and cognitive systems, and top-down modulation of visual input based on conscious interpretation (Hanson et al., 2007; Iaria et al., 2008). An individual's current psychological state and past experiences with emotionally charged visual stimuli (e.g. images of bodies and faces for AN and BDD) are ever-present confounds in studies assessing visual processing (Rossignol et al., 2012; Schettino et al., 2012). Pre-existing or symptom-dependent abnormalities in the function of lower-order visual systems, higher-order cognitive and emotional systems, or both, could be involved in abnormal perception. The majority of studies performed in AN and BDD thus far, unfortunately, have not been designed to discern top-down from bottom-up phenomena. This review focuses on studies that have addressed visual processing in individuals with AN or BDD. We define visual processing as phenomena involved in any of the following steps: acquisition of visual input in the peripheral sensory system (ophthalmologic), relay of this information to the central nervous system, neural processing of visual information in occipital and occipito-parietal regions (from basic feature characteristics to more complex aspects), and further elaboration and integration into representations of whole percepts (e.g. face or body images) in (primarily) temporal brain areas.

Our goal was to examine evidence for abnormalities of different aspects of visual processing in AN and BDD, from the function and structure of the eye to higher order processing of human face and body images. To focus the review, we excluded studies that lacked information on visual processing itself but may have otherwise investigated consciously or unconsciously held beliefs about appearance, emotional reactions to visual stimuli (including food stimuli), facial emotional recognition, and visual memory or attention. Another goal was to compare visual processing abnormalities between these related disorders; definitive conclusions, however, were limited because no study directly compared these two groups.

We organized these studies into: a) ophthalmologic findings; b) perceptual organization as assessed through neuropsychological tests of visuospatial, global/local processing, or multi-sensory integration that included visual stimuli; c) visual processing of naturalistic images (face or body images); and d) functional and structural brain imaging studies of visual processing. The latter category could provide information about visual processing at any of the aforementioned steps. In addition, we included studies that examined evidence for any abnormalities as either state (secondary to symptoms of the illness) or trait (pre-existing) characteristics in AN or BDD.

Please cite this article in press as: Madsen SK, et al., Visual processing in anorexia nervosa and body dysmorphic disorder: Similarities, differences, and future research directions, Journal of Psychiatric Research (2013), http://dx.doi.org/10.1016/j.jpsychires.2013.06.003

2. Materials and methods

We searched for articles in ISI Web of Knowledge, PubMed, and PsychINFO databases. We used keywords of either "body dysmorphic disorder" or "anorexia nervosa" along with the following: "vision," "eye tracking", "eye movements", "visual processing," "visual perception," "body processing," "face processing," "central coherence," "global local processing," "Navon," and "Rey–Osterrieth Complex Figure Test." We also used the keyword "visual" along with "body dysmorphic disorder," but not with "anorexia nervosa" because the latter generated excessive unrelated results. We excluded articles that were not peer reviewed ($n = 15$), not written in English ($n = 4$), or did not provide data or clinical descriptions of visual processing of human bodies or faces in AN or BDD ($n = 200$). We did not include articles describing visual memory or attention alone because we felt it was impossible to disentangle elements of visual processing from top-down and bottom-up modulation from other cognitive domains. Some versions of the neuropsychological tests included in our search terms also involve a memory component, although modifications helped separate this confound in some studies. We also included relevant manuscripts that were cited by articles found through the literature search, but were not otherwise retrieved using our search terms. In addition, we performed a search on Google Scholar (www.scholar.google.com) using the same search terms to locate any relevant articles that the other search methods may have missed. We did not impose a limitation on publication date of the articles.

Forty-four journal articles for AN and 15 for BDD were included in this review, ranging in publication date from 1973 to 2012. Of these, two articles for AN and one for BDD were literature reviews, one article for AN was a meta-analysis, and three articles for AN were case reports. All studies of BDD included adults only. Most studies of AN included adults (26 total), with ten studies also including adolescents and five studies including only adolescents and children. Most BDD studies did not list illness duration; the three studies that included this information reported mean illness durations of approximately 10–20 years (Kiri, 2012; Stangier et al., 2008; Yaryura-Tobias et al., 2002). Twenty-two of the AN studies listed illness duration, with means ranging from less than a year to over 20 years across studies and substantial variability within studies. Most AN studies included only females, with the exception of three studies that included one or two males (Andres-Perpina et al., 2011; Castro-Fornieles et al., 2009; Slade and Russell, 1973) and one large study that included 7 men with AN (Stedal et al., 2012). BDD studies were generally of mixed gender, with the exception of three studies that included only women (Clerkin and Teachman, 2008; Deckersbach et al., 2000; Stangier et al., 2008). A minority of studies included populations that were medication-free (six BDD studies, seven AN studies), with most studies not listing medication status, or else including individuals taking antidepressants, anxiolytics, or antipsychotics. Most studies excluded individuals with neurologic conditions or substance abuse, yet allowed other psychiatric comorbidities – with depression, anxiety, and OCD being the most common.

3. Results

3.1. Anorexia nervosa

3.1.1. Ophthalmologic findings

Two published studies have investigated vision at the ophthalmologic level in AN. Both found decreased retinal nerve fiber layer thickness in patients compared to healthy controls (Caire-Estevez et al., 2012; Moschos et al., 2011). One study specifically found lower mean foveal thickness in AN (Moschos et al., 2011). In the two studies, there were inconsistent differences in visual acuity and visual fields; Moschos et al. found no differences between AN patients and controls in visual acuity or visual field, whereas Caire-Estevez et al. found worse visual acuity and visual field sensitivity in the AN group. It is unclear whether these differences are secondary to malnourishment and weight loss, as each tested underweight patients. Further research in recovered patients would help understand whether these differences persist after nutrition is improved.

3.1.2. Neuropsychological tests of visuospatial and global/local processing

Studies evaluating visuospatial abilities in AN have focused primarily on the integration of sensory information and on cognitive style, the latter suggesting that "weak central coherence" is present in AN (Lopez et al., 2008). Weak central coherence implies a lack of global and integrated processing and enhanced focus on detail (Frith, 2003). Studies investigating central coherence often use the Rey–Osterrieth Complex Figures Task (RCFT) (Shin et al., 2006) or a variation of the Embedded Figures Task (Witkin, 1950).

The RCFT requires participants to draw a complex figure and can be scored on different aspects, including performance and strategy on copy, although the interpretation of visual processing is confounded by memory in both immediate and delayed recall conditions. Studies measuring the accuracy of copy have shown either equivalent (Castro-Fornieles et al., 2009; Danner et al., 2012; Lopez et al., 2008; Sherman et al., 2006; Stedal et al., 2012) or poorer performance in AN relative to control groups (Kim et al., 2011; Lopez et al., 2009). One study found that underweight participants with AN performed worse than controls on copy, but improved after gaining 10% of body weight (Kingston et al., 1996), suggesting that the deficit may be weight-dependent. The majority of studies, which included adolescents and children along with adults, found significantly worse delayed recall in AN (Andres-Perpina et al., 2011; Camacho, 2008; Favaro et al., 2012; Lopez et al., 2008, 2009; Mathias and Kent, 1998; Pendleton-Jones, 1991; Sherman et al., 2006; Stedal et al., 2012; Tenconi et al., 2010; Thompson, 1993), or a trend for worse delayed recall (Castro-Fornieles et al., 2009), but some found equivalent performance (Danner et al., 2012; Kim et al., 2011; Kingston et al., 1996; Murphy et al., 2002).

A few of the studies that found poorer recall on the RCFT in individuals with AN compared to healthy controls also investigated potential mechanisms for this deficit. Three studies, one of which included children and adolescents (Stedal et al., 2012), evaluated the order of construction and found that individuals with AN draw the detailed aspects of the figure first and show less continuity in their drawing (Lopez et al., 2008; Sherman et al., 2006; Stedal et al., 2012). In two of these studies, copy organization significantly mediated the relationship between diagnostic group and recall accuracy, suggesting that individuals with AN may not encode information efficiently for accurate retrieval (Lopez et al., 2008; Sherman et al., 2006).

Most of these studies involved underweight participants, which may explain poorer cognitive ability. However, one study tested a sample of females at risk for developing an eating disorder based on subclinical symptoms (Alvarado-Sanchez et al., 2009). This group evidenced more fragmented completion of the figure, although overall accuracy was equivalent to a non-risk comparison group. Two studies of weight-restored participants with AN showed a lack of significant differences on accuracy compared to healthy controls on copy and recall (Kingston et al., 1996; Pendleton-Jones, 1991), but did not evaluate strategy or style. A recent study found worse performance on the RCFT and lower central coherence in a cohort of underweight AN participants, but no significant difference between a separate cohort of recovered AN participants and healthy controls (Favaro et al., 2012).

Please cite this article in press as: Madsen SK, et al., Visual processing in anorexia nervosa and body dysmorphic disorder: Similarities, differences, and future research directions, Journal of Psychiatric Research (2013), http://dx.doi.org/10.1016/j.jpsychires.2013.06.003

Other studies have examined central coherence with the Embedded Figures Task (EFT), in which participants locate a shape embedded in a complex figure, with shorter response times attributed to bias toward detailed processing. Studies have also used the similar Matching Familiar Figures (MFF) test, which asks participants to identify which one of eight figures matches one previously viewed. Both of these tasks require detailed searching of the test images and visual working memory to recall the previously viewed figure.

Studies utilizing the EFT have shown inconsistent results. Three studies, one including adolescents, found that individuals with AN identified the embedded figures more quickly and with higher accuracy than healthy controls when the embedded figure was available for reference during the task (Lopez et al., 2008, 2009; Tokley and Kemps, 2007). However, Pendleton-Jones et al. (1991) found that longer time was required in both underweight and weight-restored AN adults relative to healthy controls, using the original version of the test, which required holding the figures in working memory, creating a confound between visual processing and memory. When adults and adolescents were administered a time-constrained EFT task, the AN group correctly located fewer shapes than controls (Kim et al., 2011).

Two studies have tested individuals with AN using the MFF. One study in adults (Toner et al., 1987) found superior accuracy in AN, suggesting a bias toward detail level processing. They also found faster response time; while this is generally interpreted as suggesting less bias toward detail processing, which requires greater time to perform, it could alternatively be suggestive of bias toward attention to detail along with abnormally high speed of detail processing. The other study in adolescents and adults found no difference in performance or response time compared to controls (Southgate et al., 2008).

Other studies have utilized novel methods to investigate visuospatial processing, as well as sensory integration, in individuals with AN. In a task requiring participants to compare two visual stimuli, AN participants performed as quickly and accurately as healthy controls, although they were slower when the comparison was lexical (Eviatar et al., 2008). In order to evaluate body perception while minimizing the confounding emotional impact of body images, Nico et al. (2010) had participants follow a stimulus on a trajectory and estimate whether it would hit their body (Nico et al., 2010). Participants with AN were worse at detecting their left body boundary, showing a tendency to underestimate it. Although this was incongruent with feelings of "fatness," which is expected to expand the body boundary, it was similar to the performance of stroke participants with right parietal damage, who were also evaluated. Another study of visuospatial processing used a task of manually matching the angle of a moveable bar. Adolescents with AN performed worse than healthy controls when using their right hand (Grunwald et al., 2002). Taken together, findings from these two studies (Grunwald et al., 2002; Nico et al., 2010) suggest deficits both on the left and right side of the body. This could be due to problems with hemispheric integration, since integration of multisensory information occurs in the right posterior parietal cortex (Grunwald et al., 2002). Individuals must perceive the visuospatial field before they can act on it, possibly explaining why one study found *perceptual* differences on the left side of the body (Nico et al., 2010) and another found *performance* differences on the right (Grunwald et al., 2002).

Guardia et al. (2012) also found evidence of visuospatial deficits in adolescents and adults. Participants with AN overestimated their body size (but not the body size of others) compared to healthy controls when asked to estimate if the body would be able to pass through a doorway (Guardia et al., 2012).

Integration between sensory modalities is important for adjusting visual perception and correcting errors in perception. This integration can be tested with a size–weight illusion, where one must integrate tactile with visual information to estimate weight in two differently sized objects of the same weight. One such study showed that individuals with AN perform better than controls, suggesting a reduced reliance on visual information in judgment of weight (Case et al., 2012). A possible explanation is greater reliance on proprioceptive information, although the mechanism of enhanced performance is unclear.

3.1.3. Visual processing of naturalistic images

Studies in AN in adults and adolescents have found abnormalities in attention, and overestimation of body size, specific to images of their own bodies (Garner et al., 1976; Slade et al., 1973; Smeets et al., 1997; Urgesi et al., 2012). An eye tracking study showed that AN participants focus visual attention on body parts they are dissatisfied with, whereas controls tend to scan the whole body image (Freeman, 1991). Another study showed that AN participants saccade more quickly to their own picture compared to other pictures, unlike controls (Blechert et al., 2010). These differences are consistent with symptoms of increased attention to body areas that evoke strong feelings of dissatisfaction. Without further investigations into visual processing, however, one cannot conclude if these findings are due to abnormalities in sensory-level visual information processing, cognitive and evaluative processes related to AN, or both.

Several studies indicate that adults and adolescents with AN overestimate their overall body size (Garner et al., 1976; Slade et al., 1973; Smeets et al., 1997; Urgesi et al., 2012), even though processing of their own body parts (Garner et al., 1976; Slade et al., 1973; Smeets et al., 1997; Urgesi et al., 2012) and of the body size of other women (Garner et al., 1976; Slade et al., 1973; Smeets et al., 1997; Urgesi et al., 2012) does not differ or is more accurate than controls. These studies also found that AN participants correctly judge height, body movements (Garner et al., 1976; Slade et al., 1973; Smeets et al., 1997; Urgesi et al., 2012), and objects (Garner et al., 1976; Slade et al., 1973; Smeets et al., 1997; Urgesi et al., 2012). These findings suggest a specific disturbance of own body image. However, other studies have found perceptual abnormalities when viewing images of others' bodies. AN adults are better at detecting "thinner than" differences in others' bodies (Smeets et al., 1999) and are more accurate than controls in a delayed matching-to-sample task of pictures of male bodies, with no performance differences when matching pictures of body movements in adolescence (Urgesi et al., 2012). In summary, there appears to be evidence in AN for disturbances in visual processing of both own and others' bodies, although there may be slightly different patterns in each.

3.1.4. Brain imaging studies of visual perception

Several brain imaging studies presenting naturalistic images of bodies to participants with AN found abnormal brain activity. In a review, Pietrini et al. (2011) report relatively consistent findings of abnormal activity in frontal (anterior cingulate, and frontal visual system (right superior frontal (Beato-Fernandez et al., 2009) and right dorsolateral prefrontal (Wagner et al., 2003), parietal (inferior parietal lobule), and striatal (caudate) regions (Pietrini et al., 2011). In one functional magnetic resonance imaging (fMRI) study, AN participants showed higher ventral striatal activity when viewing underweight images compared to normal weight bodies, and also preferred underweight images, unlike controls (Fladung et al., 2010). When asked to compare their own body to an image of another body, AN participants showed less activation in the insula and premotor areas and more activation in the anterior cingulate compared to controls (Friederich et al., 2010). This comparison of own vs. other body was associated with greater anxiety in AN participants, who, unsurprisingly, were less satisfied with their

Please cite this article in press as: Madsen SK, et al., Visual processing in anorexia nervosa and body dysmorphic disorder: Similarities, differences, and future research directions, Journal of Psychiatric Research (2013), http://dx.doi.org/10.1016/j.jpsychires.2013.06.003

own body image. Another study contrasted own body images that had been altered to appear overweight vs. unaltered images. Left medial prefrontal cortex activation was reduced for the restrictive subtype of AN compared to healthy controls, while amygdala activation was normal for the combined AN group (Miyake et al., 2010). A structural MRI study found reduced gray matter density in the left extrastriate body area, which is involved in processing images of human body parts, in individuals with AN compared to controls (Suchan et al., 2010).

Taken together, the functional and structural brain imaging evidence suggests that AN participants demonstrate functional and structural abnormalities in brain areas that are involved in processing visual images of human bodies, as well as, systems involved in anxiety and emotion. Pre-existing abnormalities in brain function/structure could predispose individuals to developing AN; however this is difficult to separate from the effects of low weight and poor nutrition, as these were predominantly studies of underweight individuals.

3.1.5. State vs. trait

Some aspects of abnormal visual processing in AN may represent state characteristics (secondary to weight, nutrition, or other symptoms, and modifiable by treatment and recovery) while others represent traits (pre-existing and usually stable across time). Weight gain in underweight AN participants was associated with improved copy scores on tests of global vs. local processing (Kingston et al., 1996) and reduced overestimation of own body width (Slade et al., 1973).

Treatment and recovery from AN have also been associated with changes in functional brain activity. After recovery, AN participants showed normalized activation in the amygdala and fusiform gyrus for happy and fearful faces (Cowdrey et al., 2012). After treatment with cognitive behavioral therapy that reduced negative body-related thoughts compared to a waitlist group, participants showed increased brain activation when viewing pictures of their own bodies compared to pre-treatment, whereas the non-treatment group actually showed a decrease in activity (Vocks et al., 2011). The increase in activation after treatment was seen in areas that process human body images (extrastriate body area (Downing et al., 2001), left middle temporal gyrus (Weiner and Grill-Spector, 2011)) and self-awareness (bilateral middle frontal gyrus (Platek et al., 2008)).

On the other hand, certain abnormalities in global-local processing may be stable traits of individuals predisposed toward AN, as they have been found in studies of recovered AN participants, unaffected relatives, and at-risk populations with sub-clinical symptoms. (Of note, certain pathophysiological processes evident in recovered AN individuals may represent "scars," or lasting effects of the underweight state or other aspects of the illness that persist after weight has been restored.) Superior attention to detail and poor central coherence compared to controls was observed in both active and recovered AN participants and their unaffected sisters, for adults and adolescents (Roberts et al., 2012; Tenconi et al., 2010). A strong correlation between altered central coherence and deficits in set shifting also persisted in recovered AN participants (Danner et al., 2012). Females at risk for developing AN, with sub-clinical symptoms, also demonstrate worse organization (fragmented completion of figure) on the RCFT (Alvarado-Sanchez et al., 2009). Overall, there is some disagreement on whether and how global-local processing changes with treatment in AN. There is no available literature on the stability of other aspects of visual processing in AN.

3.2. Body dysmorphic disorder

3.2.1. Ophthalmologic findings

There are no published studies yet on ophthalmologic abnormalities in BDD.

3.2.2. Neuropsychological tests of visuospatial and global/local processing

Several studies have investigated visuospatial processing in BDD. One study found that individuals with BDD, similar to those with OCD, performed normally on visuospatial construction and memory on the RCFT (Hanes, 1998). A subsequent neuropsychological study, on the other hand, found that the BDD group performed worse than controls on the RCFT (Deckersbach et al., 2000). In this study, group differences in free recall were mediated by deficits in organizational strategies, in which the BDD group selectively recalled details instead of larger organizational design features. The authors suggested that abnormalities in executive functioning might have explained these results. However, earlier perceptual abnormalities in global and local visual processing, or differences in selective attention, may have also contributed, since this task involved viewing and encoding a complex visual figure.

Dunai et al. (2010) administered a battery of executive functioning tests of planning, organization, working memory, and motor speed to participants with and without BDD (Dunai et al., 2010). They found several domains of executive functioning were impaired in BDD, including difficulty manipulating visual information held in working memory on the Spatial Working Memory Task.

3.2.3. Visual processing of naturalistic images

Early experimental evidence that BDD may involve aberrant own-face perception comes from a study in which BDD participants and healthy controls viewed an image of their own face and indicated if any alterations had been made. A higher proportion of the BDD group perceived distortions of their faces, when in fact none were made (Yaryura-Tobias et al., 2002). Another study investigated asymmetry detection in individuals with BDD (Reese et al., 2010). Participants viewed others' faces that were unaltered or altered in symmetry, and also viewed arrays of dots that were symmetric or asymmetric. Individuals with BDD did not differ significantly from controls in accuracy of detecting asymmetry with faces or dot arrays, although they were slower in making decisions about symmetry. In another study, BDD participants were more accurate than controls at detecting changes made to facial features (e.g, distance between the eyes) of photos of others' faces (Stangier et al., 2008).

Another investigation of face processing demonstrated that individuals with BDD were slower and less accurate than controls in matching the identity of an emotional face to the same face with a neutral expression (Feusner et al., 2010a). This was evident regardless of the type of emotional expression. This suggests general abnormalities in visual processing of faces, which may be more pronounced when features are in a different configuration, such as occurs with emotional expressions.

The "face inversion effect" is a phenomenon in which recognition of inverted (upside down) faces is less accurate and slower relative to recognition of upright faces, due to the absence of a holistic template for inverted faces (Farah et al., 1995). In a study using this task, the BDD group demonstrated a smaller inversion effect during the longer duration stimuli, but no differences were seen for shorter duration stimuli (Feusner et al., 2010b). This suggests that BDD individuals may have an imbalance in global vs. local processing, with a tendency to engage in highly detailed processing of faces, whether upright or inverted. This is in contrast to controls, who may primarily engage holistic processing for upright faces, yet rely on detailed processing for inverted faces (Freire et al., 2000). This may explain the BDD group's advantage in speed for inverted faces, yet only when stimuli were presented long enough to engage detail processing. Another study used inverted faces to test face recognition in individuals with BDD and healthy controls (Kiri, 2012). Although the study did not test the "inversion effect" per se, they

Please cite this article in press as: Madsen SK, et al., Visual processing in anorexia nervosa and body dysmorphic disorder: Similarities, differences, and future research directions, Journal of Psychiatric Research (2013), http://dx.doi.org/10.1016/j.jpsychires.2013.06.003

found that individuals with BDD relative to controls had enhanced ability to recognize inverted famous faces, but did not demonstrate significant differences for upright famous faces.

Clerkin and Teachman (2008) tested visual processing of images of own faces morphed with those of highly attractive or unattractive others, in individuals with either high or low BDD symptoms (Clerkin et al., 2008). The low BDD symptom group demonstrated a normative self-enhancement bias (tendency to rate more attractive morphed image as representing themselves), which was not evident in the high BDD symptom group. This resulted in a non-significant trend for interaction between morphed photograph type and group.

A study using eye tracking investigated selective visual attention in BDD, social phobia, and healthy controls (Grocholewski et al., 2012). Only the BDD group showed selective attention to their own areas of perceived defects of their faces, as measured by number of fixations per degree of visual angle.

Results from these psychophysical experiments suggest that imbalances in holistic vs. detailed processing may explain performance advantages in individuals with BDD relative for inverted faces (Feusner et al., 2010b), as well as for change detection in facial features of others' faces (Stangier et al., 2008), and may be an inefficient or inaccurate strategy for identity recognition across facial expressions (Feusner et al., 2010a). In addition, heightened vigilance to details, particularly for areas of perceived defects (Grocholewski et al., 2012), may also increase susceptibility to errors of commission. This could result in "false positive" errors when scrutinizing own-face images (Yaryura-Tobias et al., 2002).

3.2.4. Brain imaging studies of visual perception

The first fMRI study to investigate the neural correlates of visual perception in BDD used others' faces as stimuli (Feusner et al., 2007). BDD participants and healthy controls were scanned with fMRI while matching photographs of others' faces with normal, high or low spatial frequencies (creating images that contained primarily high detail or configural/holistic information, respectively). The BDD group demonstrated left hemisphere hyperactivity relative to controls in an extended face-processing network for normal and low spatial frequency images. Within-groups results suggested that healthy controls only engaged the left hemisphere for high spatial frequency (high detail) images, whereas BDD participants engaged the left hemisphere for all image types.

An fMRI study using own-face stimuli in BDD participants and healthy controls found abnormal hypoactivity in the BDD group in striate and extrastriate visual cortex for low spatial frequency images, and hyperactivity in orbitofrontal cortex and caudate for normal images (Feusner et al., 2010c). BDD symptom severity correlated with orbitofrontal-striatal and extrastriate visual cortex activity. In a secondary data analysis of the same experiment, anxiety scores in BDD were regressed against fMRI signal changes in brain areas implicated in anxiety and visual processing of details (Bohon et al., 2012). Intermediate anxiety scores were associated with higher levels of brain activity than high or low scores in ventral visual processing areas. Interestingly, the relationship between anxiety and activity in ventral visual processing systems held regardless of BDD symptom severity.

Another fMRI experiment used inanimate object stimuli to investigate general abnormalities in visual processing in BDD (Feusner et al., 2011). BDD participants and healthy controls matched photographs of houses that included normal, high or low spatial frequencies. The BDD group demonstrated abnormal hypoactivity in secondary visual processing systems for low spatial frequency images.

These functional neuroimaging studies provide evidence of abnormal visual processing in BDD, although they utilized relatively small sample sizes. The studies found abnormalities in primary and/or secondary visual cortical, temporal, and prefrontal systems and suggest imbalances in detailed vs. global/configural processing. Moreover, this overall pattern is evident not only for own and other's appearance-related stimuli, but also for inanimate objects, suggesting more general aberrancies in visual processing.

3.2.5. State vs. trait

There are currently no published studies on visual processing abnormalities in BDD as being either state or trait features.

4. Discussion

4.1. Summary of findings

Overall, the literature on AN and BDD suggests a pattern of abnormalities in visual processing and perceptual organization that includes over-attention to detail and reduced processing of larger global features. In both AN and BDD, cognitive strategy and attention may at least partially mediate abnormalities, as these groups tend to focus more on symptom-specific details (body parts in AN and facial features in BDD), and misperceive aspects of their own images. However, visuospatial abnormalities are also evident in both disorders for non-appearance related stimuli. In brain imaging studies, both disorders show abnormal brain activation in frontal, parietal, striatal, and visual systems. Since no study has yet to directly compare visual processing in AN and BDD, we consider the following conclusions separately for each group.

In AN, there is evidence of over-attention to detail and reduced processing of larger holistic features, which likely contribute to lower accuracy on visuospatial tasks. AN individuals tend to overestimate their own body size in images. There is also evidence of abnormal reward circuit and limbic system activity for specific, salient body images. Integration of information between the left and right hemispheres in the brain may also be impaired.

Several studies have found that patterns of visual processing in those with AN may depend on body weight. However, possible effects of weight on visual processing of bodies may be intertwined with the severity of the disorder or degree of recovery. For example, at lower body weight several domains of AN symptoms may be more severe, and ability to gain weight or successfully maintain a normal weight may be linked to improvement in different symptom (e.g. cognitive rigidity or anxiety related to weight gain). Thus, it can be difficult to determine whether differences in visual processing after weight gain are related to changes in weight or nutrition, or to improvement in other symptoms.

In BDD, we also see evidence for increased attention to detail, reduced global processing, and poorer performance in visuospatial tasks. In this group, spatial working memory has been found to be impaired, which may contribute to these effects. Individuals with BDD may employ brain systems normally reserved for detailed image processing and underutilize brain regions responsible for configural and holistic processing. They also identify non-existent distortions in their own face images and show abnormal sensitivity to detecting change in others' faces, possibly due to heightened vigilance to details. Abnormal performance in tests of visual perception and brain activation patterns in BDD are present for own face images, other face images, and inanimate objects.

However, findings in both disorders at this point should still be considered inconclusive, as there are some discrepancies in results across studies. Some of the discrepancies may be explained by differences in the study populations, which could have affected the measurements being analyzed. All BDD and some AN studies included only adults, with several AN studies also investigating adolescents. For example, age differences may explain discrepancies in studies using the MFF; studies of AN adults showed higher

Please cite this article in press as: Madsen SK, et al., Visual processing in anorexia nervosa and body dysmorphic disorder: Similarities, differences, and future research directions, Journal of Psychiatric Research (2013), http://dx.doi.org/10.1016/j.jpsychires.2013.06.003

accuracy and detailed processing, while studies of adolescents found no difference between AN and controls. All BDD studies were of adults, so no clear conclusions about age in this group can be made. Differences in illness duration across studies may explain discrepancies in results. For example, studies including individuals with AN with longer durations of illness demonstrated abnormally slow performance. This may be due to an accumulation of damage to the brain as a result of longer standing malnutrition, anxiety, depression, etc. In general, duration of illness was either not listed or spanned such a broad range (months to decades in some cases), that no clear conclusions can be drawn. Comparisons between AN and BDD should also be made in light of the fact that BDD studies included both genders, while AN studies included only women (with one exception (Stedal et al., 2012)). Thus AN findings may be more specific to women, while BDD findings may be more generalizable to males and females. Two additional factors that could affect results across studies are comorbidities with other psychiatric disorders (some studies included individuals with AN or BDD who had comorbid anxiety, depression, and OCD, along with other disorders), and current use of psychoactive medications. It is also important to note that not all studies provided detailed descriptions of their study populations, making it difficult to assess these factors thoroughly.

Also limiting conclusions is the fact that in general there is an insufficient body of research on visual processing in AN and BDD. In particular, many aspects of visual processing have not been investigated in either disorder (e.g. sensory-level striate and extrastriate visual cortical functioning).

4.2. Recommendations for future studies

.The following recommendations are meant to address limitations in the current literature, and to expand our understanding of pathological processes that cross diagnostic boundaries. It is difficult to make conclusions about visual processing abnormalities in AN and BDD because few studies have adequately disentangled abnormalities in visual processing from effects due to factors that influence visual perception, particularly emotionally salient stimuli. These modifying variables may include anxiety (both general, disease-related, and task-provoked anxiety), depression, personality traits (such as perfectionism and cognitive rigidity), specific symptom severity (obsessive thoughts, or fear of being fat), insight/delusionality, or weight in AN (current weight, or weight gain longitudinally, under-weight vs. weight-restored). While some of these factors may be modeled as covariates, others could be manipulated experimentally to provide more power and sensitivity to detect subtle effects on visual processing. For example, emotionally neutral figures and objects can be presented in various degrees of complexity, contrast, and spatial frequency. Emotional or physical experiences can also be manipulated in experiments to understand their effects on visual processing. Future studies should include stimuli that both do and do not elicit a disease-related emotional response to separate the influence of emotion on visual processing.

Abnormalities in visuospatial performance on neuropsychological tasks in AN and BDD could be mediated by abnormal cognitive strategies for encoding or retrieval of visual information in working memory. Some studies used modified versions of these tasks to reduce confounds with memory. It would also be worthwhile for future studies to specifically investigate visual memory and attention abnormalities in AN and BDD, using studies designed to disentangle these cognitive functions from basic visual processing abnormalities. This could be done, for example, with eye-tracking studies using basic visual as opposed to symptom-relevant stimuli, or studies assessing the difference in response of individuals asked to consciously shift their attention to different stimulus features. As an example of the former, Pallanti et al. (1998) found that the severity of abnormalities in smooth eye movements and saccadic performance in AN to moving, low level visual stimuli was correlated with OCD symptoms, perfectionism, drive for thinness, and interoceptive awareness (they did not, however, measure perceptual distortions in their participants) (Pallanti et al., 1998). Widely used and well-validated, low level, neutral visual stimuli such as sine-wave gratings (Campbell and Green, 1965) or the contour integration task (Kovacs et al., 2000) could be employed to assess relatively early visual system functioning. Moreover, brain imaging techniques such as electroencephalography (EEG) or magnetoencephalography (MEG) have the temporal resolution to discriminate early vs. later visual processing abnormalities, which is not possible with fMRI.

Conclusions about similarities and differences between AN and BDD are limited by the fact that these groups have not yet been directly compared on the same experimental tasks. To more definitively compare and contrast visual processing in these related disorders of body image, future studies should include both AN and BDD subjects, along with matched controls, within the same experiment to ensure methodological consistency. In addition, studies in large, analog populations that are assessed for dimensionality of body image disturbances and visual perceptual distortions may uncover dimensional abnormalities in visual processing that map to dysfunctional brain networks. Another line of research yet to be performed is an investigation of if, and how, prior trauma may relate to the development of aberrant visual processing.

Whether visual abnormalities are a contributing cause or a consequence of AN and BDD is still unclear. We attempted to address this question in the State vs. Trait section of our Results; however no papers were available on this topic for BDD. For AN, several studies suggest that heightened attention to detail and poor central coherence are stable traits that could have contributed to the development of the disorder. However, this inference is based on individuals in recovery or at-risk for AN, rather than currently unaffected individuals who later went on to develop AN. This type of powerful longitudinal study has not been done in AN or in BDD due to practical barriers, although it would be extremely valuable.

Replication of the current studies with larger sample sizes is also needed to understand which measures (neuropsychological assessments, behavioral measures, MRI measures etc.) are most reliable and informative for assessing visual processing in these populations. Multi-site studies are likely necessary to obtain large enough samples, due to difficulty in recruitment of these populations. Finally, it will be important to perform longitudinal studies to determine whether these putative phenotypes predict course of illness and response to treatment.

Role of funding source

This research was made with Government support under and awarded by a DoD, Air Force Office of Scientific Research, National Defense Science and Engineering Graduate (NDSEG) Fellowship, 32 CFR 168a (Sarah K. Madsen), a NIMH grant 2T32MH073517 (Dr. Cara Bohon), and National Institute of Mental Health grants K23 MH079212 and R01MH093535 (Dr. Jamie D. Feusner).

Contributors

Sarah K. Madsen performed the literature search, wrote portions of the first draft, and edited completed drafts. Cara Bohon wrote portions of the first draft and edited completed drafts. Jamie Feusner wrote portions of the first draft and edited completed drafts. All authors have contributed to and have approved the final manuscript.

Please cite this article in press as: Madsen SK, et al., Visual processing in anorexia nervosa and body dysmorphic disorder: Similarities, differences, and future research directions, Journal of Psychiatric Research (2013), http://dx.doi.org/10.1016/j.jpsychires.2013.06.003

Konstantakopoulos G, Varsou E, Dikeos D, Ioannidi N, Gonidakis F, Papadimitriou G, et al. Delusionality of body image beliefs in eating disorders. Psychiatry Research 2012;200:482–8.
Koran LM, Abujaoude E, Large MD, Serpe RT. The prevalence of body dysmorphic disorder in the United States adult population. CNS Spectrums 2008;13:316–22.
Kovacs I, Polat U, Pennefather PM, Chandna A, Norcia AM. A new test of contour integration deficits in patients with a history of disrupted binocular experience during visual development. Vision Research 2000;40:1775–83.
Lamme VA, Roelfsema PR. The distinct modes of vision offered by feedforward and recurrent processing. Trends in Neurosciences 2000;23:571–9.
Lopez C, Tchanturia K, Stahl D, Treasure J. Central coherence in eating disorders: a systematic review. Psychological Medicine 2008;38:1393–404.
Lopez C, Tchanturia K, Stahl D, Treasure J. Weak central coherence in eating disorders: a step towards looking for an endophenotype of eating disorders. Journal of Clinical and Experimental Neuropsychology 2009;31:117–25.
Mancuso SG, Knoesen NP, Castle DJ. Delusional versus nondelusional body dysmorphic disorder. Comprehensive Psychiatry 2010;51:177–82.
Mathias JL, Kent PS. Neuropsychological consequences of extreme weight loss and dietary restriction in patients with anorexia nervosa. Journal of Clinical and Experimental Neuropsychology 1998;20:548–64.
Miyake Y, Okamoto Y, Onoda K, Kurosaki M, Shirao N, Yamawaki S. Brain activation during the perception of distorted body images in eating disorders. Psychiatry Research 2010;181:183–92.
Moschos MM, Gonidakis F, Varsou E, Markopoulos I, Rouvas A, Ladas I, et al. Anatomical and functional impairment of the retina and optic nerve in patients with anorexia nervosa without vision loss. The British Journal of Ophthalmology 2011;95:1128–33.
Moutoussis K. Brain activation and the locus of visual awareness. Communicative & Integrative Biology 2009;2:265–7.
Murphy R, Nutzinger DO, Paul T, Leplow B. Dissociated conditional-associative learning in anorexia nervosa. Journal of Clinical and Experimental Neuropsychology 2002;24:176–86.
Nico D, Daprati E, Nighoghossian N, Carrier E, Duhamel JR, Sirigu A. The role of the right parietal lobe in anorexia nervosa. Psychological Medicine 2010;40:1531–9.
Pallanti S, Quercioli L, Zaccara G, Ramacciotti AB, Arnetoli G. Eye movement abnormalities in anorexia nervosa. Psychiatry Research 1998;78:59–70.
Pendleton-Jones B. Cognition in eating disorders. Journal of Clinical and Experimental Neuropsychology 1991;13:711–28.
Phillips KA, Coles ME, Menard W, Yen S, Fay C, Weisberg RB. Suicidal ideation and suicide attempts in body dysmorphic disorder. Journal of Clinical Psychiatry 2005a;66:717–25.
Phillips KA, Diaz SF. Gender differences in body dysmorphic disorder. Journal of Nervous and Mental Disorders 1997;185:570–7.
Phillips KA, Kaye WH. The relationship of body dysmorphic disorder and eating disorders to obsessive-compulsive disorder. CNS Spectrums 2007;12:347–58.
Phillips KA, Menard W. Suicidality in body dysmorphic disorder: a prospective study. American Journal of Psychiatry 2006;163:1280–2.
Phillips KA, Menard W, Fay C, Weisberg R. Demographic characteristics, phenomenology, comorbidity, and family history in 200 individuals with body dysmorphic disorder. Psychosomatics 2005b;46:317–25.
Phillips KA, Menard W, Pagano ME, Fay C, Stout RL. Delusional versus nondelusional body dysmorphic disorder: clinical features and course of illness. Journal of Psychiatric Research 2006;40:95–104.
Phillips KA, Wilhelm S, Koran LM, Didie ER, Fallon BA, Feusner J, et al. Body dysmorphic disorder: some key issues for DSM-V. Depression and Anxiety 2010;27:573–91.
Pietrini F, Castellini G, Ricca V, Polito C, Pupi A, Faravelli C. Functional neuroimaging in anorexia nervosa: a clinical approach. European Psychiatry: The Journal of the Association of European Psychiatrists 2011;26:176–82.
Platek SM, Wathne K, Tierney NG, Thomson JW. Neural correlates of self-face recognition: an effect-location meta-analysis. Brain Research 2008;1232:173–84.
Rabe-Jablonska Jolanta J, Sobow Tomasz M. The links between body dysmorphic disorder and eating disorders. European Psychiatry 2000;15:302–5.
Reese HE, McNally RJ, Wilhelm S. Facial asymmetry detection in patients with body dysmorphic disorder. Behaviour Research and Therapy 2010;48:936–40.
Rief W, Buhlmann U, Wilhelm S, Borkenhagen A, Brahler E. The prevalence of body dysmorphic disorder: a population-based survey. Psychological Medicine 2006;36:877–85.
Roberts ME, Tchanturia K, Treasure JL. Is attention to detail a similarly strong candidate endophenotype for anorexia nervosa and bulimia nervosa? The World Journal of Biological Psychiatry: The Official Journal of the World Federation of Societies of Biological Psychiatry 2012.
Rosen JC, Ramirez E. A comparison of eating disorders and body dysmorphic disorder on body image and psychological adjustment. Journal of Psychosomatic Research 1998;44:441–9.
Rossignol M, Campanella S, Maurage P, Heeren A, Falbo L, Philippot P. Enhanced perceptual responses during visual processing of facial stimuli in young socially anxious individuals. Neuroscience Letters 2012;526:68–73.
Ruffolo J, Phillips K, Menard W, Fay C, Weisberg R. Comorbidity of body dysmorphic disorder and eating disorders: severity of psychopathology and body image disturbance. International Journal of Eating Disorders 2006;39:11–9.
Schettino A, Loeys T, Bossi M, Pourtois G. Valence-specific modulation in the accumulation of perceptual evidence prior to visual scene recognition. PloS One 2012;7:e38064.
Schneider N, Frieler K, Pfeiffer E, Lehmkuhl U, Salbach-Andrae H. Comparison of body size estimation in adolescents with different types of eating disorders. European Eating Disorders Review: The Journal of the Eating Disorders Association 2009;17:468–75.
Sherman BJ, Savage CR, Eddy KT, Blais MA, Deckersbach T, Jackson SC, et al. Strategic memory in adults with anorexia nervosa: are there similarities to obsessive compulsive spectrum disorders? The International Journal of Eating Disorders 2006;39:468–76.
Shin MS, Park SY, Park SR, Seol SH, Kwon JS. Clinical and empirical applications of the Rey–Osterrieth complex figure test. Nature Protocols 2006;1:892–9.
Slade PD, Russell GF. Awareness of body dimensions in anorexia nervosa: cross-sectional and longitudinal studies. Psychological Medicine 1973;3:188–99.
Smeets MA, Ingleby JD, Hoek HW, Panhuysen GE. Body size perception in anorexia nervosa: a signal detection approach. Journal of Psychosomatic Research 1999;46:465–77.
Smeets MA, Smit F, Panhuysen GE, Ingleby JD. The influence of methodological differences on the outcome of body size estimation studies in anorexia nervosa. The British Journal of Clinical Psychology/the British Psychological Society 1997;36(Pt 2):263–77.
Southgate L, Tchanturia K, Treasure J. Information processing bias in anorexia nervosa. Psychiatry Research 2008;160:221–7.
Stangier U, Adam-Schwebe S, Muller T, Wolter M. Discrimination of facial appearance stimuli in body dysmorphic disorder. Journal of Abnormal Psychology 2008;117:435–43.
Stedal K, Rose M, Frampton I, Landro NI, Lask B. The neuropsychological profile of children, adolescents, and young adults with anorexia nervosa. Archives of Clinical Neuropsychology: The Official Journal of the National Academy of Neuropsychologists 2012;27:329–37.
Stice E, Agras WS. Predicting onset and cessation of bulimic behaviors during adolescence: a longitudinal grouping analysis. Behavior Therapy 1998;29:257–76.
Suchan B, Busch M, Schulte D, Gronemeyer D, Herpertz S, Vocks S. Reduction of gray matter density in the extrastriate body area in women with anorexia nervosa. Behavioural Brain Research 2010;206:63–7.
Sullivan PF. Mortality in anorexia nervosa. American Journal of Psychiatry 1995;152:1073–4.
Sutandar-Pinnock K, Blake Woodside D, Carter JC, Olmsted MP, Kaplan AS. Perfectionism in anorexia nervosa: a 6-24-month follow-up study. The International Journal of Eating Disorders 2003;33:225–9.
Swinbourne JM, Touyz SW. The co-morbidity of eating disorders and anxiety disorders: a review. European Eating Disorders Review 2007;15:253–74.
Tenconi E, Santonastaso P, Degortes D, Bosello R, Titton F, Mapelli D, et al. Set-shifting abilities, central coherence, and handedness in anorexia nervosa patients, their unaffected siblings and healthy controls: exploring putative endophenotypes. The World Journal of Biological Psychiatry: The Official Journal of the World Federation of Societies of Biological Psychiatry 2010;11:813–23.
Thompson SBN. Implications of neuropsychological test results of women in a new phase of anorexia nervosa. European Eating Disorders Review 1993;1:152–65.
Tokley M, Kemps E. Preoccupation with detail contributes to poor abstraction in women with anorexia nervosa. Journal of Clinical and Experimental Neuropsychology 2007;29:734–41.
Toner BB, Garfinkel PE, Garner DM. Cognitive style of patients with bulimic and diet-restricting anorexia nervosa. The American Journal of Psychiatry 1987;144:510–2.
Urgesi C, Fornasari L, Perini L, Canalaz F, Cremaschi S, Faleschini L, et al. Visual body perception in anorexia nervosa. The International Journal of Eating Disorders 2012;45:501–11.
Veale D, Boocock A, Gournay K, Dryden W, Shah F, Willson R, et al. Body dysmorphic disorder. A survey of fifty cases. British Journal of Psychiatry 1996;169:196–201.
Vocks S, Schulte D, Busch M, Gronemeyer D, Herpertz S, Suchan B. Changes in neuronal correlates of body image processing by means of cognitive-behavioural body image therapy for eating disorders: a randomized controlled fMRI study. Psychological Medicine 2011;41:1651–63.
Wagner A, Ruf M, Braus DF, Schmidt MH. Neuronal activity changes and body image distortion in anorexia nervosa. Neuroreport 2003;14:2193–7.
Weiner KS, Grill-Spector K. Not one extrastriate body area: using anatomical landmarks, hMT+, and visual field maps to parcellate limb-selective activations in human lateral occipitotemporal cortex. NeuroImage 2011;56:2183–99.
Witkin HA. Individual differences in ease of perception of embedded figures. Journal of Personality 1950;19:1–15.
World Health Organization. The ICD-10 classification of mental and behavioural disorders: clinical descriptions and diagnostic guidelines. Geneva, Switzerland: WHO; 1992.
Yaryura-Tobias J, Neziroglu F, Chang R, Lee S, Pinto A, Donohue L. Computerized perceptual analysis of patients with body dysmorphic disorder. CNS Spectrums 2002;7:444–6.
Zeki S, Bartels A. Toward a theory of visual consciousness. Consciousness and Cognition 1999;8:225–59.

Please cite this article in press as: Madsen SK, et al., Visual processing in anorexia nervosa and body dysmorphic disorder: Similarities, differences, and future research directions, Journal of Psychiatric Research (2013), http://dx.doi.org/10.1016/j.jpsychires.2013.06.003

4.2 Neuroscience outreach

This section is adapted from the following paper.

Romero-Calderon, R., O'Hare, E., Suthana, N. A., Scott-Van Zeeland, A. A., Rizk-Jacson, A., Attar, A., **Madsen, S. K.,** Ghiani, C. A., Evans, C. J., Watson, J. B. (2012). Project Brainstorm: Using Neuroscience to Connect College Students with Local Schools, PLoS Biology, 10(4), e1001310. doi:10.1371/journal.pbio.1001310.

OPEN ACCESS Freely available online

PLoS BIOLOGY

Community Page

Project Brainstorm: Using Neuroscience to Connect College Students with Local Schools

Rafael Romero-Calderón[1], Elizabeth D. O'Hare[2], Nanthia A. Suthana[3], Ashley A. Scott-Van Zeeland[4], Angela Rizk-Jackson[5], Aida Attar[6], Sarah K. Madsen[6], Cristina A. Ghiani[7], Christopher J. Evans[7,8], Joseph B. Watson[7,8]*

1 Department of Molecular, Cell and Developmental Biology, University of California, Los Angeles, Los Angeles, California, United States of America, **2** Department of Neurology, David Geffen School of Medicine, University of California, Los Angeles, Los Angeles, California, United States of America, **3** Department of Neurosurgery, David Geffen School of Medicine and Semel Institute For Neuroscience and Human Behavior, University of California, Los Angeles, Los Angeles, California, United States of America, **4** Scripps Genomic Medicine, Scripps Translational Science Institute and Scripps Health, La Jolla, California, United States of America, **5** Department of Radiology, Center for the Imaging of Neurodegenerative Disease, University of California, San Francisco, San Francisco, California, United States of America, **6** Interdepartmental Ph.D. Program in Neuroscience, University of California, Los Angeles, Los Angeles, California, United States of America, **7** Department of Psychiatry and Biobehavioral Sciences, University of California, Los Angeles, Los Angeles, California, United States of America, **8** Brain Research Institute, University of California, Los Angeles, Los Angeles, California, United States of America

Currently, a large component of college science classes focuses on the acquisition of factual material. Although a solid knowledge base is essential for a successful career in science, the large volume of memorized material tends to make these classes tedious [1]. Importantly, simply knowing facts but not knowing how to apply them or understanding how they are relevant can leave undergraduate students woefully unprepared for the job market or graduate school. A number of initiatives have started to change the focus of science education in college [2,3], making it more interactive and relevant for students and instructors alike. In fact, this radical shift in teaching science has percolated down the education pipeline to include schools in the kindergarten to 12th grade levels (K-12) [4,5].

Here we describe a field course called Project Brainstorm that asks third- and fourth-year undergraduate students to apply their knowledge of neuroscience in practice and communicate it effectively to school children in the greater Los Angeles area (see http://www.bri.ucla.edu/bri_education/scienceoutreach.asp). Our model provides undergraduates with a real-world experience in neuroscience and also connects them with the public at large. First, students summarize the structure and function of the brain to their peers, requiring them to fully understand the concepts and most importantly how to effectively speak to school children about how the human brain works in a simple yet accurate way. Second, students must create a hands-on activity that showcases an essential brain function and in turn reflects their solid grasp of the theory behind it. Thus the driving force for the course is that undergraduates test their knowledge of neuroscience as they use it in a real-world context by teaching it (Figure 1).

Project Brainstorm also provides undergraduates with the opportunity to improve their writing and oral communication skills while gaining teaching experience. Perhaps just as important, Project Brainstorm serves as an outreach program that allows undergraduates to interact with both school children and teachers at the K-12 level in the local community, make connections outside the university campus, and explore options for using their degree after graduation. Notably, the course is also designed so that neuroscience graduate students benefit as well from Project Brainstorm. By serving as teaching assistants (TAs), graduate students actively train neuroscience undergraduates and proctor school visits, gaining valuable teaching experience at both the K-12 and college level. Considering the lack of comprehensive teaching opportunities in most graduate programs [6] and the increasing movement of young PhDs into "alternative" careers [7], Project Brainstorm offers a much-needed training opportunity for graduate students.

An essential component of the Project Brainstorm course is the formal guidance that undergraduate students receive in preparing cogent lesson plans. More specifically teams of 2–3 undergraduate students are assigned a K-12 classroom to teach and given a general outline of the material they should master (see course syllabus; Text S1). Subsequently they are expected to create a novel, age-appropriate lesson plan of 45 min to showcase the structure and function of the nervous system. This type of independent, group learning has been shown to increase the retention of facts [8] and encourages students to use their creativity to consolidate their knowledge and identify gaps in their understanding [9]. During the introductory meetings, the TA and course instructor coach students on

The Community Page is a forum for organizations and societies to highlight their efforts to enhance the dissemination and value of scientific knowledge.

Citation: Romero-Calderón R, O'Hare ED, Suthana NA, Scott-Van Zeeland AA, Rizk-Jackson A, et al. (2012) Project Brainstorm: Using Neuroscience to Connect College Students with Local Schools. PLoS Biol 10(4): e1001310. doi:10.1371/journal.pbio.1001310

Published April 17, 2012

Funding: Project Brainstorm was supported by the Center for Community Learning at UCLA, the Interdepartmental Neuroscience Departments (graduate and undergraduate) at UCLA, and by the Brain Research Institute. The funders had no role in study design, data collection and analysis, decision to publish, or preparation of the manuscript.

Competing Interests: The authors have declared that no competing interests exist.

* E-mail: jwatson@mednet.ucla.edu

Figure 1. UCLA neuroscience undergraduate students teaching local school children about the brain. (A) Explaining how the water in a jar protects an egg from breaking in much the same way that the cerebrospinal fluid protects the brain from damage. (B) School children look at healthy and diseased human brains wrapped in plastic. (C) Undergraduate neuroscience student introduces the brain to a classroom of seventh grade students. (D) Classroom of fifth grade students learn the gross anatomy of the brain from an undergraduate student holding a model human brain. All participants in this study (legal guardians of school children, undergraduate and graduate students) provided signed consent to publication of their likeness as part of this project.
doi:10.1371/journal.pbio.1001310.g001

effective presentation skills such as voice projection, poise, audience engagement, and appropriate use of PowerPoint and/or a black/whiteboard. Similarly, before students are formally allowed to go into the school classrooms, they perform a dress rehearsal of their lesson plan in front of their peer classmates, the TA, the course instructor, and a small panel of invited neuroscience graduate students (including former TAs) and faculty. The practice run allows the presentations to be checked for factual accuracy, appropriateness for the student age group, and improvements in the teaching style. See Text S2 for a sample Microsoft PowerPoint presentation that includes the introduction and brain-in-perspective components.

Assuming that the school children have no significant background in neuroscience, the undergraduate presenter's lesson plan starts with a 5-min introduction of the nervous system. This covers basic gross anatomy (the principal cortical lobes, cerebellum, and brain stem), comparative anatomy, and the structure/function of a neuron. Next, the teams introduce a brain-in-perspective topic to the school children through a 10 min presentation focusing on one age-appropriate topic of interest. Examples include (but are not limited to) senses, memory and learning, motor systems and reflexes, and brain injury (5–9 y of age); any of the previous topics, plus sleep and dreaming, handedness, and pain (10–13 y of age); and any of the previous topics, plus drugs and the brain, nerve impulse conduction, gender differences in the brain, circadian rhythms, stroke, and neurodegenerative diseases (14–18 y of age).

To conclude the lesson plan, the undergraduates guide a 30 min hands-on practicum aided by numerous hands-on teaching props. To encourage active participation in science during the practicum, school students are divided into smaller groups that rotate through a number of different stations, including (a) comparative anatomy (real animal brains, ranging from fruit flies to sheep), (b) human dura matter and spinal cord, (c) human whole brain and sectioned hemispheres, (d) brain injury with pathological human brains sections, and (e) student-developed exercises that highlight their brain-in-perspective topic. See Video S1 to glimpse the hands-on practicum dynamic in the classroom and Text S3 for examples of typical brain-in-perspective activities.

At the conclusion of the course, the undergraduate students submit a 2–3 page instructive lesson plan on their project formatted so that other educators (school teachers, fellow student mentors, or college faculty) can quickly and independently utilize their lesson. These lesson plans (see Text S4 for an example) are simple enough that teachers with limited science backgrounds can implement them on their own within the school's science curricula and can be easily modified to meet the changing needs of the school classroom—two conditions that are thought to improve the efficacy of an outreach program in K-12 schools [10].

We acknowledge that there will be substantial differences in the way the material is delivered in the classrooms, reflecting the styles and personalities of the undergraduates. However, both the quantity and quality of the material are carefully controlled during the practice runs and remain fairly standard between groups. In the process, we have generated an ongoing archive of interactive and concise lesson plans that use the brain as a teaching tool to advocate both the importance and fun of science. Indeed Project Brainstorm's primary goal is not to introduce school children to neuroscience per se but rather to create interaction between college and school students. These interactions will hopefully (1) allow K-12 students to learn about research first-hand and maybe inspire them to pursue higher education and a career in science and (2) provide undergraduates with insight into the educational system and highlight ways in which outreach efforts in general can have a positive impact in society. Moreover, this course format should translate well to any other discipline in the life or physical sciences and could have broad appeal to many educational institutions.

The outreach component of the course has also been quite successful in reaching a large number of school children. In the past five years, over 100 neuroscience undergraduates have completed the Project Brainstorm course and have visited more than 60 classrooms in 30 Los Angeles schools, to reach over 1,900 K-12 students with hands-on and interactive learning experiences focused on neuroscience. This course is unique in its ability to reach large student audiences of varying socioeconomic backgrounds (Table S1). Because a majority of schools in the greater Los Angeles area are classified as Title 1 (at least 40% of its students come from families that qualify as low-income under the United States Census's definitions), we are effectively reaching a large number of students who may not have

access to these educational experiences and have fewer opportunities to interact with college students. Although the number of underrepresented minorities earning a science bachelor's degree has risen slightly over the last 15 years, they currently range below 17% of all science degrees conferred in 2007 [11], roughly half of what would be expected based on the demographic representation levels of minorities in the general population [12].

Targeting a younger demographic provides some added advantages. First, school children have an instinctive curiosity about natural phenomena that facilitates their interest and retention of the subject matter [13]. Second, we take advantage of the fact that older students are teaching younger students, a pedagogical strategy that has successfully introduced active science into the classroom in the past [14,15]. Interestingly, based on anecdotal experiences over the past five years, the younger the student's age (especially 3rd–5th grades), the greater is the student's enthusiasm, spontaneity, questions, and curiosity about neuroscience and the brain. We are currently measuring Project Brainstorm's impact on K-12 students' perception of science, before and after each school visit, in order to provide a more quantitative assessment of our outreach efforts. Additionally, the school presentations will serve as the performance task that helps evaluate the effectiveness of our methodology [16]. Determining how well the K-12 students understood the material during the classroom visits will provide a measure of how successful our program is at both consolidating neuroscience concepts in undergraduate college students and communicating science to school children.

Although the employment prospects for recent college graduates appear to be poor [17], historically evidence shows that having a college degree significantly increases the earning potential and decreases unemployment [18]. Project Brainstorm primarily aims to provide college students practical use of their knowledge through teaching, while reaching out to a newer generation of students to motivate them to pursue a higher education in the sciences. In light of the critical need for properly trained science teachers [19], exposing undergraduate neuroscience students to the K-12 environment can motivate them to consider teaching as a viable and rewarding career. Furthermore, we are also keenly aware that college enrollment in life science majors is dismally low. For instance, in 2003–2004 only 4% of entering college students declared a biological or biomedical science-related major, with only 20% of them successfully completing the bachelor's degree [20]. This lack of interest in science might stem from poor science education and achievement during primary and especially during secondary education [21,22]. However, this negative influence can be mitigated by allowing young scientists to interact with school children early on [23], something that Project Brainstorm addresses directly.

The importance of science outreach among scientists and science educators has been widely recognized. Indeed, similar programs coupling college faculty and students with schools have been successfully implemented to increase student interest and learning in science [24]. Similarly within the neuroscience community a series of innovative educational initiatives have also been developed over the last decade [25–28]. Nevertheless, there remains a persistent resistance to new educational models of instruction [29]. Our hope is that Project Brainstorm offers an additional alternative to make science real for both college undergraduates and school students and bolster the discourse between scientists and the general public.

Supporting Information

Table S1 List of schools visited and classrooms taught by Project Brainstorm during the 2006–2011 school years within the Greater Los Angeles Area. Elementary Schools represent kindergarten through fifth grade (5–10 y of age); Middle schools represent sixth through eighth grades (11–13 y); High schools represent ninth through 12th grades (14–18 y); multi-level schools represent kindergarten through eighth grade (5–13 y). *Title I school (at least 40% of students come from families that qualify as low-income under the United States Census definitions). †School visited multiple times. # 2009–10 school year data presented (except for Hawthorne Math & Science Academy and Animo Leadership Charter, for which 2008–2009 data were used), and it is representative of the 2006–2011 time period when schools were visited. The main five ethnic/racial groups are shown. AI, American Indian/Alaskan. The heading Asian includes Filipino and Pacific Islanders. The heading White only includes non-Hispanic White students. N/A, data not available or missing. Not all percentage totals will equal 100 since other ethnicities are not shown. Total number of students and ethnicity profiles were obtained by referring to the School Accountability Report Cards (SARC), which can be viewed at http://notebook.lausd.net/schoolsearch/selector.jsp (for the Los Angeles Unified School District), at http://www.smmusd.org/ (for the Santa Monica-Malibu Unified School District), at http://ccusd.org/ (for the Culver City Unified School District), at http://www.hawthorne.k12.ca.us/ (for the Hawthorne School District), and at http://www.icefla.org/ (for the ICEF Public Schools).
(RTF)

Text S1 Course syllabus for Project Brainstorm.
(RTF)

Text S2 Representative PowerPoint presentation of a Project Brainstorm school visit.
(PPT)

Text S3 Example brain-in-perspective topics for three different age groups.
(RTF)

Text S4 Example of a complete lesson plan for use in schools by teachers.
(RTF)

Video S1 Project Brainstorm classroom visit highlights.
(WMV)

Acknowledgments

We wish to thank the principals, teachers, and students at the schools that agreed to participate in Project Brainstorm. We also extend our gratitude to the neuroscience undergraduate students who organized the presentations and activities for the school classrooms, to the faculty who have participated in the dress rehearsals and to Michael Sherlock for editing Video S1.

References

1. Alberts B (2005) A wakeup call for science faculty. Cell 123: 739–741.
2. Hoskins SG, Stevens LM (2009) Learning our L.I.M.I.T.S.: less is more in teaching science. Advances in Physiology Education 33: 17–20.
3. Clark IE, Romero-Calderon R, Olson JM, Jaworski L, Lopatto D, et al. (2009) "Deconstructing" scientific research: a practical and scalable pedagogical tool to provide evidence-based science instruction. PLoS Biol 7: e1000264. doi:10.1371/journal.pbio.1000264.
4. Bhattacharjee Y (2005) Science education. New curricula aim to make high school labs less boring. Science 310: 224–225.
5. Willingale-Theune J, Manaia A, Gebhardt P, De Lorenzi R, Haury M (2009) Science education. Introducing modern science into schools. Science 325: 1077–1078.
6. Wolyniak MJ (2003) Balancing teaching and research experiences in doctoral training programs: lessons for the future educator. Cell Biology Education 2: 228–232.
7. Mervis J (2008) Science education. And then there was one. Science 321: 1622–1628.
8. Wood DF (2003) Problem based learning. BMJ 326: 328–330.
9. DeHaan RL (2011) Science education. Teaching creative science thinking. Science 334: 1499–1500.
10. Krasny ME (2005) University outreach K-12 science outreach programs: how can we reach a broad audience? Bio Science 55: 350–359.
11. National Science Board (2010) Science and engineering indicators 2010. Arlington, VA: National Science Foundation (NSB 10-01). pp 2–16, 17.
12. US Census Bureau, 2005–2009 American Community Survey. Retrieved December 12, 2011 from: http://factfinder2.census.gov/faces/tableservices/jsf/pages/productview.xhtml?pid=ACS_10_5YR_DP05&prodType=table.
13. Eshach H, Fried MN (2005) Should science be taught in early childhood? Journal of Science Education and Technology 14: 315–336.
14. Beck MR, Morgan EA, Strand SS, Woolsey TA (2006) Mentoring. Volunteers bring passion to science outreach. Science 314: 1246–1247.
15. Toolin RE (2003) Learning what it takes to teach science: high school students as science teachers for middle school students. Journal of Science Education and Technology 12: 457–469.
16. Wiggins G, McTighe J (2005) Understanding by design. Alexandria, VA: Association for Supervision and Curriculum Development.
17. Godofsky J, Zukin C, Horn CV (2011) Unfulfilled expectations: recent college graduates struggle in a troubled economy. New Brunswick, NJ: John J. Heldrich Center for Workforce Development, Edward J. Bloustein School of Planning and Public Policy, Rutgers University.
18. Crosby O, Moncarz R (2006) The 2004-14 job outlook for college graduates. Occupational Outlook Quarterly 50: 42–57.
19. Darling-Hammond L (2007) We need to invest in math and science teachers. The Chronicle of Higher Education 54: B20.
20. Snyder TD, Dillow SA, Hoffman CM (2009) Digest of education statistics 2008 (NCES 2009-020). In: National Center for Education Statistics, Institute of Education Sciences, U.S. Department of Education. Washington, DC, .
21. Grigg W, Lauko M, Brockway D (2006) The nation's report card: science 2005 (NCES 2006-466). In: Department of Education, National Center for Education Statistics. Washington, DC.
22. Gonzales P, Williams T, Jocelyn L, Roey S, Kastberg D, et al. (2008) Highlights from TIMSS 2007: mathematics and science achievement of U.S. fourth- and eighth-grade students in an international context (NCES 2009-001). In: National Center for Education Statistics IoES, U.S. Department of Education, editor. Washington, DC.
23. Organisation for Economic Co-operation and Development (2006) Starting strong II: early childhood education and care. Paris, France, . 198 p.
24. Directorate for Education and Human Resources (2006) Math and science partnership program: strengthening America by advancing academic achievement in mathematics and science. Arlington, VA: National Science Foundation (NSF-05-069).
25. Frantz KJ, McNerney CD, Spitzer NC (2009) We've got NERVE: a call to arms for neuroscience education. The Journal of Neuroscience: The Official Journal of the Society for Neuroscience 29: 3337–3339.
26. Zardetto-Smith AM, Mu K, Carruth LL, Frantz KJ (2006) Brains rule!: a model program for developing professional stewardship among neuroscientists. CBE Life Sciences Education 5: 158–166.
27. Dubinsky JM (2010) Neuroscience education for prekindergarten-12 teachers. The Journal of Neuroscience: The Official Journal of the Society for Neuroscience 30: 8057–8060.
28. Stevens C (2011) Integrating community outreach into the undergraduate neuroscience classroom. The Journal of Undergraduate Neuroscience Education (JUNE) 10: A44–A49.
29. Brainard J (2007) America's science test: the tough road to better science teaching. Chronicle of Higher Education 53: A16.

4.3 List of co-authored papers completed during graduate studies

The following is a list of the co-authored papers that I completed during my graduate studies, which cover a broad range of brain imaging techniques in various populations. The most recent publications are listed first.

Gutman, B, **Madsen, S.,** Thompson, P. (2013). A Family of Fast Spherical Registration Algorithms for Cortical Shapes, accepted at MeshMed *MICCAI 2013*, Nagoya, Japan, Sept. 22-26 2013 [8-page paper; peer-reviewed conference paper].

Dean, D.C. IIU, Jerskey, B.A., Chen, K., Protas, H., Thiyyagura, P., Roontiva, A., O'Muircheartaigh, J., Dirks, H., Waskiewicz, N., Siniard, A.L., Turk, M.N., Hua, X**., Madsen, S.K.,** Thompson, P.M., Fleisher, A.S., Huentelman, M.J., Deoni, S.C., Reiman, E.M. (submitted 2013). Brain differences in infants at differential genetic risk for late-onset Alzheimer's Disease: a cross-sectional imaging study, *JAMA Neurology*, in review.

Feusner, J.D., **Madsen, S.,** Moody, T.D., Bohon, C., Hembacher, E., Bookheimer, S.Y., Bytritsky, A. (2012). Effects of cranial electrotherapy stimulation on resting state brain activity. Brain and Behavoir, 2(3), 211-220.

Foland-Ross, L.C., Bookheimer, S.Y., Lieberman, M.D., Sugar, C.A., Townsend, J., Fischer, J., Torrisi, S., Penfold, C., **Madsen, S.K.,** Thompson, P. M., & Altshuler, L. L. (2011), Normal amygdala activation but persistent ventrolateral prefrontal hypoactivation in adults with bipolar disorder during euthymia. *NeuroImage*, 59(2012), 738-744.

Hua, X., Thompson, P.M., Leow, A.D., **Madsen, S.K**., Caplan, R., Toga, A.W., Levitt, J.G. (2012). Brain growth rate abnormalities visualized in adolescents with autism, *Human Brian Mapping*, 34(2), 425-436.

Looi, J.C., Rajagopalan, P., Walterfang, **Madsen, S.K.,** Thompson, P.M., Macfarlane, M.D., Ching, C., Chua, P., Velakoulis, D. (2012). Differential putaminal morphology in Huntington's

disease, frontotemporal dementia, and Alzhiemer's disease, *Australian and New Zealand Journal of Psychiatry*, 46(120, 1145-1157, DOI: 10.1177/0004867412457224

Rajagopalan, P., Jahanshad, N., Stein, J.L., Hua, X., **Madsen, S.K**., Kohannim, O., Hibar, D.P., Toga, A.W., Jack, C.R., Saykin, A.J., Green, R., Weiner, M.W., Bis, J.C., Kuller, L.H., Riverol, M., Becker, J.T., Lopez, O.L., Alzheimer's Disease Neuroimaging Initiative (ADNI), Cardiovascular Health Study (CHS) (2012). Common folate gene variant, MTHFR C677T, is associated with brain structure in two independent cohorts of people with mild cognitive impairment, *Neuroimage: Clinical*, 1(1), 179-187.

Romero-Calderon, R., O'Hare, E., Suthana, N.A., Scott-Van Zeeland, A. A., Rizk-Jacson, A., Attar, A., **Madsen, S. K.,** Ghiani, C. A., Evans, C. J., Watson, J. B. (2012). Project Brainstorm: Using Neuroscience to Connect College Students with Local Schools, *PLoS Biology*, 10(4), e1001310. doi:10.1371/journal.pbio.1001310.

Bearden, C.E., van Erp, T.G.M., Dutton, R.A., Boyle, C., **Madsen, S.,** Luders, E., Kieseppa, T., Tuulio-Henriksson, A., Huttenen, M., Patronen, T., Kaprio, J., Lonnqvvist, J., Thompson, P.M. (2011). Mapping Corpus Callosum Morphometry in Twin Pairs Discordant for Bipolar Disorder. Cerebral Cortex, 21(10), 2415-2424.

Becker, J.T., Sanders, J., **Madsen, S.K**., Ragin, A., Kingsley, L., Maruca, V., Cohen, B., Goodkin, K., Martin, E., Miller, E.N., Sacktor, N., Alger, J.R., Barker, P.B., Saharan, P., Carmichael, O.T., Thompson, P.M. (2011). Subcortical brain atrophy persists even in HAART-regulated HIV disease. *Brain Imaging and Behavior*, 5(2), 77-85.

Foland-Ross, L.C., Thompson, P.M., Sugar, C.A., **Madsen, S.K.,** Shen, J.K., Penfold, C., Ahlf, K., Rasser, P.E., Fischer, J., Yang, Y.L., Townsend, J., Bookheimer, S.Y., Altshuler, L.L. (2011). Investigation of Cortical Thickness Abnormalities in Lithium-Free Adults with Bipolar I Disorder Using Cortical Pattern Matching. *American Journal of Psychiatry*, 168(5), 530-539.

Ho, A.J., Raji, C.A., Saharan, P. DeGiorgrio, A., **Madsen, S.K.,** Hibar, D.P., Stein, J.L., Becker, J.T., Lopez, O.L., Toga, A.W., Thompson, P.M. (2011). Hippocampal volume is related to body mass index in Alzheimer's disease. *Neuroreport*, 22(1), 10-14.

Stein, J.L, Hibar, D.P., **Madsen, S.K**., Khamis, M., McMahon, K.L., de Zubicaray, G.I., Hansell, N.K., Montgomery, G.W., Martin, N.G., Wright, M.J., Saykin, A.J., Jack, C.R. Jr., Weiner, M.W., Toga, A.W., Thompson, P.M. (2011), Discovery and replication of dopamine-related gene effects on caudate volume in young and elderly populations (N=1198) using genome-wide search. *Molecular Psychiatry*, 16(9), 927-937.

Chou, Y.Y., Lepore, N., Saharan, P., **Madsen, S.K.,** Hua, X., Jack, C.R. Jr., Shaw, L.W., Trojanowski, J.Q., Weinier, M.W., Toga, A.W., Thompson, P.M., & the Alzheimer's Disease Neuroimaging Initiative. (2010). Ventricular maps in 804 ADNI subjects: correlations with CSF biomarkers and clinical decline. *Neurobiology of Aging: ADNI Special Issue*, 31(8), 1386-1400.

Foland-Ross, L.C., Altshuler, L.L., Bookheimer, S.Y., Lieberman, M.D., Townsend, J., Penfold, C., Ahlf, K., Shen, J.K., **Madsen, S.K**., Rasser, P.E., Toga, A.W., & Thompson, P.M. (2010). Amygdala reactivity in healthy adults is correlated with prefrontal cortical thickness. *Journal of Neuroscience*, 30(49), 16673-16678.

CHAPTER 5

Future Works

5.1 Combining multiple risk factors and brain measures in an integrated model

In actuality, the risk factors and brain measures that I explored in my graduate work do not exist independently of each other. Future work will combine several health factors (cardiovascular, hormonal, metabolic, etc.) that relate to Alzheimer's disease risk along with multiple different type of brain imaging measures (cortical and subcortical gray matter, white matter, etc.). In terms of methods, joint independent components analysis (jICA) could be applied to investigate these relationships and attempt to tease apart the various components involved.

5.2 Interaction of genetics and modifiable health factors in the brain

Several studies have found that thyroid hormones levels are under strong genetic influence (possibly up to 65% heritable) [25-28] and that thyroid hormone receptor genotypes relate to brain differences [29]. Future studies include comparing structural brain differences in elderly individuals with varying genotypes coding for different thyroid hormone receptors and thyroid hormone transporters [29-32]. The Alzheimer's Disease Neuroimaging Initiative (ADNI) and Cardiovascular Health Study (CHS) datasets which I analyzed in my graduate work both have a large amount of clinical, as well as, genetic information for several hundreds of elderly subjects. Using the data, I will investigate how different receptor and transporter profiles interact with

modifiable health factors and how this interaction relates to structural brain differences in the elderly.

5.3 Structural connectivity differences associated with modifiable health factors

There is evidence to suggest that thyroid hormones play a major role in white matter development and maintenance in adulthood [33, 34]. A logical continuation of this work is to look for associations between thyroid hormone variables and white matter measures obtained in diffusion tensor imaging (DTI) analyses. To expand on the results I found in cortical gray matter measures, future studies will determine if there are also differences in the underlying white matter fibers that connect regions where we found gray matter thinning. In terms of the MRI biomarkers I investigated, future studies will investigate if longitudinal change in ventricle volume can predict differences in white matter, which would be a new finding to complement our results in cortical gray matter.

BIBLIOGRFAPHY:

1. Kinsella K, H.W., *An Aging World: 2008*, 2009, US Census Bureau: Washington, DC.

2. Shattuck, D.W., et al., *Magnetic resonance image tissue classification using a partial volume model.* NeuroImage, 2001. **13**(5): p. 856-76.

3. Mayeux, R. and Y. Stern, *Epidemiology of Alzheimer disease.* Cold Spring Harbor perspectives in medicine, 2012. **2**(8).

4. Albert, M.S., et al., *Predictors of cognitive change in older persons: MacArthur studies of successful aging.* Psychology and Aging, 1995. **10**(4): p. 578-589.

5. Landau, S.M., et al., *Association of Lifetime Cognitive Engagement and Low beta-Amyloid Deposition.* Archives of neurology, 2012. **69**(5): p. 623-629.

6. Parrott, M.D. and C.E. Greenwood, *Dietary influences on cognitive function with aging - From high-fat diets to healthful eating.* Healthy Aging and Longevity, 2007. **1114**: p. 389-397.

7. Vilatela, M.E.A., M. Lopez-Lopez, and P. Yeseas-Gomez, *Genetics of Alzheimer's Disease.* Archives of Medical Research, 2012. **43**(8): p. 622-631.

8. Wilson, R.S., et al., *Proneness to psychological distress is associated with risk of Alzheimer's disease.* Neurology, 2003. **61**(11): p. 1479-1485.

9. Xu, W.L., et al., *Midlife overweight and obesity increase late-life dementia risk A population-based twin study.* Neurology, 2011. **76**(18): p. 1568-1574.

10. Kalmijn, S., et al., *Subclinical hyperthyroidism and the risk of dementia. The Rotterdam study.* Clinical Endocrinology, 2000. **53**(6): p. 733-737.

11. Yeap, B.B., et al., *Higher Free Thyroxine Levels Predict Increased Incidence of Dementia in Older Men: The Health In Men Study.* Journal of Clinical Endocrinology & Metabolism, 2012. **97**(12): p. E2230-E2237.

12. de Jong, F.J., et al., *Thyroid function, the risk of dementia and neuropathologic changes: The Honolulu-Asia Aging Study.* Neurobiology of Aging, 2009. **30**(4): p. 600-606.

13. Tan, Z.S., et al., *Thyroid function and the risk of Alzheimer disease: The Framingham Study.* Archives of Internal Medicine, 2008. **168**(14): p. 1514-1520.

14. Volpato, S., et al., *Serum thyroxine level and cognitive decline in euthyroid older women.* Neurology, 2002. **58**(7): p. 1055-1061.

15. Stuerenburg, H.J., S. Arlt, and T. Mueller-Thomsen, *Free thyroxine, cognitive decline and depression in Alzheimer's disease.* Neuroendocrinology Letters, 2006. **27**(4): p. 535-537.

16. Ceresini, G., et al., *Thyroid Function Abnormalities and Cognitive Impairment in Elderly People: Results of the Invecchiare in Chianti Study.* Journal of the American Geriatrics Society, 2009. **57**(1): p. 89-93.

17. Lehmann, M., C.G. Gottfries, and B. Regland, *Identification of cognitive impairment in the elderly: Homocysteine is an early marker.* Dementia and Geriatric Cognitive Disorders, 1999. **10**(1): p. 12-20.

18. Riggs, K.M., et al., *Relations of vitamin B-12, vitamin B-6, folate, and homocysteine to cognitive performance in the normative aging study.* American Journal of Clinical Nutrition, 1996. **63**(3): p. 306-314.

19. Morris, M.S., et al., *Hyperhomocysteinemia associated with poor recall in the third National Health and Nutrition Examination Survey.* American Journal of Clinical Nutrition, 2001. **73**(5): p. 927-933.

20. Seshadri, S., et al., *Plasma homocysteine as a risk factor for dementia and Alzheimer's disease.* New England Journal of Medicine, 2002. **346**(7): p. 476-83.

21. Carter, C.L., et al., *Sex and Gender Differences in Alzheimer's Disease: Recommendations for Future Research*. Journal of Women's Health, 2012. **21**(10): p. 1018-23.

22. Reitz, C., et al., *Epidemiology of Alzheimer's disease*. Nature Reviews Neurology, 2011. **7**(3): p. 137-52.

23. Corbett, A., et al., *New and emerging treatments for Alzheimer's disease*. Expert review of neurotherapeutics, 2012. **12**(5): p. 535-43.

24. Sadowsky, C.H., et al., *Guidelines for the management of cognitive and behavioral problems in dementia.* Journal of the American Board of Family Medicine : JABFM, 2012. **25**(3): p. 350-66.

25. Hansen, P.S., et al., *Major genetic influence on the regulation of the pituitary-thyroid axis: A study of healthy Danish twins.* Journal of Clinical Endocrinology & Metabolism, 2004. **89**(3): p. 1181-1187.

26. Panicker, V., et al., *Heritability of serum TSH, free T4 and free T3 concentrations: a study of a large UK twin cohort.* Clinical Endocrinology, 2008. **68**(4): p. 652-9.

27. Arnaud-Lopez, L., et al., *Phosphodiesterase 8B gene variants are associated with serum TSH levels and thyroid function.* American journal of human genetics, 2008. **82**(6): p. 1270-80.

28. Atzmon, G., et al., *Genetic Predisposition to Elevated Serum Thyrotropin Is Associated with Exceptional Longevity.* Journal of Clinical Endocrinology & Metabolism, 2009. **94**(12): p. 4768-4775.

29. Dixson, L., et al., *Thyroid hormone transporter genes and grey matter changes in patients with major depressive disorder and healthy controls.* Psychoneuroendocrinology, 2011. **36**(6): p. 929-934.

30. Schwartz, C.E. and R.E. Stevenson, *The MCT8 thyroid hormone transporter and Allan-Herndon-Dudley syndrome.* Best Practice & Research Clinical Endocrinology & Metabolism, 2007. **21**(2): p. 307-321.

31. van der Deure, W.M., et al., *Polymorphisms in the brain-specific thyroid hormone transporter OATP1C1 are associated with fatigue and depression in hypothyroid patients.* Clinical Endocrinology, 2008. **69**(5): p. 804-811.

32. Fuchs, O., et al., *Elevated serum triiodothyronine and intellectual and motor disability with paroxysmal dyskinesia caused by a monocarboxylate transporter 8 gene mutation.* Developmental Medicine and Child Neurology, 2009. **51**(3): p. 240-244.

33. Powell, M.H., et al., *Magnetic resonance imaging and volumetric analysis: Novel tools to study the effects of thyroid hormone disruption on white matter development.* Neurotoxicology, 2012.

34. Harsan, L.A., et al., *Recovery from Chronic Demyelination by Thyroid Hormone Therapy: Myelinogenesis Induction and Assessment by Diffusion Tensor Magnetic Resonance Imaging.* Journal of Neuroscience, 2008. **28**(52): p. 14189-14201.